CHEMICAL SYNTHESIS OF HYDROXYAPATITE AND STUDY OF ITS ANTIMICROBIAL PROPERTY

DISSERTATION-II

Submitted in partial fulfilment of the requirements for the award of the degree of

Master of Technology
(BIOTECHNOLOGY)

Submitted by
BHUMIKA BERRY
(11506401)

Under the guidance of
Dr. ANJUVAN SINGH
(Associate Professor)
(15950)

SCHOOL OF BIOENGINEERING AND BIOSCIENCES LOVELY PROFESSIONAL UNIVERSITY

PHAGWARA-144411, PUNJAB, INDIA.

CERTIFICATE

I hereby certify that the work being presented in the dissertation entitled "**CHEMICAL SYNTHESIS OF HYDROXYAPATITE AND STUDY OF ITS ANTIMICROBIAL PROPERTY**" in partial fulfillment of the requirement of the award of the Degree of master of technology and submitted to the Department of Bioengineering and Biosciences f Lovely Professional University, Phagwara, is an authentic record of my own work carried out under the supervision of **Dr. Anjuvan Singh**, **Associate Professor,** School of Bioengineering And Biosciences, Lovely Professional University. The matter embodied in this dissertation has not been submitted in part or full to any other University or Institute for the award of any degree.

(Date)

Bhumika Berry

Registration no. 11506401

This is to certify that the above statement made by the candidate is correct to the best of my knowledge.

(Date) (Dr. Anjuvan Singh)

(U.ID - 15950)

Chapter 1

Introduction

Hydroxyapatite, abbreviated as HAP, is a bioceramic material that is frequently used in various biomedical applications. Mr. Abraham Gottlob Werner, a German geologist coined the term apatite in the year 1786. Apatite is a mineral that ` often mistaken for other minerals. Word Apatite has Greek origin. This is a derivative of the word 'apatein' which implicates deceiving or deceptive.

1.1 Classification

In general; APATITE means a group of minerals that contain phosphates as major component. Apatite include three common members referred to as hydroxylapatite, fluorapatite and chlorapatite, as these carry high concentrations of various ions i.e., OH^-, F^- and Cl^- ions, respectively in their resulting crystals.

Table 1 Formulation of Various individual minerals

$Ca_{10}(PO4)6(OH)_2$	Hydroxyapatite
$Ca_{10}(PO4)6(F)_2$	fluoroapatite (strongly resists acid attack)
$Ca_{10}(PO4)6(Cl)_2$	chloroapatite

A relatively rare form of apatite carrying numerous carbonate and acid phosphate substitutions but minimal but minimal or nil hydroxyl groups is a large component of animal bone material. Hydroxyapatite has a chemical formation as $Ca_{10}(PO_4)_6(OH)_2$.

The purpose of conducting this study was to assess the efficacy of the method to produce HAP. In the present study, HAP is being synthesized using Wet Chemical Method. The method is definitely proficient enough to manufacture HAP with minimal impurities. HAP produced was characterized by FTIR, SEM, TEM and also by XRD analysis. HAP is remarkably biocompatible. It is also assessed to possess antimicrobial efficacy upto an enhanced degree. And as such it can be used to replace normal human tissues as and when required medically. Main purpose of undertaking this project is to establish that HAP can be competently used as a substitute for dental implant. Dental implants are one of the most extensively performed implants on human body.

1.2 USES

HAP has numerous medical applications in various physical forms i.e., porous, dense and granular states. This being the natural inorganic substance of Teeth along with Bones, has been widely used in the biomedical field. It is commonly employed in dentistry and in orthopedics for the reason that it has likeness to inorganic element of a tooth as well as that of bones. Hydroxyapatite is frequently being used for filling of periodontal lesions.

Apatite is produced and used in procedures pertaining to biological micro-environmental systems. One more name for hydroxyapatite is hydroxylapatite. It is found out to be the main component enamel of teeth and bony minerals. The eminent role of HAP is known in medical applications. Hydroxyapatite; a ceramic material is being used for bone reengineering and also in medicine delivery systems because it is biocompatible. (Pandey, H.M.et.al.,2012). HAP has major biological and industrial roles. The porous character of HAP allows good binding affinity for pharmacologicals including antibiotics, enzymes, hormones, steroids, antibody fragments. (Sadjadi M.S. et al 2010). The porosity character allows HAP in the treatment of diseases such as osteomyelitis, bone cancers etc. The synthesized HAP has osteoconductive properties. Therefore it is used to replace hard tissues. The role of HAP in biomedical uses is basically measured according to its similarity with body apatite, which comprises the calcified mineral phases of dentine and bone.Moreover it is usually applied as powder form to supplement Calcium drugs, in both ceramic and composite forms connecting the bones along with their repair. Also it is coated on metals and various alloys forming bone splints and screws. HAP has rapid activity to form direct bonding with the living bone lacking connective tissue as intermediate source.

HAP is widely used as a calcium supplement drug, as a ceramic, for connecting the bone, in orthopedics for repairing bone and as filler to replace amputated bone. It is enormously being used in dentistry as coating material to promote growth inside dental implants and for augmentation. In powder form it is used as a drug to supplement calcium; to connect bones it is to be in ceramic or composite form alloys used for bone splins , to link or repair the bone and coating on metals,. Nano crystalline HAP is similar to natural bone as far as composition and crystalline structure are concerned. Its controlled reabsorption in the body fluids following implantation makes it an ideal bone graft substitute.

Implant steadiness is being prejudiced by local as well as and skeletal bone densities.(Merheb, J.et. al. 2016).

Nano HAP stimulates adhesion in bone cells and assist their proliferation. It promotes deposition of bone on bioceramic material surface. Hence particle size, composition morphology of HAP are important parameters. (Sasikumar S. and Vijayaraghavan R. 2006)

1.3 PROPERTIES

Hydroxyapatite ceramics are never toxic. Moreover these do not possess any inflammatory response or pyrogenetic response. HAP never leads on to fibrous tissue development between the placed insert and the host bone tissue. Hydroxyapatite has high bioactivity. Its non-toxicity is a major feature to promote its applications. Hydroxyapatite is approximately seventy percent by weight and fifty percent by volume as present in bones. Biological apatite is different from pure HAP. Variations are present in biological reactivity, Composition, Crystallinity, Solubility, Structure and other physical and mechanical properties.

Biological apatite is reported to be Calcium insufficient. It has low crystallinity and is generally carbonated. Approximately Carbonate amounts to 3-8% by weight of the hard tissues constituting human body. Besides Ca^{2+} and $PO_4^{3-,}$ Carbonate ($CO_3^{2-)}$ makes the major secondary ions weights in HAP that is to be used biologically However, HAP has tremendous intrinsic brittleness. It has poor mechanical properties. Such features restrict its approach in respective applications associated with load-bearing. [Susmita M.et. al.,2014]

Calcium hydroxyapatite is the most stable but the slightest dissolvable phosphate salt of calcium at pH more than 4.2. HAP powders possess relatively high thermal stability in highly alkaline media and also good phase purity at temperature ranging between 1100-1300^{0}C.It was analysed that synthesized HAP, with Calcium-Phosphorus ratio of 1.67, was stable at a temperature less than 1200^{0}C. It was seen that beyond 1200^{0}C, HAP gets deprived of hydroxyl groups and is modified to oxyapatite ($Ca_{10}(PO_4)6O$). At a temperature beyond 1450^{0}C, it further breaks down into trisodium phosphate, calcium pyroclore and tetracalcium phosphate. Pure HAP powder synthesized using pure water withstand temperature upto 1300^{0}C when heated up using dry air for a period of hours without getting decomposed. (Tas et al 1990).

Hydroxyapatite shows fast bone regeneration capability. It bonds directly with the bone of living host bone. Non connective tissue is required as an intermediate .It is versatile because of high biocompatibility & surface active properties, non-toxigenicity, non-inflammatory quality and also non-immunogenic behaviour.

Nano HAP stimulates proliferation of bony cells and their adhesion. Simultaneously it increases proliferation of bone on bioceramic material surface. It also reduces apoptotic cell death.

Main characteristics of Hydroxyapatite include ratio i.e., Ca/P, size of crystals, morphology, specific surface area, uniform distribution of particles, resorption and associated biological activity.

It has been reported as a better replacement in case of graded materials. It provides bioactivity and good mechanical properties. Its physicochemical properties especially solubility and crystallographic details are directly proportional to the mineralization processes in living systems.

1.4 PREPARATION

There are many methods to synthesize HAP. These include Wet Chemical Process, Deposition by Biomimetic means , Damp Chemical Precipitation, Electro-deposition, Spray Drying, Microemulsion,Hydrothermal Tfchnique, chemical Vapour Deposition,Co-precipitation and so on.

Two commonly used methods for the preparation of HAP. Chemical Methods including wet precipitation processes and hydrothermal technologies. Secondly Solid State Reaction Method: dry method. HAP is found to be sable thermodynamically at physiological pH, as well as osteoconductive. (Chaudhry et al., 2006).

Hydroxyapatite (HAP) nanocrystals have been synthesized by chemical precipitation technique. Advantages of chemical synthesis are simple equipment, lower cost, capability to produce HAP powder as nano particles , high scale production; associated elevated purity.

$$10\ Ca(OH)_2 + 6\ H_3PO_4 \rightarrow Ca_{10}(PO_4)_6(OH)_2 + 18\ H_2O.$$

The best method for synthesis of HAP remains sonication followed by precipitation.[Anjuvan S. et. al.,]

1.5 Preparation modifications

A more recent approach to developing porous, ceramic fibers is by use of electrospinning. In this case, the inorganic solution (precursor to the ceramic) is mixed with a polymer solution followed by electrospinning at voltage of 10 to 30 kV(Defne Bayraktar et al 1999). Some methods need high temperature for processing. The raw material is costly and the process is complex. Interaction of antimicrobials with HAP powder prepared by chemical method which is precipitation based has been studied. The respective zones of inhibition produced there of are to be analysed.

TiO_2 have been studied for inhibiting growth of bacteria. Hence, HAP and TiO_2 mixture is used to form composite material that can decompose organic materials and kill bacteria. It is good for antibacterial applications and decomposition of the biomaterials photocatalytically, like proteins and lipids. In the biomedical field, many implantation failures are due to creation of microbes at implanted sites. If implant materials possess the aptitude of antimicrobial movement within those, then problem of failure goes reduced.Also, microorganisms causing wide variety of human infections;also animal diseases spread through universal places as door - knobs, bath - room tiles and space filler materials.Prevention can be done by the antimicrobial coatings. Present work is focused primarily on the biocompatibility as well as antimicrobial activity of the hydroxyapatite.

1.6 Nanostructure Confirmation

The structural analysis is performed order to check the composition, morphology and structural parameters. Analysis is done by using FTIR, XRD, SEM , TEM techniques.

1.7 Antimicrobial Activity

The antimicrobial efficacy is accessed by Well-Diffusion Method as well as Disk (Pellet) Diffusion method against pathogenic bacteria such as Escherichia coli and Staphylococcus species like aureus.{Baur et.al.,1966)

1.8 Human Skeleton and HAP

Our human skeleton is made up of around 206 bones. Bones not only provide strength to our body but also us to walk. One of the longest bone which is present in our body is called femur i.e. also known as thigh bone. Whereas our smallest bone is present in the ear and named as

step bone. Even our hand consists of 26 bones. In Our body, only ear and nose are the organs which are made up flexible material called cartilage, and is not hard like bone. Bones are interconnected to each other by joints. There are several types of joints, comprises of stagnant joints (which is found in skull, and comprises of many bones), pivoted joints (which are found in the fingers as well as toes), and other type of joint is ball-and-socket (which are found in the shoulders and hips). Bones is made up of calcium and helps in manufacturing of blood cells as well as also help in storing important minerals. Organs such as kidney, liver and muscle the bones are also made up of living tissue which interacts with their own environment. While responding to a stimulus two basic course of action take place.

Bone modelling is generally done in small children or adolescents so that bone growth can take place in length as well as in cross-sectional area. The development of bones by the aggregation of material onto endosteum or periosteum region which facilitate in the modelling process, and can occur for lifetime. Bone remodeling generally includes removal or replacement of bone. Thus, it facilitates us for the continuous recycling of the bones whereas healthy tissue stay away from micro-cracks that may lead to fatigue seizure of that structure. This type of process is commonly seen during the healing process of fracture.

Hydroxyapatite (HAP) is an artificial biomaterial which is commercially used in repairing of bone tissue. HAP, general formula is $Ca_{10}(PO_4)_6(OH)_2$, that is primarily made up of Ca and phosphorous interrelated by hydroxide ions which gets eliminated at high temperature. HAP among the other Ca/P minerals have been extensively employed as material for implant from long time since it has exceptional biocompatibility and adhesiveness because of its structural as well as the similarity in the composition with the mineral phase material of the hard tissue which is present in the human bones. HAP coatings have virtuous ability thus can employed due to its biocompatibility assisted with bone bonding capability similar to that of the ceramic, whereas additionally using the mechanical properties of other substrates like Ti6-Al4-V and various other alloys that are biocompatible. These metallic materials which are used with HAP not only contributes in the mechanical properties, but they also provide the osteoconductive surface for the accumulation of the material for the bone growth, implant anchoring and relocating burden over the skeleton, additionally also help in combatting during atrophy of the bone.

Ratio of Ca/P ratio is around 1.52±2.0 that makes it an exceptional choice among the dentist and orthopedic as it has useful application as it can be used as a bio-ceramic coating. The prominence of a coating is largely reliant on its by and large qualities and features of powder which has been synthesized. Thus, attributes consist of phase composition, clarity, crystallinity, particle size and its distribution, and surface area of the particle, density of the particle and morphology of the particle. These important features that determines the success rate of HAP coating aggregated onto implanted teeth with the plasma thermal spraying. The chemical quality of HAP, however, contributes itself as a substitution, which means that synthesis of nonstoichiometric HAP is there. The most usual substitutions are CO_3^{-2}, F^- and Cl^- that replace the hydroxyl groups, whereas deficiency in HAP causes the developing of certain defects.

The reason for selecting the HAP because of its versatile nature and properties. It shows excellent biocompatibility and surface active ability. It has non-toxic nature, non-inflammatory behavior, non-immunogenic response. It is analogous to mineral constituent of innate bone; also it promotes regeneration of bones at targeted site.

. A relatively rare form of apatite carrying numerous carbonate and acid phosphate substitutions, but minimal or nil hydroxyl groups, is a large component of animal bone material .Hydroxyapatite has a chemical formation as $Ca_{10}(PO_4)_6(OH)_2$.

Antimicrobial substance is one that is capable of capable of inhibiting or killing disease-causing microorganisms.

There is a huge list of antibiotics that are antimicrobial like Ampicillin, Gentamycin, Ciprofloxacin and so on. Apart from antibiotics there are many herbal antimicrobials. These include various spices and herbs like cloves, cinnamon mustard, black pepper, red pepper, ginger etc. Spices / herbs are being used ever since ancient age. People understood the use of spices - herbs to preserve foods and even learnt their medicinal utility. Scientists also acknowledged the antimicrobial qualities of some spices / herbs; their sub constituents as well. Cinnamon, cloves and mustard possess strong antimicrobial efficacy. Whereas coriander and cumin have medium degree of activity; but black pepper, red pepper and ginger are weak antimicrobials.

Studies conducted in the past decade have proved that growth of various foodborne bacteria and fungi can be prevented by cloves, cinnamon, sage, onion, and other spices. For any food,

its water content along with fat, protein, and salt components influences the microbial resistance. Spices / herbs help in preserving pickles and eatables.

The normal amount of spices added to foods for flavor cannot completely prevent microbial growth. Antimicrobial effectivity is highly variable. It depends on kind of spice or herb, medium used for testing, and variety of the microorganism concerned. Addition of spices aids to preserve eatables at low temperature i.e., refrigeration temperature, at which division of microorganisms is at low rate.

DONE HERE

Chapter 2

Terminology

H AP	Hydroxyapatite
FTIR	Fourier Transform Infrared Spectroscopy
XRD	X-ray diffraction
SEM	Scanning Electron Microscopy
TEM	Transmission Electron Microscopy
E.coli	Escherichia coli
S.aureus	Staphylococcus aureus

Chapter 3

Review Of Literature

[Mohandes,F.1,M.et.al.2013] There are many derivates of calcium phosphate.These are as follows: Monocalcium phosphate with Calcium / Phosphorus =0.5 as molar ratio. Molar ratio is 1.0 (Ca/P) in case of dicalcium phosphate ; and that in case of calcium pyrophosphate with formula as $Ca_2P_2O_7$ is 1.13. Tricalcium phosphate has been formulated as $[Ca_3(PO_4)_2]$. Ca/P = 1.5 represents its molar ratio. Tetracalcium phosphate formulated $[Ca_4(PO4)_2]$ and with molar ratio of 2.0 i.e., Ca/P. Hydroxyapatite has a molar ratio of 1.67) i.e. Ca/P. $(Ca_{10}(PO_4)_6(OH)_2$ is chemical formula of hydroxyapatite. Among all these members, hydroxyapatite is one of the most effective salts as far as clinical applications are concerned. HAP is known for its excellent biocompatibility. It has such surface active properties that make it compatible with the living tissues.

[Maisara S.et.al., 2011] Hydroxyapatite (HAP) was set up by co-precipitation method usingcalcium chloride using phosphoric corrosive but β- TCP has readied utilizing ammonium as hydrogen phosphate salt along with $CaCl_2$ (calcium chloride).Wet powders obtained through both these arrangements had been centrifuged followed by sonication. Then the samples were autoclaved. Finally these were calcinated to produce the desired nanoparticles. They were analyzed by FTIR, XRD and SEM. Sintered as well as green circles of both examples were likewise arranged. Hydroxyapatite nanoparticles which were bar shaped structures had measurements amounting to 65±1.0 nanometers (nm) for length; and 25±1.0 nanometers (nm) for width but β-TCP had bigger size having measurement for length equal to 200±10 nanometers (nm) and that for width evaluating to 100±10 nanometers (nm).Hardness of the sintered hydroxyapatite circle had been observed to be more as compared to that of β-TCP in sintered form.

[Eslami et. al., 2008] Diammonium as hydrogen phosphate, also calcium nitrate in 4-hydrate were taken as initial gradients. Sodium hydroxide (NaOH) solution was utilized to adjust pH of the product. Accordingly, it was seen that hydroxyapatite in form of nanocrystals can be produced by processing wet precipitation mode. Bulk synthesized hydroxyapatite was processed to determine Ca/P molar ratio which was determined to be 1.71.It was found out to be more than stoichiometric ratio with a value of 1.667.Such a ratio difference is expected as it signifies HAP in pure phase.

[Ciobanu,C.et.al.,[2013] Ag: HAP nanoparticles are obtained by an inexpensive
Technology. These nanoparticles work to protect from macrophages. These also take care against cytotoxicity. Their activity is to be monitored to get rid of unwanted immune responses in the human body. So optimization of doses is essential.

[Senthilarasan K. et al 2014] Nano HAP-Agar composite was synthesized by a modified wet chemical method. FTIR conforms various functional groups including (-OH), ester group and

phosphate group. XRD patterns reveal its compositeness. TEM image visualizes HAP and size of the prepared nano composite varying from 20-100 nm. The developed Agar/nHAP composite may have applications as a biocomposite, for drug delivery and bone tissue reconstruction.

[Núria C et.al., 1975]In field of cell biology, TEM (transmission electron microscopy) is an important tool of different types of microscopies exploited till date, electron microscopy remains the most advantageous technique and therefore it to decipher the cell architecture as well as its functional capability.

[Nery et al., 1975] For the first time in dentistry, the effect of tricalcium phosphate reagent in intrabony defects in dogs was studied, but later it was demonstrated that it was a mixture of hydroxyapatite and tricalcium phosphate.

[Anita L. J. 2015]It is notable that the aqueous temperature assumes a key part in the controlling the crystallite estimate, level of crystallinity and the stoichiometric proportion Be that as it may, the got powders were exceptionally agglomerated and their estimate circulation is similarly vast. Subsequently surfactant helped course is best used to incorporate nanopowders, nanorods and Along these lines, hydrothermal union utilizing a cationic surfactant Cetyl Trimethyl ammonium bromide (CTAB) as delicate format can adequately control the morphology as well as it has an impact on the synthesis, crystallite size and stoichiometry of hydroxyapatite particles is explored. HPA is porous ceramic as required for the particular applications.

[Binnaz, H.Y. Yeliz, K. 2009] The impact of three diverse mixing methods attractive, ultrasonic and two fold stage blending on properties of HAP was researched. The utilized precipitation procedures were reasonable to generate HAP powders in nano form. Test interpretation accomplished by XRD, FTIR and SEM.

[Mukherjeea, S. et all 2013] The vast majority of the – earthenware production require the utilization of exactness techniques. In the present work, we received an option and savvy shear blending system to get ready CNT–HAP composites with various extents of perfect CNT particles and examined the impact of the fortification on the physical, mechanical, biological and invitro bioactivity properties of HAP.

[Zhou W. et al2008] The nanoemulsion procedure was assessed to incorporate carbonated hydroxyapatite (CHAP) nanospheres which could be utilized to create composite tissue designing frameworks. CHAP nanospheres were effectively incorporated by blending a CH3)2CO arrangement of $Ca(NO3)_2$ _ $4H_2O$ with a watery arrangement of $(NH4)_2HPO_4$ and NH_4HCO_3. Wet slurries of CHAP from the nanoemulsions were dried to powder form. X-Ray Diffraction (XRD) demonstrated that the integrated CHAP nanoparticles were mostly in a formless state. Following calcination at 900 ^{0}C, the apatite turned out to be very much solidified.

[Jamarun,N.et al 2016] Limestone (calcium carbonate) was made to converted to calcium oxide, a precursor in hydroxyapatite synthesis. The source of phosphate was from orthophosphoric acid [H_3PO_4]. Also diammonium hydrogen phosphate [$(NH_4)_2HPO_4$] and NH_3 were used. Synthesized samples had characterized done by XRD, FTIR and SEM.

[Kumar, G.S. et.al., 2015] All in all, HAP in form of nanorods has been effectively incorporated by using snail shells to provide calcium and by means of simple microwave light technique in quick way utilizing EDTA as a chelating operator. The acquired item was identified to be a B type of carbonated HAP having hexagonal structure. The arrangement of nanorods was anisotropic with development of propensity for HAP crystallites on exposure to microwave light. Subsequently, there could be novel prospects for improvement of various biomaterials to be applied in orthopedics field. The nanorods formation is subject to the growth of HAP crystallites in anisotropic manner on exposure to microwave irradiation. Consequently there can be numerous prospects in the orthopedical biomaterial applications.

[Craig D.et.al., 1998] BoneSource^{TM}-hydroxyapatite concrete is another calcium phosphate concrete biomaterial. It is self-setting. It has exceptional biocompatibility and physical properties. So it is used in r craniofacial skeletal recreation. The general properties were investigated.

[Fabbri, M. et.al., 1995] At the demand of restorative groups from the maxillofacial part, an exceedingly permeable artistic bolster based. HAP powder was produced by reacting $(NH_4)_2HP0_4$ and $CaCl_2$ .This led to enhanced refinement in particle size, its distribution, and agglomeration. XRD showed pure crystalline HAP on calcinations at 800°C. Whereas conventionally prepared HAP after calcination temperatures up to l200°C, showed impurities like CaO. Therefore microemulsion process is more beneficial to provide a homogeneous powder than conventional process.

[Lopez, M.A.et.al.,1998] The mixing procedure determines the final stoichiometry of the precipitated HAP particles with controlled stoichiometry were precipitated from solution by forced hydrolysis. Solution was mixture of calcium and phosphate salts. HAP produced had narrow size with some aggregation traced using light scattering. The Ca/P ratio was found to depend on the specific preparation route.

[Mansour1,S.et.al.,2016] Using co-precipitation method HAP; and also dicalcium phosphate dihydrate were produced. These nano particles were subjected to XRD, FTIR, SEM &TEM. The morphology and microstructure were studied. Depending on pH values HAP had needle as well as rice like shape.

[Kapoor, S. et al 2012] HAP was produced by Sol-Gel performance. Tetrahydrate salt of $CaNO_3$ and dihydrogen phosphate of the metal potassium were utilized to produce calcium and phosphorus respectively.Point by point contemplate on its change amid calcination at

different temperatures was attempted. Blended nanoparticles were calcined at 600^0C and 800°C. The outcomes uncovered the gotten powders as hydroxyapatite.

[Mishra V. et al 2016] Techniques used to study HAP distinctives include: X-RD, SEM, TEM, Raman Spectroscopy, [LIBS] Laser Induced Breakdown Spectroscopy. The morphology of HAP can be varied by varying pH of the solution. The needle like structure change to flower like structure on performing SEM. At pH above 10 followed by calcination the structures at microscopic level are more dense & homogeneous than at pH below 10. EDTA acts as a capping or chelating agent. It helps to prevent agglomeration of particles. Other parameters include initial ingredients, physical & chemical conditions, Calcination temperature, Microwave Power, doping with a non-reacting metal. These lead to variation in the structure, shape, size as well as bonding pattern of HAP crystal. Also effects optical distinctives.

At pH 9 peaks of X-RD Sample were obtained between 25-30 & 50-60. These disappear as pH is increased to 11 or 13. X-Ray peaks change due to: change in lattice parameter, residual stress or impurity element, defect concentration.
SEM Sample after undergoing calcination at 600^0C shows similar surface morphology (needle like Structure). But this is drastically changed on heating at 900^0C (Changes to capsule like structure). This deals with the synthesis of HAP using Calcium Nitrate & Diammonium Hydrogen ortho phosphate. Further the precipitated was made dry & washed .The chemical analysis of powders are carried out by atomic absorption spectroscopy, trimetry, gravimetry, spectrophotometry, FTIR, XRD , SEM .

[Kapoor, S. et al 2012] HAP in nano form has been produced using sol-gel methodology. Potassium dihydrogen phosphate as well as calcium nitrate tetrahydrate were used as forerunners for phosphorus in addition to Ca respectively. Change in the midst of calcination carried out at two different basic temperatures was endeavored.Mixed powder was calcined at 600^0C furthermore also at 800^0C for dissimilar periods.The results revealed that the gotten powders in the wake of calcining at 600^0C and 800^0C are definitely hydroxyapatite.

[Mohandes,F.1,M.et.al.2013] There are many derivates of calcium phosphate.These are as follows: Monocalcium phosphate has 0.5 as molar ratio. Molar ratio (Ca/P) is one for dicalcium phosphate:. Calcium pyrophosphate has molar ratio of Ca/P = 1.13); it has formula as Ca2P2O7. Tricalcium phosphate has been formulated as [Ca3(PO4)2]. Ca/P = 1.5 represents its molar ratio. Tetracalcium phosphate formulated [$Ca_4(PO_4)_2$] and with molar ratio of 2.0 i.e., Ca/P. Hydroxyapatite has a molar ratio of 1.67) i.e. Ca/P. ($Ca_{10}(PO_4)_6(OH)_2$ is chemical formula of hydroxyapatite. Among all these members, hydroxyapatite is one of the most effective salts as far as clinical applications are concerned. HAP is known for its excellent biocompatibility. It has such surface active properties that make it compatible with the living tissues.

[Werner E.G.et al.,2016] There is very high prevalence of dental hypersensitivity in many regions of the world. Treatment of such disorder is too costly. Rarely it may show a are very life threatening outcome. Using, By fabrication of natural polymer i.e., polyphosphate, microparticles in amorphous form were prepared.These were used to treat the hypersensitivity.It is done by resealing the dentinal tubules that got exposed.

[Yukai S et.al.,2013] Surface-modification of HAP was done by the addition of beta alanine. A inorganic-organic composite was prepared successfully.During the progression of HAP

modifications, morphology got changed from rod to sheet and next distorted from flakes towards needles. The principal amino-terminated hydroxyapatite is an outstanding originator for polymerization through ring-opening of amino acid named as N-carboxyanhydride, which could even be dissolved in a solution of chloroform.

[Frayssinet et al 1998]Over the last few decades, bone substitutes have been used for human surgery enormously. Such materials have been used to guide as well as to expand the healing of bone tissue and thereby to get integrated within that. It resembles remodeling process in the actual bone. Hydroxyapatite rods were rapidly produceded by a continuous hydrothermal three pump mechanism utilising a water feed. The product obtained was highly crystalline and found to be a phase pure material.

[Ciobanu,C.et.al.,2013] Ag: HAP nanoparticles are obtained by an inexpensive technology. These nanoparticles work to protect from macrophages. These also take care against cytotoxicity. Their activity is to be monitored to get rid of unwanted immune responses in the human body. So optimization of doses is essential.

[Mohammad,N.F.et.al.,2014] Common methods used in the preparation of mesoporous hydroxyapatite (HAP) have been discussed. Surfactants (ionic or nonionic) were used as pore template. Wet precipitation methods are used. These included chemical precipitation, hydrothermal as well as emulsion techniques. Mesoporous HAP nanoparticles were found to be useful because these have sustained release properties.

[Raizda, P. et.al. 2016] The photo-catalytic effectiveness of BiOCl/HA nanocomposites was assessed for the debasement of OTC. Sun based photo-catalytic debasement was less expensive and less complex strategy for the expulsion of OTC using BiOCl/HA (Bismuth Oxychloride Hydroxyapatite). Concurrent adsorption and catalysis process was very productive for OTC expulsion. The debasement of OTC is ideal at pH 5. The rate of response was maximal at 60 mg/50 ml of BiOCl/HA stacking and1.0 x 10-3 M of OTC fixation. The rate consistent had maximal esteem at ideal grouping of H2O2 (1 x 10-3 mol dm-3). The blend of H2O2 and BiOCl/HA under sunlight based light was observed to be productive for the corruption of OTC.

[Nery et al., 1975] In dentistry, the effect of tricalcium phosphate reagent on intra-bony defects present in dogs was studied.Afterwards it was demonstrated that actually it was a mixture of hydroxyapatite and tricalcium phosphate.

[J. Anita Lett 2015] It is notable that the aqueous temperature assumes a key part in the controlling the level of crystallinity and the stoichiometric proportion.The got powders were exceptionally agglomerated and their estimate circulation is similarly vast. Subsequently surfactant helped course is best used to incorporate nanopowders, nanorods and Along these lines, hydrothermal union utilizing a cationic surfactant Cetyl Trimethyl Ammonium Bromide (CTAB) as delicate format can adequately control the morphology as well as it has an impact on the synthesis, crystallite size and stoichiometry of hydroxyapatite particles is explored. HPA is porous ceramic as required for the particular applications. However, in recent years, nano sized hydroxyapatite (nHAP).

[Eslami, H. et al. 2010] Bioactivity of HAP materials depends on many factors during process of synthesis. These include reagents used, impurities present, size of crystals with morphology status, concentration of reagents with their mixture order, temperature of procedure and pH value.

[Dorozhkin, S. V. 2010] Late improvements in biomineralization have officially shown that HAP particles assume a vital part in development of hard tissues of creatures i. e., bones and teeth. Likewise, the structures of both dental lacquer and bones can be mirrored by a situated conglomeration of nanosized calcium orthophosphates, dictated by the biomolecules. The application and imminent utilization of dimensional and crystalline calcium orthophosphates for a clinical repair of harmed bones and teeth are likewise known. For instance, a more noteworthy suitability and a superior multiplication of different sorts of cells were distinguished on littler precious stones of calcium orthophosphates. Along these lines, the dimensional and crystalline kinds of Ca orthophosphates have an incredible potential to reform the field of hard tissue designing beginning from bone repair and enlargement to the restricted medication conveyance gadgets. This paper surveys recent condition of information and late advancements of this subject beginning from the blend and portrayal to biological applications. More to the point, this survey gives conceivable headings of future innovative work.

[Suresh Kumar G.et.al., 2015] All in all, HAP in form of nanorods has been effectively incorporated by using snail shells to provide calcium and by means of simple microwave light technique in quick way utilizing EDTA as a chelating operator. The acquired item was identified to be B type of carbonated HAP with hexagonal structure. The arrangement of nanorods was expected to the anisotropic with development of propensity for HAP crystallites on exposure to microwave light. Subsequently, there could be novel prospects for improvement of various biological materials to be applied in orthopedics field. The nanorods development is subject to growth of HAP crystals in anisotropic manner on exposure to irradiation using a microwave.Consequently there could be numerous set-ups in the orthopedical biomaterial applications.

[Craig D.et.al., 1998] BoneSourceTM-hydroxyapatite concrete is another calcium phosphate concrete biomaterial. It is self-setting. It has exceptional biocompatibility and physical properties. So it is used in r craniofacial skeletal recreation. The general properties were investigated.

[Cristina & Julian 2003)] Hydroxyapatite suspension was extruded utilising a range of nozzles with diameter ranging between 100 nanometres and 330 nanometres from a driven syringe. standard latticework scaffolding was done by merged deposition.Hydroxyapatite suspensions were expelled through a scope of spouts with similar dimensions using a syringe. General latticework platforming was done by melded statement displaying a strong free forming technique, on a three-pivot table utilizing 330 nanometre width fiber. The platforming was acquainted with refined human being osteoblasts.Following a period of 48 hours, the surfaces were completely secured with dynamic cells.Then on culturing on to human osteoblast cells for a period of 48 hours, the surfaces were completely covered with dynamic cells.

[Lopez,M. et.al., 1998] The mixing procedure determines the final stoichiometry of precipitated HAP [Ca10(PO4)6(OH)2; or HAP] particles with controlled stoichiometry were precipitated from solution by forced hydrolysis. Solution was mixture of calcium and phosphate salts. HAP having narrow size distribution was formed;although there was some aggregation traced by light scattering. The Ca/P ratio was found to depend on the specific preparation route.

CALCINATION

[Toropkov et al.2016] It was found that the items blended essentially comprise of hydroxyapatite. The conditions for acquiring a nanocrystalline item (20-27 nm) with a HA part of 70 to 90 wt.% were resolved. Depleting antecedents at a temperature near the breaking point gives dynamic convection, uniform conveyance of the reagents in the mass that quickens the union. It is desirable over keep the precipitation in the mother alcohol over a day and up to two weeks to expand the substance of nanocrystalline stage. Assist calcination the item is not sensible as a result of the low vitality proficiency of the procedure.
It is demonstrated that the underlying state and the technique for the warming forerunner impact irrelevantly on the crystallinity, Ca/P proportion and the substance of the nanocrystalline stage.

[Fabbri, M. et.al.,1995] At the demand of restorative groups from the maxillofacial part, an exceedingly permeable artistic bolster based HAP as a powder prepared by directly reacting (NH4)2HP04 solution and CaCl2 solution.This microemulsion led to a momentous sophistication in the particles' dimension as well as their agglomeration. XRD investigation conveyed towering purity. Crystals appeared on calcination to 800°C.

FTIR, SEM, TEM, XRD

[Mishra V. et al 2016] Techniques used to study HAP characteristics include: X-RD, SEM, TEM, Raman Spectroscopy, [LIBS] Laser Induced Breakdown Spectroscopy. The morphology of HAP can be varied by varying pH of the solution. The needle like structure change to flower like structure on performing SEM. At pH above 10 followed by calcination the structures at microscopic level are more dense & homogeneous than at pH below 10. EDTA acts as a capping or chelating agent. It helps to prevent agglomeration of particles. Other parameters include initial ingredients, physical & chemical conditions, Calcination temperature, Microwave Power, doping with a non-reacting metal. These lead to variation in the structure, shape, size, morphology and bonding pattern of HAP crystal. Also effects optical characteristics.
At pH 9 peaks of X-RD Sample were obtained between 25-30 & 50-60. These disappears pH is increased to 11 or 13 X-Ray Peaks change due to: change in lattice parameter, residual stress or impurity element, defect concentration.
SEM Sample after undergoing calcination at 600^0C shows similar surface morphology (needle like Structure). But this is drastically changed on heating at 900^0C (Changes to capsule like structure). This deals with the synthesis of HAP using Calcium Nitrate & Diammonium Hydrogen ortho phosphate. Further the precipitated was made dry & washed .The chemical analysis of powders are carried out by atomic absorption spectroscopy, trimetry, gravimetry, spectrophotometry, FTIR, XRD , SEM . THE Ca : P ratio was assessed as 1.65

[Chaudhry et al., 2006] XRD procedure was performed. Distinctive peaks of HAP were revealed. Impurities as per peaks were not present in any sample.SEM(scanning electron microscopy) results suggested that samples' surface morphology was not altered due to doping components. There was homogeneousness for all the prepared samples. According to this study, hydroxyapatite can be synthesized avoiding ageing step followed by heat treatment.

[Ohta, k. et. al., 2013] Spindle-shaped, (20-50nm) nano-HAP particles were prepared of the Dentine surface treated with nano-HAP on FE-SEM procedure indicated that there was uniform

occlusion of dentinal tubules. There was formation of dentinal plug which was formed along protective layer laid on surface of dentine. As such nano-HAP is an effective agent for occluding dentinal tubules.

[Sridhara et. al., 2010] TEM means Transmission Electron Microscopy and it is a basic tool to investigate microstructure of HAP. It provides crystallographic information along with nanometeric scale composition.
Specimen preparation includes thinning of the sample up to the extent of electron transparent thickness which could result in formation of artifacts and those could be briefly reported.

[Senthilarasan, K. et al 2014] Nano HAP-Agar composite was synthesized by a modified wet chemical method. FTIR conforms various functional groups including (-OH), ester group and phosphate group. XRD patterns reveal its compositeness. TEM image visualizes HAP and size of the prepared nano composite varying from 20-100 nm. The developed Agar/nHAP composite may have applications as a biocomposite, for drug delivery and bone tissue reconstruction. Nano- Batch hydrothermal syntheses of HAP in a normal manner yields crystalline HAP rods that are usually agglomerated. No organic templating agents were used. But basic solutions of calcium nitrate and ammonium phosphate were used in a mixer.
[Maisara S.et.al., 2011] Hydroxyapatite (HAP) was set up by co-precipitation method using calcium chloride and phosphoric corrosive but β- TCP has readied utilizing ammonium as hydrogen phosphate salt along with CaCl2 (calcium chloride).Wet powders obtained through both these arrangements had been centrifuged followed by sonication. Then the samples were autoclaved. Finally these were calcinated to produce the desired nanoparticles. They were analyzed by FTIR, XRD and SEM. Sintered as well as green circles of both examples were likewise arranged. Hydroxyapatite nanoparticles which were bar shaped structures had measurements.Amounting to 65±1.0 nanometers (nm) for length; and 25±1.0 nanometers (nm) for width but β-TCP had bigger size having measurement for length equal to 200±10 nanometers (nm) and that for width evaluating to 100±10 nanometers (nm).Hardness of the sintered hydroxyapatite circle had been observed to be more as compared to that of β-TCP in sintered form.

[Binnaz H Y, Yeliz K 2009] The impact of three diverse mixing methods attractive, ultrasonic and two fold stage blending on properties of HAP was researched. The utilized precipitation procedures were observed to be reasonable for the generation of HAP powders.Finally FTIR, XRD and SEM were done for final analysis.

[Jamarun N. et al 2016] Limestone (calcium carbonate) was made to converted to calcium oxide, a precursor in hydroxyapatite synthesis. The source of phosphate was from orthophosphoric acid [H3PO4].Also diammonium hydrogen phosphate [(NH4)2HPO4] and ammonia (NH3 were used). Synthesized samples had characterized done by Fourier Transform Infrared method, X-ray Difraction etc.

[Ohta, k. et al 2013] Spindle-shaped, (20-50nm) nano-HAP particles were prepared of the dentine surface treated with nano-HAP on FE-SEM procedure indicated that there was uniform occlusion of dentinal tubules. There was formation of dentinal plug which was formed along protective layer laid on surface of dentine. As such nano-HAP is an effective agent for occluding dentinal tubules.

[Zakaria, S. M. et. al. 2013] HAP is bio-compatible substance which is utilized as a part of substitution and recovery of bone material. In nature, HAP is fundamental part display in tough body tissues. Henceforth, the best in class in nanotechnology can be abused to coordinate nanophase HAP that has comparable properties with regular HAP. Feasible strategies to mass-deliver engineered HAP nanoparticles are being produced to take care of the expanding demand for these materials and to additionally build up the advance made in hard tissue recovery, particularly for bones and teeth defects. This article surveys the present improvements in nanophase HAP through different assembling strategies and changes.

[Sridhara et al 2010] TEM means Transmission Electron Microscopy and it is a basic tool to investigate microstructure of HAP. It provides crystallographic information along with nanometeric scale composition.Specimen preparation includes thinning of the sample up to the extent of electron transparent thickness which could result in formation of artifacts and those could be briefly reported.

[Martínez-Castañón et.al,2012] Hydroxyapatite nanostructured powder was set up with various crystallinity degrees, gem measures and morphologies utilizing a straightforward watery precipitation technique differing as per pH and temperature parameters.It was found that at higher pH values the precious stone size develops and crystallinity was enhanced; at higher temperatures there is additionally a gem estimate development and crystallinity enhancing however this change is more huge, an adjustment in the morphology of the nanopowders was likewise watched. Utilizing XRD examples and Rietveld examination it was found that the precious stone size changes from 9.15 to 26.4 nm. The readied powders are exceedingly agglomerated with a pseudo-round and bar like morphology.The prepared powders are highly agglomerated with a pseudo-spherical and rod-like morphology .

[Salimi and Anuar, 2012] The most widely recognized quality vectors utilized were infection based viruses.But non-viral vectors are better because of greaer biocompatibility. The HAP particles got made by the sol-gel technique.Various temperatures (20^{o}C, 30^{o}C or 40^{o}C) and the mixing rates (200 rpm, 400 rpm or 600 rpm) were used.The analysers were FTIR for distinguishing useful gatherings followed by XRD for stage structure. It was assessed that at lower temperature tiny molecule were framed.It was other way round for mixing rates.

[Chaudhry et al., 2006] XRD procedure was performed. distinguishing peaks of HAP got revealed. Impurities as per peaks were not present in any sample.SEM(scanning electron microscopy) results suggested that samples' surface morphology was not altered due to doping components. There was homogeneousness for all the prepared samples. Presence of calcium, phosphorous oxygen and silver in Ag: HAP compound was two analyses i.e., by EDAX and by XPS without So subsequent heat treatment is not valuable at all.

[Zhou, W. et. al. 2008] The nanoemulsion procedure was assessed to incorporate carbonated hydroxyapatite (CHAP) nanospheres which could be utilized to create composite tissue designing frameworks. CHAP nanospheres were effectively incorporated by blending Ca(NO3)2 _ 4H2O with a watery arrangement of $(NH_4)2HPO_4$ and NH_4HCO_3. Wet slurries of CHAP from the nanoemulsions were dried to powder form. X-Ray Diffraction (XRD).
(XRD) demonstrated that the integrated CHAP nanoparticles were mostly in a formless state. Following calcination at 900 0C, the apatite turned out to be very much solidified.

[Ragab, H. S. et. al. 2014] HAP nano - particles were manufactured by precipitation route by means of calcium hydroxide, phosphoric acid as phosphorus (P) and calcium (Ca) precursors and sodium hydroxide (NaOH). Its crystal configuration was subjected to analysis by XRD, FTIR, EDS and TEM. Additionally, HAP nanoparticles were subjected to various kinds of bacteria to assess its action. Results indicated its exceptional wide spectrum doings. Therefore it be applied in medical field..

[Jadalannagari S. et al 2013].Silver doped HAP was synthesized at 1000^{o}C. XRD showed that the particles were fully crystalline. These had hexagonal structure and size of 25 nm. These showed good activity against microbes.

[Marcos D. et al 2009] Ag-HAP composite in nano form was made by colloidal procedure chemically and then subjected to heating by 350 0 C. This was analysed by TEM, XRD and spectroscopy. The effectiveness against bacteria was assessed. The outcome showed high antimicrobial activity against Staphylococcus aureus, Pneumococcus and E.coli. Hence it is a promising antimicrobial biomaterial which can be employed for implants in human body.

[Werner E.G.et,al.,2016**]** There is very high prevalence of dental hypersensitivity in many regions of the world. Treatment of such disorder is too costly. Rarely it may show a are very life threatening outcome. By fabrication of natural polymer i.e., polyphosphate, microparticles in amorphous form were prepared. These were used to treat the hypersensitivity. I t is done by resealing the dentinal tubules that got exposed .

[Yukai S et.al.,2013] Surface-modification of HAP was done by the addition of beta alanine. An inorganic-organic composite was prepared successfully. During the process of modification of HAP, the morphology got altered. Rods and flakes changed to sheets and needles respectively. HAP, which was amino-terminated, was found out to be a good initiator of polymerization of N-carboxyanhydride amino acid .

[Frayssinet et al 1998] Over the last few decades, bone substitutes have been used for human surgery enormously. Such materials have been used to guide as well as to expand the healing of bone tissue and thereby to get integrated within that. It resembles remodeling process in the actual bone. Hydroxyapatite rods were rapidly produceded by a continuous hydrothermal three pump mechanism utilising a water feed. The product obtained was extremely crystalline plus a pure material.

[Mohammad N.F.et.al.,2014] Common methods used in the preparation of mesoporous hydroxyapatite (HAP) have been discussed. Surfactants (ionic or nonionic) were used as pore template. Wet precipitation methods are used. These included chemical precipitation, hydrothermal as well as emulsion techniques. Mesoporous HAP nanoparticles were found to be useful because these have sustained release properties.

[Nzeako, B. C. et. al] Oil of thyme is used as a flavor enhancer in a wide range of refreshments, candy store items and in perfumery for the scenting of cleansers and lotions. It has sterile, bronchiolytic, antispasmodic and antimicrobial properties that make it prominent as a restorative herb and as an additive for foods. Clove, whose scientific name is Syzygium

aromaticum, is a plant generally developed in Spice Islands, Indonesia, Pemba and Zanzibar. However prior creation of the plant was in China. Like thyme, it is utilized as a part of the flavoring of food. Its antimicrobial activity is on bacteria and some fungi. The antimicrobial action of clove is inferable from eugenol, oleic acids and lipids found in its basic oils.

[Sofia P. K. et al 2006] Evaluation of the activity of spices-extracts,like clove, mustard, garlic etc. was conducted against bacteria. These are in use in traditional medicines. The antimicrobial activity of these was assessed against against Escherichia coli / Bacillus cereus / Staphylococcus aureus. Antimicrobial testing was done by paper disc method.Clove, cinnamon and mustard showed good inhibition, while garlic exhibited moderate activity. Ginger and mint possessed minute antibacterial activity.

[Pandey B. et al 2013] In the present review, the antimicrobial movement of flavors has been researched as another option to anti-toxins keeping in mind the end goal to handle these risks. Looking for bioactive compound, methanol concentrate of 5 Indian flavors were screened for antibacterial property. The antibacterial action of five normal Indian flavors specifically clove, ajwain, turmeric, dalchini and dark pepper against two microscopic organisms The outcomes uncovered that the methanol concentrates had high antimicrobial effect on the microbes . These flavors contain high measure of optional metabolites and because of these metabolites they have high antimicrobial movement and it can be utilized as great bio-preservater and it can likewise used for restorative **reason.**

[Yujie C. et al 2014] The antimicrobial effectiveness of vanillin, turmeric and curcumin on. Staphylococcus aureus, Listeria monocytogenes Shigella sonnei, Salmonella typhimurium and Escherichia coli has been assessed. Turmeric exhibited promising antimicrobial efficacy.

[Jirawan O. et al 2006] The spices of Zingiberaceae family were evaluated for antimicrobial activity. Their ethanol extracts were taken. The substances included galangal, ginger, turmeric and krachai. The microbes utilized in the study included Staphylococcus aureus and Escherichia coli. Galangal extract exhibited the highest consequence on Staph. aureus i.e., inhibited it to the maximum.TEM verified that galangal extract damaged outer and inner membranes and also led to cytoplasm coagulation.

Chapter 4
Rationale And
Scope Of Study

4.1 Scope

The biomaterials are being most extensively found so that these can be used as alternative material in human body implanting. Hydroxyapatite, is one of the biomaterial among the others. The major reason for choosing the hydroxyapatite as a biomaterial in our study remains that it is quite similar to the natural bone. Due to these abilities, it has been extensively employed for tissue engineering of the bones.

As we observe nowadays, large amount of people are suffering from various orthopaedic abnormalities. These are many reasons that lead to these defects which either be due to accident or ageing. The orthopaedic injuries majorly make the sport person suffer due to the associated trauma risk. As such hydroxyapatite is mostly used in treating the bone defects. But it is not being used for the dental problems associated with cavities in teeth.

Thus, this current study focus on synthesizing the hydroxyapatite by different methods and to evaluate the nature and properties of the synthesized hydroxyapatite. The various biomaterials have been found and explored. As it has various advantages such as biocompatibility, high porosity and many other. Now our target is to use this material in treating the dental problems. Apart from having excellent biocompatibility, HAP is having good antimicrobial activity . Because of its antimicrobial capability, HAP is safe as an implant in human body. It has much better antimicrobial activity when compared with other natural antimicrobials like clove, turmeric and Indian gooseberry. It is potently active against bacteria (Staph. aureus as well as E. coli) and both these bacteria are common human pathogens in wide variety of infections.

Chapter 5
Objectives Of Study

5.1 Objective

- To Synthesize the Hydroxyapatite by chemical precipitation method (wet chemical synthesis method)
- To evaluate properties (physical and chemical) of HAP.
- To check the efficacy of synthesized and development of the tablet of HAP.
- To study antimicrobial efficacy of synthesized HAP
- To compare antimicrobial properties of synthesized HAP with Clove , Turmeric and Indian gooseberry.

Chapter 6
Material And Research Methodology

Table 2 List of Instruments & Equipments used

Table 3 List of Chemicals used

List of Instruments & Equipments used

Sr. No	Material	Company
1	Glasswares & Burrete	Borosil and Borosil
2	Plastic wares	AdvLab and Co.
3	pH Meter	REMI
4	Hot Air Oven	Labtech instruments Co.
5	Weighing Balance	REMI

List of Chemicals required for HAP Synthesis

Sr. No	Chemical	Company
1	Calcium Hydroxide	Central Drug House (P) Ltd.
2	Orthophosphoric Acid	Central Drug House (P) Ltd.
3	Calcium Nitrate	Central Drug House (P) Ltd.
4	di-Ammonium Hydrogen Orthophosphate	Central Drug House (P) Ltd.
5	Ammonia	Central Drug House (P) Ltd.
6	Ammonium Hydroxide	Central Drug House (P) Ltd.

6.1 Preparation of HAP using Calcium Hydroxide & Ortho-Phosphoric Acid

Chemicals used

- Calcium Hydroxide
- Ortho-Phosphoric acid
- Ammonia
- Distilled Water

Procedure [Nicolae, D. et al] [Sibta, S. et al 2013]

Titration

A glass beaker was placed over a magnetic stirrer fixed over the base of the stand. The beaker contained magnetic beads to assist in stirring during the procedure. In the beaker 0.5M calcium hydroxide was dissolved in ammonia. With the help of clamps, fixed up a burette to deliver its contents into the beaker. A funnel was placed at the top of burette containing filter paper. In second beaker 0.3M phosphoric acid was added in water (distilled) . That was done drop by drop through the burette into the beaker. Steering speed was 800 rpm and temperature was maintained at 60-80^{0}C.During experiment the pH level was maintained at 10.Value of pH was maintained using ammonium hydroxide

Removal of excess Amonia

The precipitate that was obtained were allowed to settle for 24 hours. It is then washed the prepared chemical with water 7-8 times to remove excess ammonia until the smell was lost completely. Further processing can be done by four methods as described below.

1. Raw Preparation

It was filtered by pouring through filter paper. It was further removed by using a spatula and transfer that into a Petri plate. Then it was made dry in a hot air oven at 80^{0}C over time period of 3-4 hours until it became completely dry.Finally grinded the product to a fine powder using a mortar/pestle. Stored the prepared powder in a petri plate.

2. Ultraspurification

Ultrasonicator was used to ultra-purify the sample for 30 mins. Then it sas filtered by pouring through filter paper. It was further removed by using a spatula and transfer that into a Petri plate.Then it was made dry in a hot air oven at 80^{0}C over time period of 3-4 hour until it became completely dry. Finally grinded the product to a fine powder using a mortar/pestle. Stored the prepared powder in a petri plate. Now performed crystallography by FTIR.

3. Raw Preparation and Heating at 800^0 C (Calcination)

Then it was filtered by pouring through filter paper. It was further removed by using a spatula and transfer that into a Petri plate. Then it was made dry in a hot air oven at 800^{0}C over time period of 3-4 hours until it became completely dry. Finally grinded the product to a fine powder using a mortar/pestle. Stored the prepared powder in a petri plate. Powder was put in the crucibles and heated at 800^{0}C for 2hours. Finally performed crystallography by FTIR.

4 .Ultrapurification and Heating at 800^0C (calcination)

Ultrasonicator was used to ultra-purify the sample for 30 mins.Then it is filtered by pouring through filter paper. It was further removed by using a spatula and transfered that into a petri plate. Then it is desiccated in a hot air oven at 80^0C over time period of 3-4 hours. Until it became completely dry. Finally grinded the product to a fine powder using a mortar/pestle. Stored the prepared powder in a petri plate. Powder was put in the crucibles and heated at 800^0C for 2 hours. Now performed crystallography by FTIR.

The following reaction took place: -

$5Ca(OH)_2 + 3H_3PO_4$ ----> $Ca_5(PO_4)_6(OH)_2 + 19H_2O$

.

Molarity wais calculated by using the formula given below -:

Molarity = Mass / Mol. Wt x 1000/vol. [vol is 100] Flow

6.2 Alternate method Preparation of HAP using Calcium Nitrate & Di-ammonium Hydrogen Phosphate

Chemicals Used were Calcium Nitrate, Di-ammonium Hydrogen Phosphate and Ammonia.

Procedure [Dakshnamoorthy A. et.al., 2013]

Placed a glass beaker over a magnetic stirrer fixed over the base of the stand. The beaker contained magnetic beads to assist in stirring during the procedure. In the beaker 0.6M calcium nitrate was dissolved in ammonia. With the help of clamps, fixed up a burette to deliver its contents into the beaker. A funnel was placed at the top of burette containing filter paper. In second beaker 0.4M diammonium hydrogen phosphate was dissolved in distilled water. That was poured slowly and droply through the burette into the beaker. The reaction was conducted under a stirring rate of 800 rpm at 60-80^0C. Maintained pH of 10.8 during the experiment. added ammonium hydroxide if ph droped. The obtained precipitate was allowed to settle for 24 hours. Then washed the prepared chemical with water 7-8 times to remove excess ammonia and till smell goes away.

Further processing can be done by 4 methods

1. Raw Preparation

Then it was filtered by pouring through filter paper. It is further removed by using a spatula and transferred that into a Petri plate. Then it was made dry in a hot air oven at 80^0C over time period of 3-4 hours. Until it became completely dry. Finally grinded the product to a fine powder using a mortar/pestle.Stored the prepared powder in a petri plate.

2. Ultraspurification

Ultrasonicator was used to ultra-purify the sample for 30 mins. Then it was filtered by pouring through filter paper. It was further removed by using a spatula and transfered that into a Petri plate. Then it was made dry in a hot air oven at 800C over time period of 3-4 hours until it became completely dry. Finally grind the product to a fine powder using a mortar/pestle. Stored the prepared powder in a petri plate. Now performed crystallography by FTIR.

3. Raw Preparation and Heating at 800^0 C (Calcination)

Then it was filtered by pouring through filter paper. It was further removed by using a spatula and transfered that into a petri plate.

Then it was made dry in a hot air oven at 80^0C over time period of 3-4 hours until it became completely dry. Finally grinded the product to a fine powder using a mortar/pestle. Stored the prepared powder in a petri plate. Powderwais put in the crucibles and heated at 800^0C for 2hours. Now performed crystallography by FTIR.

4 .Ultrapurification and Heating at 800^0 C(calcination)

Ultrasonicator is used to ultra-purify the sample for 30 mins. Then it was filtered by pouring through filter paper. It was further removed by using a spatula and transfered that into a petri plate. Then it was made dry in a hot air oven at 80^0C over time period of 3-4 hours until it became completely dry. Finally grinded the product to a fine powder using a mortar/pestle. Stored the prepared powder in a petri plate. Powder was put in the crucibles and heated at 800^0C for 2 hours. Now performed crystallography by FTIR.

The following reaction took place: -

$10\ Ca(NO_3)_2 + 6\ (NH_4)_2HPO_4 + 8\ NH_4OH \rightarrow Ca_{10}(PO_4)_6 + 20\ NH_4NO_3 + 6H_2O$

Molarity was calculated by using the formula given below -:

Molarity = Mass / Mol.Wt x 1000/vol. [vol. was 100]

6.3 Figures for Synthesis of HAP

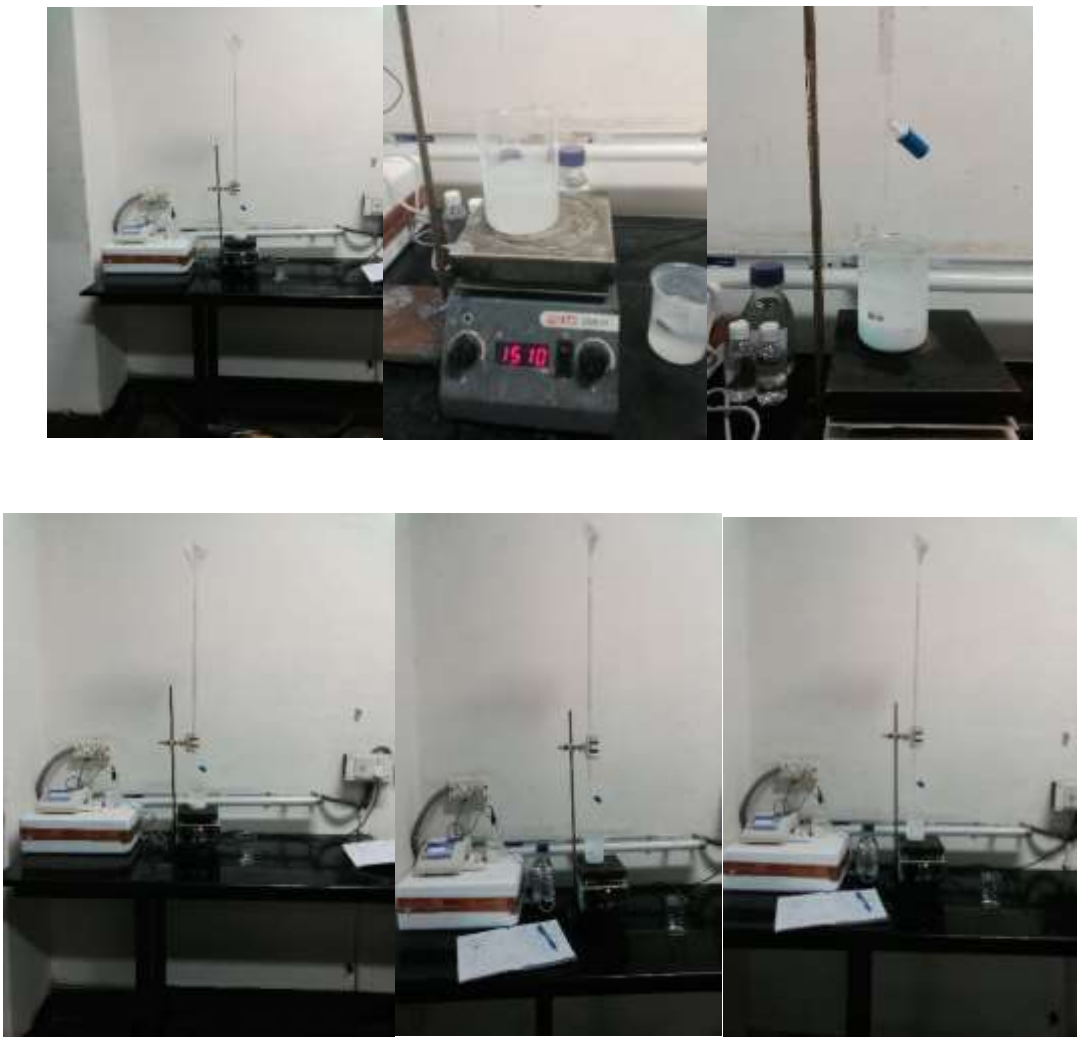

Figure 1. Ttitration of HAP

0.5M calcium hydroxide was dissolved in ammonia & 0.3M phosphoric acid was added in distilled water. T Alternatively 0.6M calcium nitrate was dissolved in ammonia & 0.4M diammonium hydrogen phosphate dissolved in distilled water. This is poured slowly and drop wise through the burette into the beaker. Stirring rate of 800 rpm at 60-800C & pH of 10.8 is maintained during the experiment.

Figure 2. Weighing Balance

This is used to weigh calcium nitrate diammonium hydrogen phosphate

Figure 3. pH Meter

This is used to maintain a pH of 10.8 during the titration.

Figure 4. Washing of HAP

The obtained precipitate will be followed by settling for 24 hours. Then wash the prepared chemical with water 7-8 times to remove excess Ammonia until smell goes away.

Figure 6. Filteration

This is used to remove excess water and to obtain pure HAP. Funnel along with filter paper is used for the same. Concentrated ?HA|P remains in the filter paper and excess water gets filtereed out.

Figure 6. Transfer to Prtri Plate

When most of the water is removed the precipitate of HAP is transferred from the filter paper to the petri plate with the help of spatula

Figure 7. Crushing with Mortar &Pestle

After the powder has dried it is transferred into mortar & pestel from the petri plates. It is then grinded to form a v fine powder. It is then sieved through a sieve.

6.4 Characterisation of HAP

6.4.1 FTIR

Principle

FTIR, standing for Fourier Transform Infra Red (IR) Spectroscopy, is the ideal technique. In this technique, Infra Red waves are passed all the way from end to end of the sample ; some of those get absorbed and rest are being transmitted.

Working

This is used to characterize HAP at microscopic level. On performing FTIR distinctive bands were obtained. The peaks obtained in the graph signify the bonding pattern of the compound and absorption distinctives of HAP. To study the spectral distinctives of the chemical bonding, IR characterization was carried out. This is used to characterize HAP at Microscopic Level. On performing FTIR distinctive bands were obtained. The peaks obtained in the graph signify the bonding pattern of the compound and absorption distinctives of HAP. To learn the spectral uniqueness of chemical bonding, IR characterization was carried out

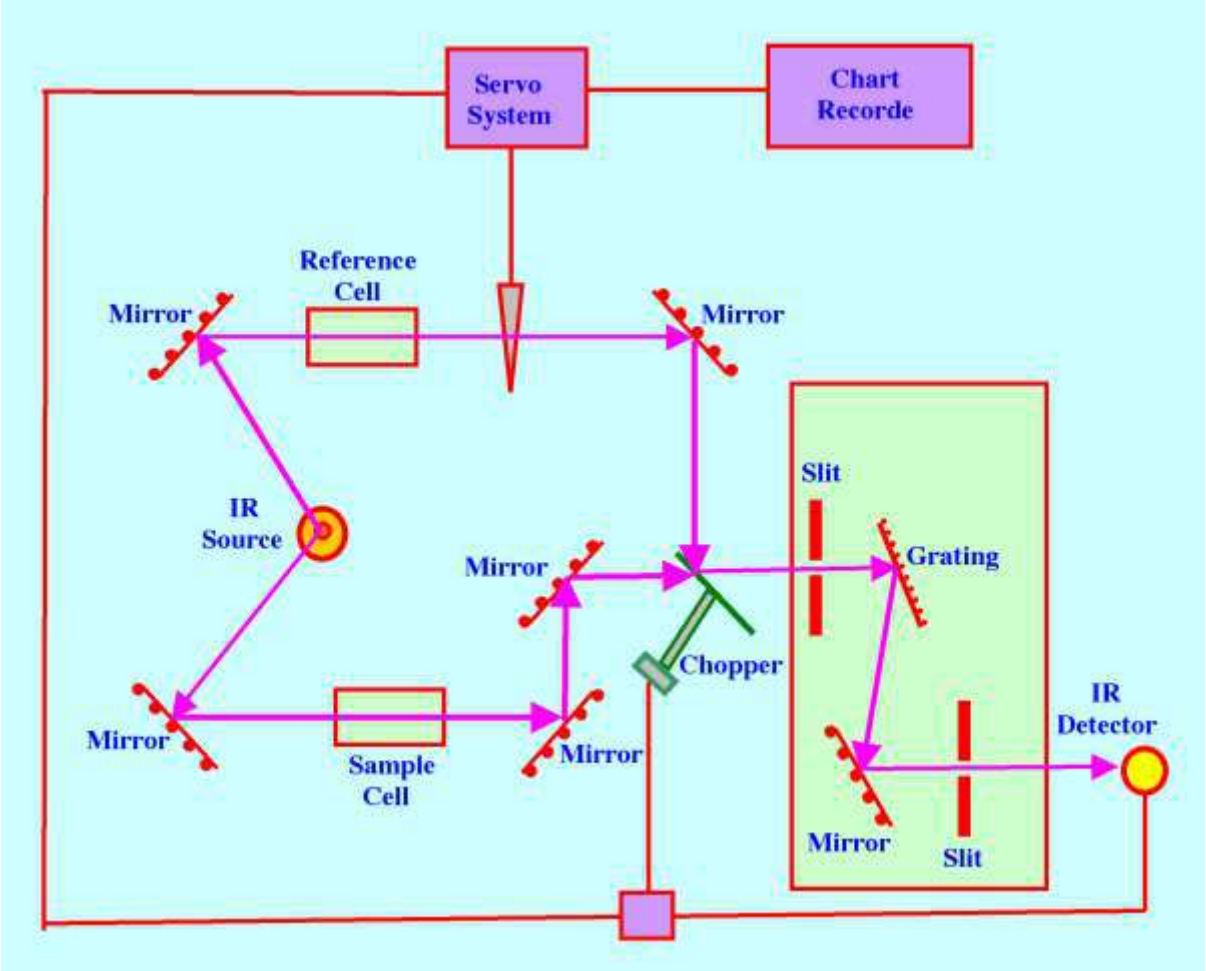

Figure8: Layout of FTIR

6.4.2 X RAY DIFFRACTION

Principle

XRD is an important tool; non-destructive in nature and is used to analyze varied matter and materials—ranging between fluids to powders and also respective crystalline forms. XRD is one of the indispensable methods used for characterization of various materials as well as in quality control assessment. A range of diffractometers are bieng established for specific use in academic as well as in industrial fields, which provide us with versatile technically advanced and cost-effective ways out today.

Working

XRD is a rapid analytical system principally used for phase recognition of crystalline matter and can make available information regarding unit cellular proportions. Analyzed material is delicately ground; homogenized followed by measuring average bulk composition. X-rays orignated by cathode – ray- tube are filtered for gaining mono-chromatic radiations which are concentrated by collimation, and are directed towards the sample.Then the constructive kind of interference gets created by the inter-action of incident rays with the specific sample particles. Bragg's Law ($n\lambda = 2d \sin\theta$) is to be satisfied in this process. In equation $n\lambda = 2d \sin\theta$, n is a positive integer; λ is wavelength of the incident ray; d is interplanar expanse in a crystal and θ is scattering angie's measurement.This method can reveal the structure and function of many biological molecules,
including vitamins,drugs, proteins and nucleicacids such as DNA.

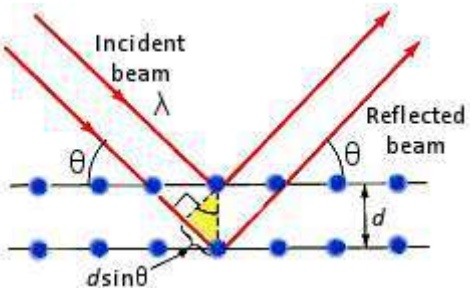

Figure9: Diagram of XRD

6.4.3 SCANNING ELECTRON MICROSCOPY (SEM)

Principal.

Scanning Electron Microscope utilizes focused beam of electrons to produce images of any specimen.The electrons interact with atoms of the sample.Thereby a range of signals emerge carrying information about the constituents of the specimen and its surface topography.These signals generated produce two-dimensional picture and also reveal information regarding the sample regarding texture i.e., external morphology and orientation of its constituents.

Working

SEM is used primarily to get three-dimensional image of the specimen surface. The image is developed via the detection of electrons (secondary) which are released from the specimen as a result of it being scanned by very high energy "primary" electrons. The primary electrons are emitted from the electron "gun" in the SEM. Most of the biological specimens are composed of non-dense material. Therefore the amount of secondary electrons produced is very low to

create an image. Hence these are generally coated with a much fine metallic layer which readily produces secondary electrons.Now a large depth of field is achievable.It can produce an image of great visual depth with a three-dimensional appearance.
The operating background of a standard scanning electron microscope dictates that high-quality preparation techniques are used. Distinctiveally, a biological specimen is chemically fixed, dehydrated through an acetone or ethanol series and then dried at the critical point. This method is used to curtail specimen distortion due to drying tensions. SEM can also be used to investigate smooth surfaces of industrial samples.

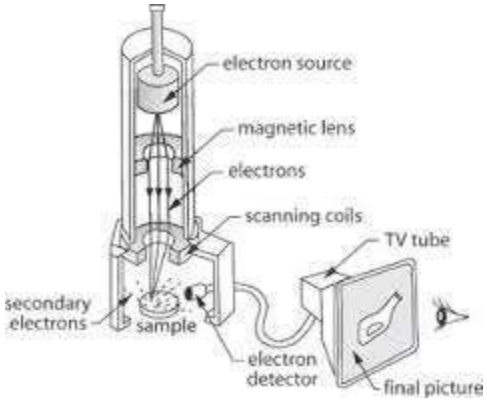

Figure10: Diagram showing layout of SEM

6.4.4 TRANSMISSION ELECTRON MICROSCOPY (TEM)

Principle

Transmission electron microscopy is the technique in which of electrons beam is transmitted through a very thin specimen, interacting with the specimen as it passes through it. An image is formed from the interaction of the electrons transmitted through the specimen; the image is magnified and directed towards a screen or to be detected by a sensor.
TEMs are capable of imaging at a significantly higher resolution owing to the small de Broglie wavelenth of electrons. This enables the instrument's user to examine fine detail—even as small as a single column of atoms, which is thousands of times smaller than the smallest resolvable object in a light microscope. TEM forms a major analysis method in a range of scientific fields i.e., physical, chemical and organic fields.

Working

TEM is a microscopical performance in which electrons in a beam are transmitted through an ultra-thin sampling. An illustration is formed from the interaction of the electrons transmitted through the sample.The image is overstated and finally gets focused on an imaging appliance. T can be a fluorescent screen, a photographic film or a sensor.

TEMs are accomplished of imaging at a significantly advanced resolution than light microscopes. It is because of diminutive de Broglie wavelength of electrons. Therefore user

can observe fine details. These could be as tiny as a single line of atoms. TEM forms a key analysis means in varied scientific fields, including physical, chemical and biological sciences. TEMs find application in cancer research, virology and material science.

Components

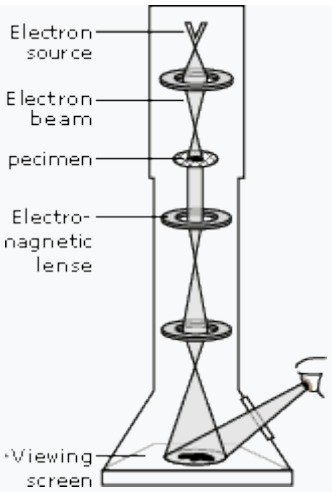

Figure11: Diagram showing layout of TEM

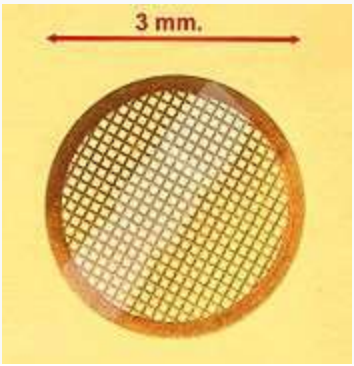

Figure12: Diagram showing Specimen Stage layout of TEM

Two main designs for stages in a TEM exist, the side-entry and top entry version. Each design must accommodate the matching holder to allow for specimen insertion without either damaging delicate TEM optics or allowing gas into TEM systems under vacuum.

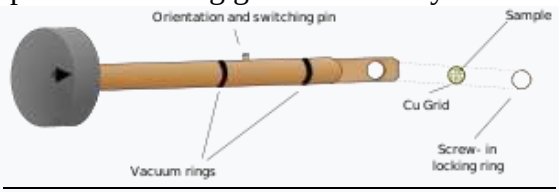

Figure13: Sample Holder For Insertion Into A TEM Goniometer.

6.5Antimicrobial Activity

6.5.1 Pellet Preparation

HAP Powder was crushed to make a uniform powder. Powder is weighed to in concentrations of 900, 720, 450, 180, 60, 150, 240, 300 mg. powder is packed in butter paper. Pellets of the HAP Powder is made using dye punch. Pellets are made in different ratios in pure form as well as by mixing it in different proportions with antimicrobial substances. Antimicrobial Substances used in pellet formation included clove, haldi and amla

HAP Conc. (Percentage)	Antimicrobial substance Conc. (Clove or Amla or Turmeric) (Percentage)	
900(100%)	0(0%)	(Control)
720(80%)	180(20%)	
450(50%)	450(50%)	
180(20%)	720(80%)	
0(0%)	900(100%)	(Control)

Amla Conc.	Clove Conc.	Turmeric Conc.	Combined Amla, Clove & Turmeric Percentage	HAP Conc. (Percentage)	
300	300	300	100%	0 (0%)	(Control)
240	240	240	80%	180(20%)	
150	150	150	50%	450(50%)	
60	60	60	20%	720(80%)	
0	0	0	0%	900(100%)	(Control)

Added the appropriate ratio of the materials (HAP & Antimicrobial Substance) in the dye. Punch was used to make the pellets. Excipient was also added to assist in the formation of pellets. To ease the formation of pellets 0.5% of polyvinyl alcohol (PVA) or polyethylene glycol (PEG) is added. PVA or PEG acts as a polymer or binder.

Pellets for these are made in the similar way as mentioned above.

6.5.2 Media Preparation

Nutrient agar and MacConkey's agar were used to study the efficacy of various prepared pellets. Microbes, against which antimicrobial efficacy was tested included Escherichia coli and Staphylococcus aureus. These are two commonest pathogenic bacteria.Taking all standard precautions, media were prepared following manufacturer's instructions. Aseptically pouring was done in various petri-plates followed by setting of the media.

Respective bacterial suspensions were prepared in normal saline and then inoculated on plates. Two to three pellets were placed on each plate. Then plates were incubated at 37^0C for 24-48 hours. The zones of inhibition were considered on all the plates. These were compared and results inferred with appropriate conclusion.

6.5.2.1 Preparation of Nutrient Agar (Hedley D. 1934)

For preparation of Nutrient Agar, took 28 gm of nutrient agar powder in a flask. To that added one liter of distilled water mixed with the suspension followed by heating. Continued heating the mixture with continuous stirring in order to completely dissolve all the components. Then autoclaved that prepared medium by heating that at 121^0C at 15 pounds (lbs.) pressure for 15 minutes for complete sterilization. Allowed the mixture to cool down; but without solidification.

Then poured the medium into a series of sterilized petri-plates and left those plates on the sterile surface till the solidification of agar. Then replaced the lid of each petri dish and stored the plates in a refrigerator at 4^0C.

6.5.2.2 Preparation Of MacConkey's Agar (Downes F P.2001)

For preparation of MacConkey's Agar took 49.53 gm of MacConkey's agar powder in a flask. To that added one litre of distilled water. Mixed the suspension followed by heating. Continued

heating the mixture with continuous stirring in order to completely dissolve all the components. Then autoclaved that prepared medium by heating that at 1210C at 15 pounds (lbs.) pressure for 15 minutes for complete sterilization. Allowed the mixture to cool down; but without solidification.

Then poured the medium into a series of sterilized petri-plates and left those plates on the sterile surface till the solidification of agar. Then replaced the lid of each petri dish and stored the plates in a refrigerator.

6.5.3 **Autoclaving of Medium**

Washed the flask with soap and water. Added distilled water and then medium contents in powder form. Mixed well with glass rod. Heated to dissolve. Closed the mouth of the flask with cotton plug and covered thewith a thread tied brown paper. Then placed the flask in an autoclave. Closed the autoclave. Maintained a temperature of 1210C at 15 psi for 13 minutes. Then switched off the autoclave and opened it after the pressure returned to the normal atmospheric pressure.

6.5.4 Preparation of Bacterial Culture

Escherichia coli and Staphylococcus aureus cultures were taken from laboratory. Suspension of each microbe was prepared in normal saline.

Antimicrobial testing was done by two methods i,e., (a) Disk Diffusion Method and (b) Well Diffusion Method.(Baur et.al.,1966)

Prepared HAP pellets and all three antimicrobials in the form of pellets were put up on the plates of nutrient agar and MacConkey's agar inoculated with Staphylococcus aureus and E.coli suspensions in two sets. The pellets were prepared in different proportions in pure as well as mixed forms. The respective diameters of inhibition zones have been depicted in various tables.

The second method to do antimicrobial susceptibility was by well diffusion method. Media plates were prepared. After setting of medium three wells were dig in each plate. Then plates were inoculated with Staphylococcus aureus and E.coli suspensions in two sets. Antimicobial substances including HAP were added into the wells in pure as well as varying mixed proportions as specified in the respective tables.

All the petri-plates were incubated at 37^0C for 24 hours. After that three zones of inhibition in different directions were calculated for each antimicrobial. A final value for each zone was calculated by taking the mean of three readings. Then comparative efficacy of various antimicrobial substances was assessed.

6.5.5 Laminar air flow

Switch ON the main eleetrical power point & clean the surface of working bench with 75% alcohol.

Switch ON the UV lamp for 15 mintes befor the using laminar air flow. Laminar air flow produeesb avery clean and dust free area. The whole of the air present in a restrained region flows with homogeneous velocity. By employing high efficiency bacteria proof filter,the air supplied to the is sterilized which will sweep all dust and air ball partielcs from the chamber through the open side, then making the whole area free of microorganisms.The operator should his hands thoroughly with alcohol etc. and wear sterilized gloves, headgear, mask and clothing.All the apparatus and equipment required to be used in the process must be sterilized properly. Switch off laminar flow and clean that.

A laminar flow hood is an enclosed work surface intended to avert contamination of biological samples. With HEPA filter air is blown in an exceedingly smooth manner towards theoperator. This cabinet is generally made of steel metal of stainless quality with nil gaps to minimize spores collection and hence contamination.

6.5.6 Inoculation of Petri Plates

Taking all standard precautions, media were prepared following manufacturer's instructions. Aseptically pouring was done in various petri-plates followed by setting of the media.

Respective bacterial suspensions were prepared in normal saline and these were inoculated on plates.These plates were divided into two sets.

First set of plates was used for antimicrobial sensitivity by using pellets. Three pellets were placed on every plate.Then plates were incubated at 37^0C for 24 hours. Growth inhibition of bacteria was assessed on all the plates.The zones surrounding the pellets were determined and compared; and results inferred with appropriate conclusion.

Second set of petri-plates was used for antimicrobial sensitivity by using well method. Three wells were made on each plate at proper spacing. Various antimicrobials in different strengths and also in various combinations were placed into these wells. Then plates were incubated at 37^0C for 24 hours. Growth inhibition of bacteria was assessed on all the plates.The zones surrounding the wells were determined and compared; and results inferred with appropriate conclusion.

48

Chapter 7
Result And Discussion

The objective of my study was to develop an efficient HAP Powder.

7.1 Synthesis of HAP

Hydroxyapatite was synthesized successfully by using chemical precipitation technique. The synthesis was done using two methods i.e First Method using Calcium Hydroxide and Orthophosphoric Acid and Second Method using Calcium Nitrate and Diammonium Hydrogen Ortho Phosphate. It was observed during synthesis that hydroxyapatite was less soluble and has remarkable stability. The figure 1 shows HAP powder obtained after Titration washing Filteration Drying & crushing with Mortar & Pestle.

Table 4 Properties of Powder:

Colour	White
Nature	Crystalline
Porosity	High

Figure 8. HAP Powder Synthesized

Figure 9.Variour samples Prepared for characterization using FTIR, XRD, SEM, TEM

7.2 FTIR Analysis of Synthesized HAP

The distinctive bands exhibited in the sample spectra:

- bands due to OH^- ions
- the band arise from PO_4^{3-} ions
- bands due to CO^{3-}

This is used to characterize HAP at Microscopic Level. On performing FTIR distinctive bands were obtained. The peaks obtained in the graph signify the bonding pattern of the compound and absorption distinctives of HAP. To study the spectral distinctives of the chemical bonding IR Characterization was carried out.

The distinctive bands exhibited in the sample spectra bands due to OH− ions, $PO4^{3-}$ ions, CO_3^{3-} ions, bands due to absorbed water.

Standards

The standard values to signify different peaks; as FTIR spectra showed, are mentioned.

The distinguishing bands of PO_4^{3-}at peaks with values 1090–1032, 960, and 600–500 cm^{-1}. Absorbed water was indicated by1640 to 1595 cm^{-1}peaks. OH^- was shown by 633 cm^{-1}. CO_3^{2-} bands were at 1550, 1460, 1445, 1415, and 870 cm^{-1} peaks. [Jose et.al.,2013].

The distinctive bands of $PO_4^{3-}$are at peaks with values 469, 599,560,962,1088 and 1046 cm^{-1}, OH^- was shown by 3700,3100,1637,3571 and 632 cm^{-1}.The absorption bands at 1482, 1424 and 875 cm-1confirmed the presence of carbonate group.[KristineS,et.al.,2010]

The presence of phosphate groups was indicated by bands of values 1042, 1034, 1089 and 962 cm-1.3437, 3448, and 3571 cm-1indicate presence of OH^- (hydroxyl) groups. [Novesar J.et.al., 2016]

Distinctive bands to indicate PO_4^{3-}appeared at 874 cm^{-1} and 1,033 cm^{-1}; the distinctive bands for CO_3^{2-} appeared at 1,637, 3,420 and 1,416 cm^{-1}. [Yukai S.et.al.,2013]

Peak at 3405.01cm-1confirms the presence of OH− (hydroxyl) groups. The peak at 1479.33cm-1 corresponds to the CO_3^{2-} group. The peak at 1041$cm^{-1}$and 603.96cm-1are assigned to phosphate(PO_4^{3-})group.[Sakthivel, P.et.al.,2014]

FTIR spectra showed the distinctive bands of $PO4^{3-}$ at 1041, 603.96, OH− was shown by 3405.01, carbonate bands were at 1479.33.The bands typical of $PO4^{3-}$ groups will be observed at 1087, 1023, 962 and 599 cm-1.

The distinctive bands of PO4 3 −at peaks with values 1085–1092, 1033-1035, and 1000, 933-962, 560-602.5 cm−1. OH− was shown by 3130, 3630, 3430 cm−1. CO3 2- bands were at 1623.6 cm−1 peaks

The distinctive bands of PO4 3 −at peaks with values 603-561 cm−1. OH− was shown by 622, 355 cm−1. CO3 2- bands were at 1600 cm−1 peaks

The distinctive bands of PO4 3 −at peaks with values 1042, 1034, 1089 cm−1. OH− was shown by 622, 355 cm−1. CO3 2- bands were at 1637 cm−1 peaks

The distinctive bands of PO4 3 −at peaks with values 874 cm−1. OH− was shown by 3437, 3448 cm−1. CO3 2- bands were at 1416 cm−1 peaks
The distinctive bands of PO4 3 −at peaks with values 1033 cm−1. OH− was shown by 3571 cm−1. CO3 2- bands were at 1471 cm−1 peaks

The distinctive bands of PO4 3 −at peaks with values 4962 cm−1. OH− was shown by 567.09 cm−1. CO3 2- bands were at 1482,1424 cm−1 peaks

The distinctive bands of PO4 3 −at peaks with values 475,575,601 cm−1. CO3 2- bands were at 875 cm−1 peaks

The distinctive bands of PO4 3 −at peaks with values 963, 1059,1100 cm−1.

After heat treatment at 8000C for 2 hours (Calcination):

None of the peaks related to CO_3^{2-} group (1420 cm^{-1}, 875 cm^{-1}) will be traced. Production of hydroxyapatite will be discovered by absence of huge peak located at 3550 cm-1 as linked to the crystallization water; which means water molecules gripped in the apatite units.Usually nonstoichiometric hydroxyapatite can retain some water moles.Presence of hydroxyl faction will be confirmed by the bands appearing at 3571 cm^{-1} and629 cm^{-1}, accredited to its stretching and flexural patterns.The distinctive bands of the PO_4^{3-} groups will be realistic at 1087, 1023, 962 and 599 cm^{-1}.

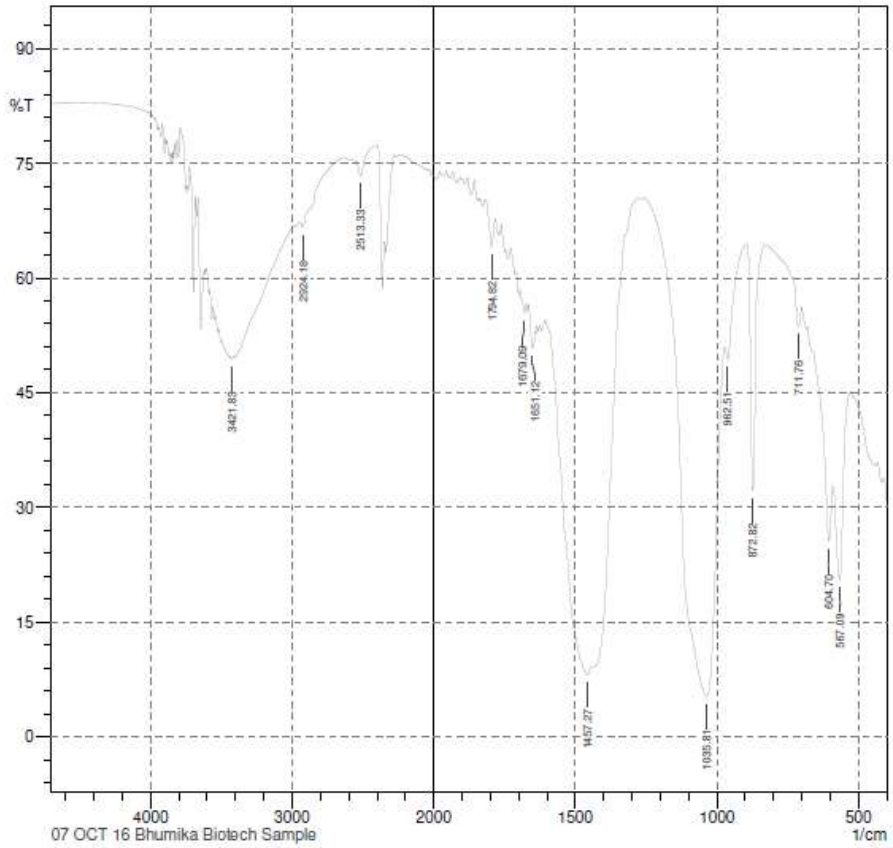

Comment;
07 OCT 16 Bhumika Biotech Sample

Date/Time; 10/7/2016 12:18:31 PM
No. of Scans;
Resolution;
Apodization;
User; Administrator

SHIMADZU

	Peak	Intensity	Corr. Inte	Base (H)	Base (L)	Area	Corr. Are
1	567.09	20.507	16.937	590.24	529.48	30.813	5.574
2	604.7	25.586	10.886	657.75	590.24	29.038	2.58
3	711.76	53.701	3.244	826.53	701.15	26.978	-0.676
4	872.82	32.223	32.19	895.96	826.53	18.468	5.199
5	962.51	49.403	3.403	973.12	895.96	18.369	-0.292
6	1035.81	5.266	49.957	1259.56	973.12	159.45	95.741
7	1457.27	8.1	4.695	1572.04	1444.73	98.708	11.342
8	1651.12	50.882	3.679	1665.59	1640.51	6.949	0.399
9	1679.09	55.476	1.452	1688.73	1672.34	4.104	0.098
10	1794.82	64.078	4.54	1814.11	1783.25	5.461	0.466
11	2513.33	73.371	2.791	2578.91	2413.99	20.046	0.711
12	2924.18	66.64	1.218	2943.47	2882.71	10.308	0.188
13	3421.83	49.414	0.368	3434.37	3408.33	7.936	0.048

Graph 1: FTIR Result of Sample 1

Sample 1

White powder obtained by chemical synthesis was subjected to FT-IR Spectroscopy for characterization. Various peaks in the graph correspond to the following compounds: Bands at 1457.27 cm-1 and 872.82 cm-1represent CO3- group. Bands at 1035.81, 962 .51 and 604.7 cm-1 are because of PO4 3- groups. Band at 567.09 cm−1 is due to OH− faction. The distinguishing bands of the $PO4^{3-}$ groups are observed at1651.21, 711.76 cm-1.

Table 4: List of Bands obtained in sample 1

group	Bands
CO3-	872.82,1457.27 cm^{-1}
$PO4^{3-}$	567.09, 604.7 , 962 .51, 1035.81 cm^{1}

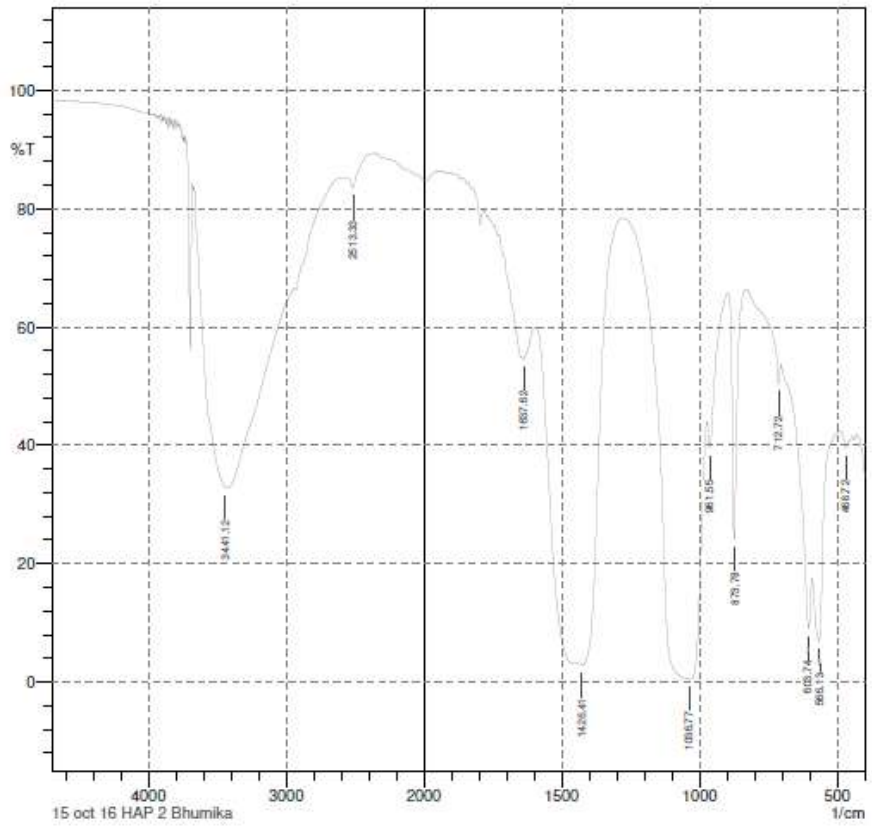

Comment;
15 oct 16 HAP 2 Bhumika

Date/Time; 10/15/2016 12:11:32 PM
No. of Scans;
Resolution;
Apodization;
User; Administrator

SHIMADZU

	Peak	Intensity	Corr. Inte	Base (H)	Base (L)	Area	Corr. Are
1	468.72	39.58	2.374	493.79	445.57	18.652	0.469
2	566.13	6.948	18.024	591.2	509.22	55.389	8.893
3	603.74	9.126	12.435	705.01	591.2	55.945	-2.377
4	712.72	50.429	4.061	829.42	705.01	26.95	-0.915
5	873.78	24.232	41.713	896.93	829.42	18.918	6.757
6	961.55	39.579	7.71	973.12	896.93	20.515	-0.018
7	1036.77	0.594	1.28	1038.7	973.12	80.321	-4.269
8	1426.41	2.784	7.978	1442.8	1278.85	105.438	-25.272
9	1637.62	54.63	0.312	1640.51	1627.97	3.252	0.015
10	2513.33	83.576	2.571	2553.84	2388.92	10.316	0.496
11	3441.12	32.902	0.202	3560.71	3439.19	52.043	1.595

Graph 2: FTIR Result of Sample 2

Sample 2

White powder obtained by chemical synthesis was subjected to FT-IR Spectroscopy for characterization. Various peaks in the graph correspond to the following compounds: Bands at 1426.41 cm-1 and 873.78 cm^{-1}represent CO3- group. Bands at 1036.77, 961 .55and 603.74 cm^{-1} are because of $PO4^{3-}$ groups. Hydroxyapatite Synthesis is indicated by absence of peak at at 3441.12 cm^{-1} ..Band at 566.13 cm^{-1} is due to hydroxyl group. The bands of the $PO4^{3-}$ groups are present at 1651.21, 711.76 cm^{-1}.

Table 5: List of Bands obtained in sample 2

group	bands
CO3-	873.78 , 1426.41 cm^{-1}
$PO4^{3-}$	468. 72, 566.13, 603.74, 961 .55, 1036.77 cm^{-1}
hydroxyapatite Synthesis	3441.12
OH−	566.13 cm^{-1}
H_2O	1637.62

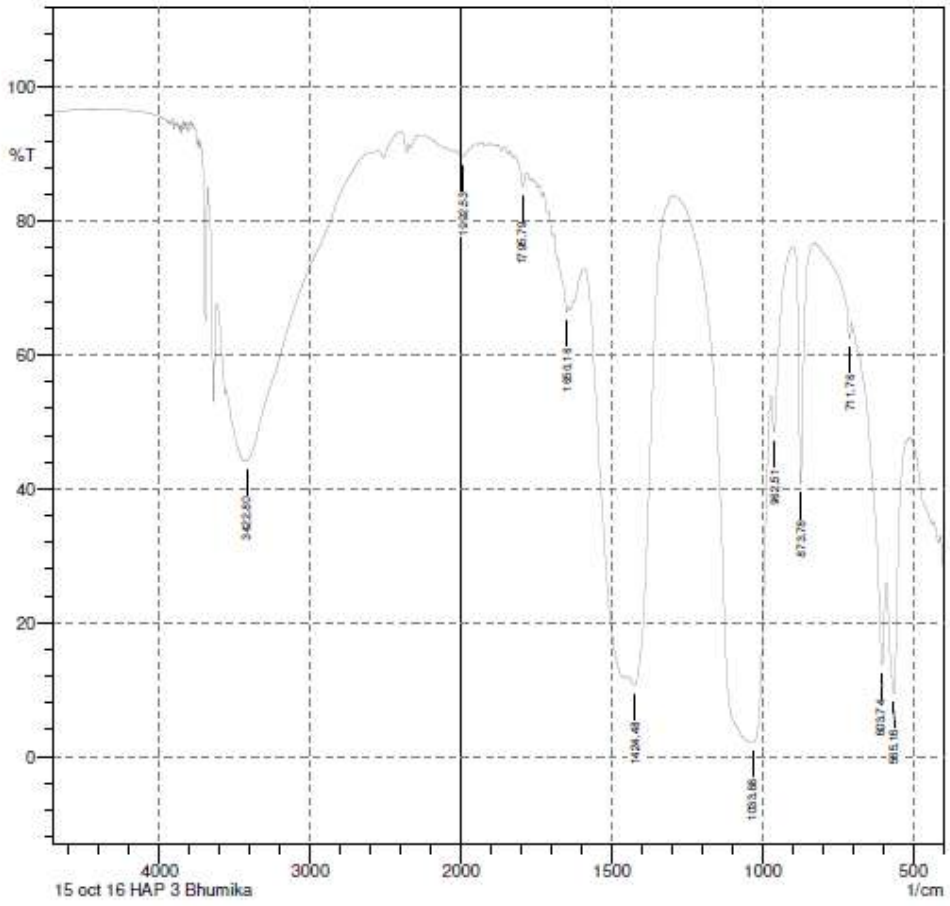

Comment;
15 oct 16 HAP 3 Bhumika

Date/Time; 10/15/2016 12:14:13 PM
No. of Scans;
Resolution;
Apodization;
User; Administrator

SHIMADZU

	Peak	Intensity	Corr. Inte	Base (H)	Base (L)	Area	Corr. Are
1	565.16	9.392	23.607	590.24	512.12	45.456	10.079
2	603.74	13.701	16.899	705.01	590.24	45.526	1.159
3	711.76	62.504	2.877	827.49	705.01	17.496	-1.109
4	873.78	40.691	35.753	899.82	827.49	12.793	4.384
5	962.51	48.442	8.543	972.16	899.82	13.763	-0.166
6	1033.88	2.044	57.679	1295.24	972.16	214.225	158.683
7	1424.48	10.691	10.553	1443.77	1295.24	65.044	-9.29
8	1650.16	66.455	1.892	1677.16	1645.33	4.937	0.152
9	1795.79	85.211	2.922	1818.93	1784.21	2.033	0.194
10	1992.53	89.682	0.509	2000.25	1950.1	2.145	0.04
11	3422.8	44.148	1.025	3439.19	2615.56	136.599	-27.576

Graph 3: FTIR Result of Sample 3

Sample 3

White powder obtained by chemical synthesis was subjected to FT-IR Spectroscopy for characterization. Various peaks in the graph correspond to the following compounds: Bands at 1424.48cm^{-1} represent CO3- group.Bands at 565.16, 603.74, 962.51, 1035.81, cm^{-1} are because of $PO4^{3-}$ groups.

Table 6: List of Bands obtained in sample 3

group	bands
CO3-	1424.48cm^{-1}
$PO4^{3-}$	565.16, 603.74, 962.51, 1035.81, cm^{-1}
hydroxyapatite Synthesis	
OH−	

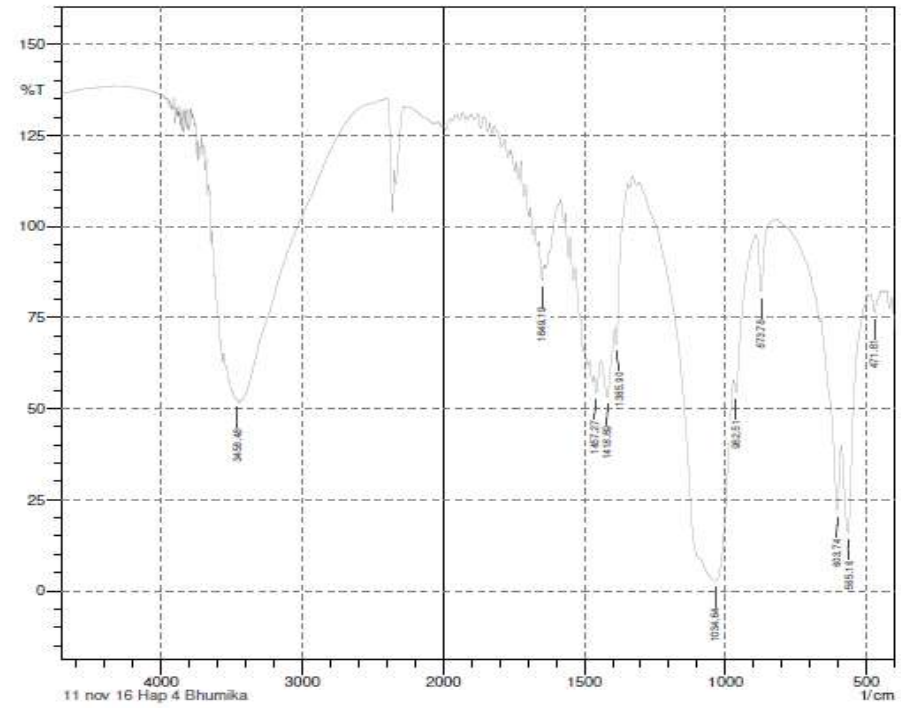

Comment;
11 nov 16 Hap 4 Bhumika

Date/Time; 11/11/2016 3:18:47 PM
No. of Scans;
Resolution;
Apodization;
User; Administrator

SHIMADZU

	Peak	Intensity	Corr. Inte	Base (H)	Base (L)	Area	Corr. Are
1	471.61	76.43	4.16	485.11	459.07	2.69	0.25
2	565.16	15.98	34.22	589.27	492.83	32.62	9.01
3	603.74	21.99	24.93	660.64	589.27	24.77	6.01
4	873.78	82.02	16.72	890.18	816.88	1.34	1.31
5	962.51	54.38	7.32	970.23	890.18	8.42	-1.48
6	1034.84	2.75	65.56	1304.89	970.23	174	142.49
7	1385.9	67.69	10.09	1392.65	1346.36	1.94	-0.25
8	1418.69	53.01	14.15	1440.87	1392.65	10.75	2.47
9	1457.27	54.31	5.74	1464.02	1440.87	5.48	0.49
10	1649.19	85.17	6.53	1660.77	1643.41	0.88	0.31
11	3458.48	52.15	0.05	3472.95	3457.52	4.32	0.01

Graph 4: FTIR Result of Sample 4

Sample 4

White powder obtained by chemical synthesis was subjected to FT-IR Spectroscopy for characterization. Various peaks in the graph correspond to the following compounds:Bands at 873.78, 1418.69, 1457.27 $cm^{-}1$ represent CO3- group.Bands at 471.61, 565.16, 603.74, 962.51, 1035.81 cm^{-} are because of $PO4^{3-}$ groups.

Table 7: List of Bands obtained in sample 4

group	bands
CO3-	873.78, 1418.69, 1457.27 cm^{-1}
$PO4^{3-}$	471.61, 565.16, 603.74, 962.51, 1035.81 cm^{-1}
hydroxyapatite Synthesis	
OH−	

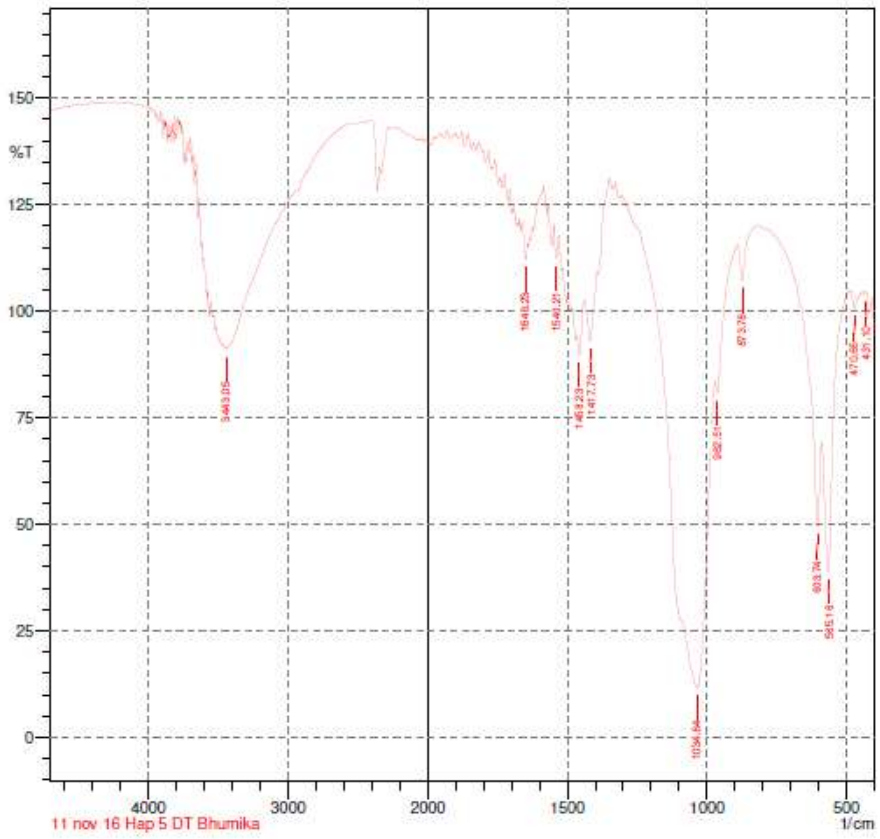

Comment;
11 nov 16 Hap 5 DT Bhumika

Date/Time; 11/11/2016 3:08:05 PM
No. of Scans;
Resolution;
Apodization;
User; Administrator

SHIMADZU

	Peak	Intensity	Corr. Inte	Base (H)	Base (L)	Area	Corr. Are
1	431.1	104.26	0.33	433.03	429.18	-0.07	0
2	470.65	100.68	3.05	483.18	461.97	-0.19	0.16
3	565.16	38.93	39.22	589.27	491.86	12.62	5.9
4	603.74	49.45	25.84	678.97	589.27	8.78	2.85
5	873.78	107.29	9.33	890.18	816.88	-4.63	0.6
6	962.51	80.87	5.95	971.19	890.18	-0.24	-0.89
7	1034.84	11.63	80.04	1306.82	971.19	83.81	88.07
8	1417.73	93.01	12.76	1438.94	1393.62	0.12	1.25
9	1458.23	89.79	6.82	1465.95	1438.94	0.6	0.4
10	1540.21	112.49	6.78	1548.89	1530.57	-1.13	0.27
11	1648.23	112.18	5.34	1662.69	1642.44	-1.3	0.2
12	3443.05	91.03	0.6	3451.73	3435.34	0.65	0.03

Graph 5: FTIR Result of Sample 5

Sample 5

White powder obtained by chemical synthesis was subjected to FT-IR Spectroscopy for characterization. Various peaks in the graph correspond to the following compounds:Bands at 873.78, 1458.23 , 1417.73 cm^{-1}represent CO3- groups. Bands at 470.65,565.16, 603.74, 962 .51, 1034.84 cm^{-1} are because of $PO4^{3-}$ groups.

Table 8: List of Bands obtained in sample 5

group	bands
CO3-	873.78, 1458.23 , 1417.73 cm^{-1}
$PO4^{3-}$	470.65,565.16, 603.74, 962 .51, 1034.84 cm^{-1}
hydroxyapatite Synthesis	
OH−	

Graph 6: FTIR Result of Sample 6

Sample 6

White powder obtained by chemical synthesis was subjected to FT-IR Spectroscopy for characterization. Various peaks in the graph correspond to the following compounds:Bands at 873.78, 1421.58 cm^{-1}represent CO3- group. Bands at 565.16, 603.74, 1033.88 $cm^{-1}$are because of $PO4^{3-}$ groups. Water bands at 1629.9 cm^{-1} .

Table 9: List of Bands obtained in sample 6

group	bands
CO3-	873.78, 1421.58 cm^{-1}
$PO4^{3-}$	565.16, 603.74, 1033.88 cm^{-1}
hydroxyapatite Synthesis	
OH^-	
H_2O	1629.9 cm^{-1}

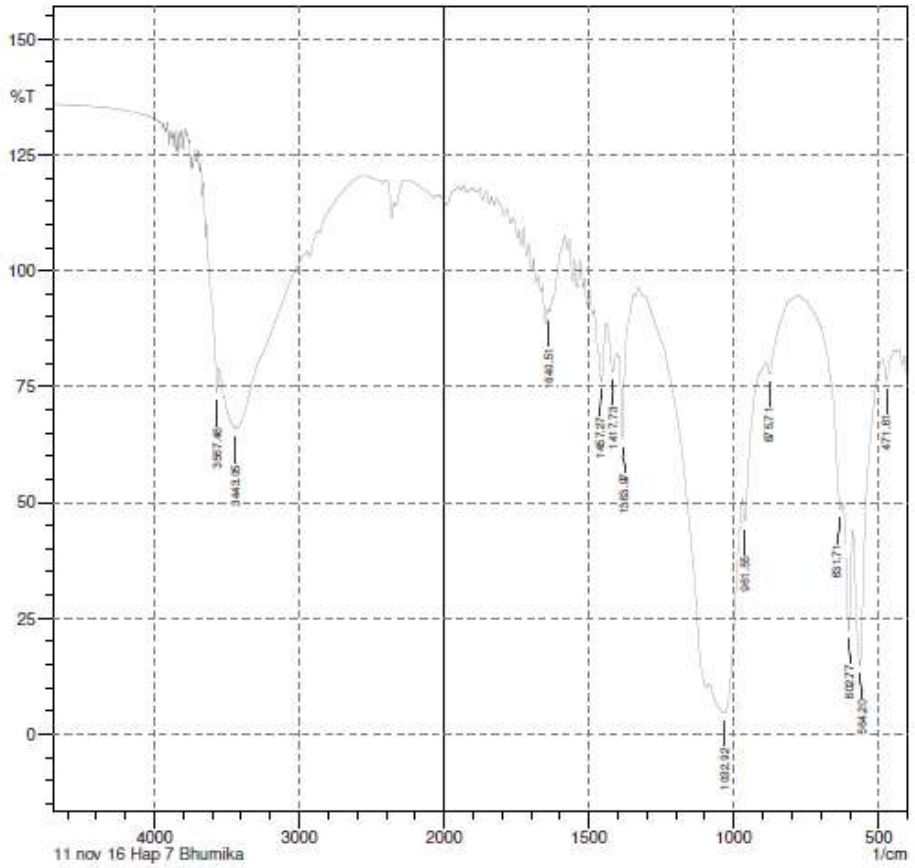

Comment;
11 nov 16 Hap 7 Bhumika

Date/Time; 11/11/2016 2:43:50 PM
No. of Scans;
Resolution;
Apodization;
User; Administrator

SHIMADZU

	Peak	Intensity	Corr. Inte	Base (H)	Base (L)	Area	Corr. Are
1	471.61	76.3	5.23	485.11	448.46	3.62	0.43
2	564.2	14.93	37.98	589.27	485.11	34.72	11.35
3	602.77	22.38	23.9	623.99	589.27	15.73	4.29
4	631.71	48.35	3.64	779.27	623.99	15.01	-10.36
5	875.71	77.68	4.2	888.25	779.27	6.02	-0.49
6	961.55	45.89	8.12	970.23	888.25	14.4	-1.54
7	1032.92	4.54	24.31	1084.03	970.23	108.07	36.56
8	1383.97	63.7	20.93	1395.54	1346.36	4.21	1.47
9	1417.73	78.17	6.67	1438.94	1403.26	3.01	0.56
10	1457.27	76.06	8.45	1466.91	1438.94	2.46	0.56
11	1640.51	91.03	0.56	1643.41	1638.58	0.19	0.01
12	3443.05	65.77	0.64	3454.62	3432.44	3.99	0.05
13	3567.46	73.69	8.8	3620.51	3556.85	4.36	1.11

Graph 7: FTIR Result of Sample 7

Sample 7

White powder obtained by chemical synthesis was subjected to FT-IR Spectroscopy for characterization. Various peaks in the graph correspond to the following compounds:Bands at 875.71, 1417.73, 1457.27 $cm^{-}1$ represent CO3- group. Bands at 471.61, 564.2, 602.77, 961 .55, 1032.92 $cm^{-1}$are because of $PO4^{3-}$ groups. Band at 3443.05, 3567.46 $cm^{-1}$is due to OH− group. Water bands at 1640.51 cm^{-1}.

Table 10: List of Bands obtained in sample 7

group	bands
CO3-	875.71, 1417.73 , 1457.27 cm^{-1}
$PO4^{3-}$	471.61, 564.2, 602.77, 961 .55, 1032.92 cm^{-1}
hydroxyapatite Synthesis	
OH−	3443.05, 3567.46 cm^{-1}
H_2O	1640.51 cm^{-1}

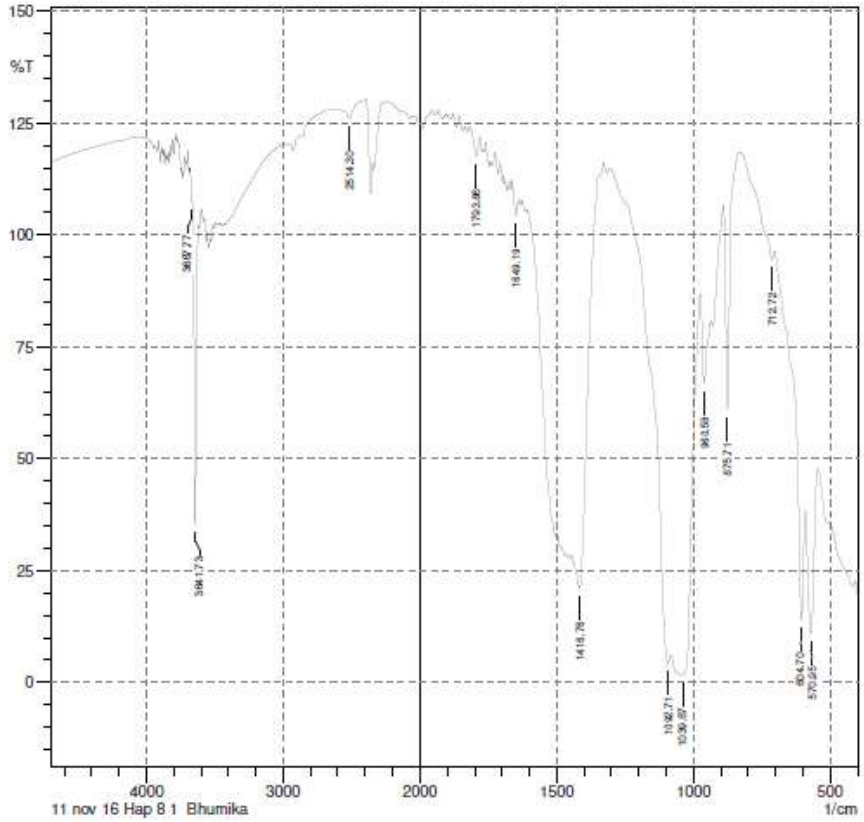

Comment;
11 nov 16 Hap 8 1 Bhumika

Date/Time; 11/11/2016 3:22:48 PM
No. of Scans;
Resolution;
Apodization;
User; Administrator

SHIMADZU

	Peak	Intensity	Corr. Inte	Base (H)	Base (L)	Area	Corr. Are
1	570.95	10.8	31.65	591.2	544.91	28.55	11.48
2	604.7	13.88	31.51	702.11	591.2	26.15	2.18
3	712.72	94.5	3.77	830.38	702.11	-3.55	0.16
4	875.71	60.87	48.81	891.14	830.38	0.45	3.54
5	960.58	66.81	17.79	975.05	936.47	4.79	1.82
6	1039.67	1.7	36.44	1082.1	975.05	113.14	44.87
7	1092.71	4.23	8.29	1248.95	1082.1	52.02	-46.83
8	1416.76	21.06	32.73	1446.66	1346.36	32.39	7.8
9	1649.19	104.35	4.63	1663.66	1641.48	-0.68	0.21
10	1793.86	117.62	5.13	1813.15	1781.32	-2.56	0.3
11	2514.3	125.99	2.85	2588.56	2393.74	-21.13	0.5
12	3641.73	35.22	69.75	3662.94	3616.65	6.02	6.95
13	3667.77	107.34	0.79	3679.34	3666.8	-0.55	0.02

Graph 8: FTIR Result of Sample 8

Sample 8

White powder obtained by chemical synthesis was subjected to FT-IR Spectroscopy for characterization. Various peaks in the graph correspond to the following compounds:Bands at 875.71, 1416.76 $cm^{-}1$represent CO3- group. Bands at 570.95, 604.7, 960 .58, 1039.67 cm^{-1} and cm^{-1} are because of $PO4^{3-}$ groups.

Table 11: List of Bands obtained in sample 8

group	bands
CO3-	875.71, 1416.76 cm^{-1}
$PO4^{3-}$	570.95,604.7, 960 .58, 1039.67 cm^{-1}
hydroxyapatite Synthesis	
OH−	

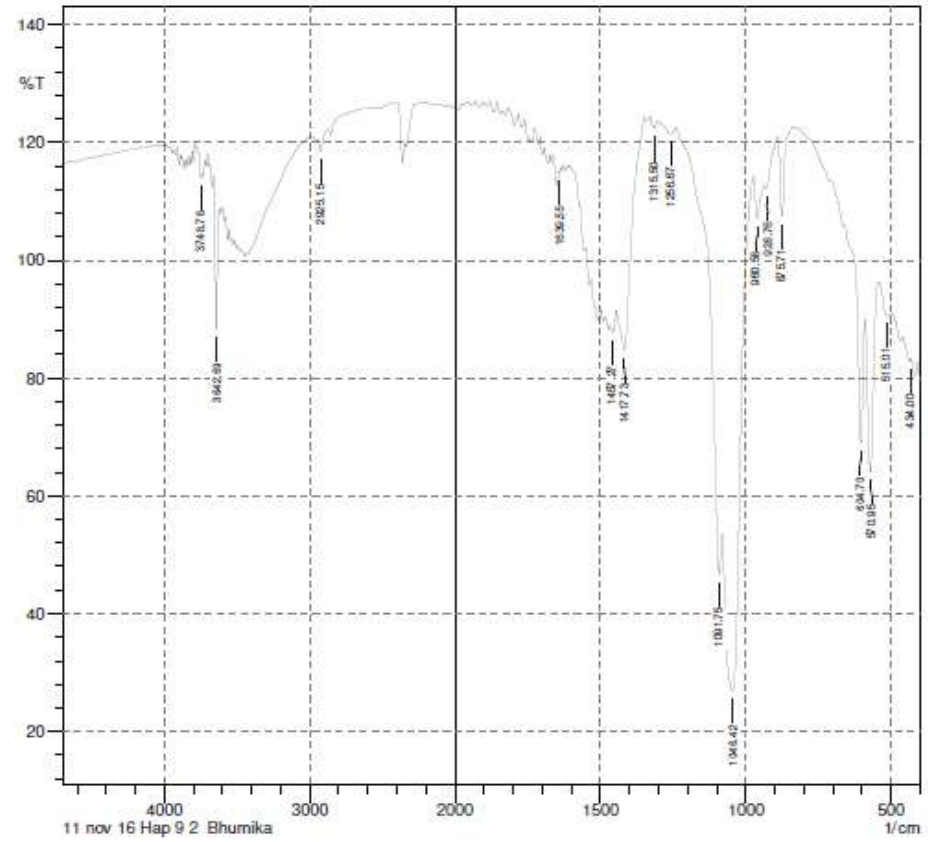

Comment;
11 nov 16 Hap 9 2 Bhumika

Date/Time; 11/11/2016 2:37:32 PM
No. of Scans;
Resolution;
Apodization;
User; Administrator

SHIMADZU

	Peak	Intensity	Corr. Inte	Base (H)	Base (L)	Area	Corr. Are
1	434	82.85	0.11	434.96	430.14	0.39	0
2	515.01	90.59	0.21	544.91	514.05	0.89	-0.02
3	570.95	64	28.72	590.24	544.91	4.56	3.16
4	604.7	68.95	24.44	658.71	590.24	2.46	1.74
5	875.71	107.5	13.49	891.14	860.28	-1.85	0.71
6	928.76	112.27	1.84	936.47	891.14	-2.96	0.1
7	960.58	107.06	6.65	974.08	936.47	-1.61	0.46
8	1046.42	26.87	46.32	1081.14	974.08	27.62	16.17
9	1091.75	46.72	11.32	1241.23	1081.14	2.16	-12.52
10	1256.67	121.47	1.41	1301.03	1241.23	-5.24	0.16
11	1315.5	122.35	1.72	1329	1301.03	-2.53	0.09
12	1417.73	84.63	16.52	1445.7	1350.22	-0.51	2.18
13	1457.27	87.78	2.41	1467.88	1445.7	1.13	0.14
14	1639.55	114.9	0.53	1641.48	1634.73	-0.42	0.01
15	2925.15	118.43	2.66	2949.26	2875	-6.01	0.24
16	3642.69	88.39	23.21	3660.05	3622.44	-0.18	1.57
17	3748.78	113.9	1.14	3762.28	3745.88	-1.04	0.03

Graph 9: FTIR Result of Sample 9

Sample 9

White powder obtained by chemical synthesis was subjected to FT-IR Spectroscopy for characterization. Various peaks in the graph correspond to the following compounds:Bands at 875.71, 1417.73, 1457.27 cm^{-1}represent CO3- group. Bands at 570.95, 604.7, 960.58, 1046.42, 1091.75 cm^{-1} are because of $PO4^{3-}$ groups.

Table 12: List of Bands obtained in sample 9

group	bands
CO3-	875.71 , 1417.73 , 1457.27 cm^{-1}
$PO4^{3-}$	570.95, 604.7, 960.58, 1046.42, 1091.75 cm^{-1}
hydroxyapatite Synthesis	
OH−	
H_2O	1639.55 cm^{-1}

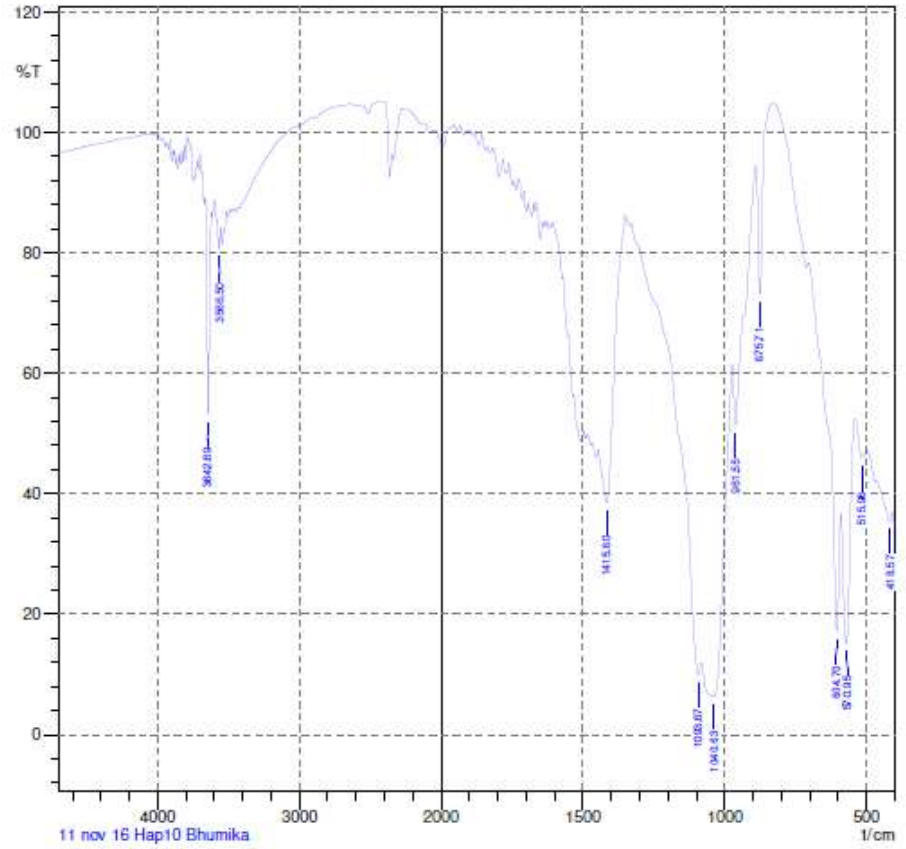

Comment;
11 nov 16 Hap10 Bhumika

Date/Time; 11/11/2016 3:10:33 PM
No. of Scans;
Resolution;
Apodization;
User; Administrator

SHIMADZU

	Peak	Intensity	Corr. Inte	Base (H)	Base (L)	Area	Corr. Are
1	418.57	35.428	1.787	430.14	407.96	9.808	0.289
2	515.98	45.843	3.693	540.09	495.72	14.203	0.729
3	570.95	15.203	27.552	590.24	540.09	27.097	9.149
4	604.7	17.177	24.872	704.04	590.24	35.084	4.324
5	875.71	73.096	24.029	890.18	836.17	1.809	1.665
6	961.55	51.306	12.586	974.08	932.61	9.222	1.568
7	1040.63	6.309	24.609	1082.1	974.08	90.25	28.906
8	1093.67	9.907	5.558	1308.75	1082.1	72.986	-41.77
9	1415.8	38.461	21.362	1446.66	1350.22	24.636	5.896
10	3566.5	80.667	4.136	3577.11	3555.89	1.797	0.278
11	3642.69	53.129	34.954	3663.91	3617.61	6.364	3.787

Graph 10: FTIR Result of Sample 10

Sample 10

White powder obtained by chemical synthesis was subjected to FT-IR Spectroscopy for characterization. Various peaks in the graph correspond to the following compounds: Bands at 875.71, 1415.8 cm^{-1} represent CO3- group. Bands at 570.95, 604.7, 961.55, 1040.63 , 1093.67 cm^{-1} are because of $PO4^{3-}$ groups.

Table 13: List of Bands obtained in sample 10

group	bands
CO3-	875.71, 1415.8 cm^{-1}
$PO4^{3-}$	570.95, 604.7, 961.55, 1040.63 , 1093.67 cm^{-1}
hydroxyapatite Synthesis	
OH^-	

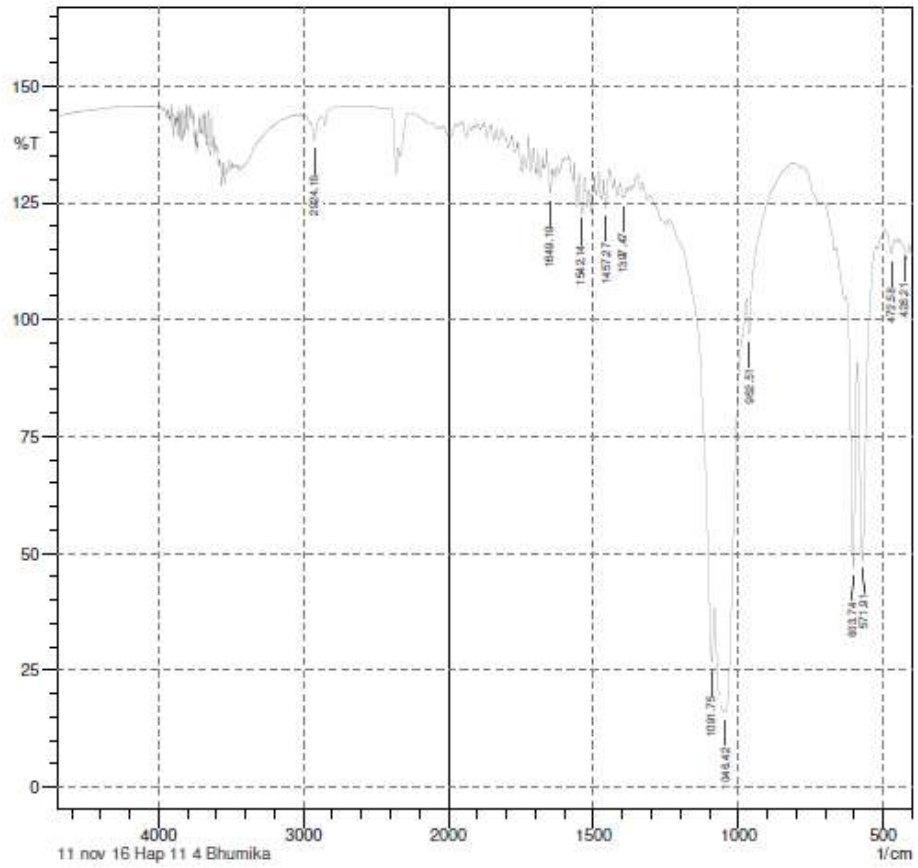

Comment;
11 nov 16 Hap 11 4 Bhumika

Date/Time; 11/11/2016 2:54:11 PM
No. of Scans;
Resolution;
Apodization;
User; Administrator

SHIMADZU

	Peak	Intensity	Corr. Inte	Base (H)	Base (L)	Area	Corr. Are
1	428.21	115.23	0.17	438.82	427.25	-0.74	0
2	472.58	114.1	3.5	493.79	463.9	-2	0.16
3	571.91	48.59	49.34	590.24	525.62	5.25	5.95
4	603.74	46.91	48.87	628.81	590.24	4.44	4.04
5	962.51	96.91	9.44	972.16	816.88	-13.44	-2.18
6	1046.42	15.99	43.94	1082.1	972.16	44.37	22.63
7	1091.75	26.7	16.94	1237.38	1082.1	9.61	-16.04
8	1397.47	125.95	1.02	1403.26	1395.54	-0.79	0.02
9	1457.27	123.87	2.23	1464.02	1455.34	-0.87	0.05
10	1542.14	123.32	1.17	1549.86	1541.18	-0.91	0.01
11	1649.19	127.12	6.8	1659.8	1643.41	-1.89	0.22
12	2924.18	138.22	4.45	2951.19	2879.82	-10.69	0.36

Graph 11: FTIR Result of Sample 11

Sample 11

White powder obtained by chemical synthesis was subjected to FT-IR Spectroscopy for characterization. Various peaks in the graph correspond to the following compounds: Bands at 1457.27 cm^{-1} represent CO3- group. Bands at 472.58, 571.91, 603.74, 962 .51, 1046.42, 1091.75 cm^{-1} are because of $PO4^{3-}$ groups.

Table 14: List of Bands obtained in sample 11

group	bands
CO3-	1457.27 cm^{-1}
$PO4^{3-}$	472.58, 571.91, 603.74, 962 .51, 1046.42 , 1091.75 cm^{-1}
hydroxyapatite Synthesis	
OH^-	

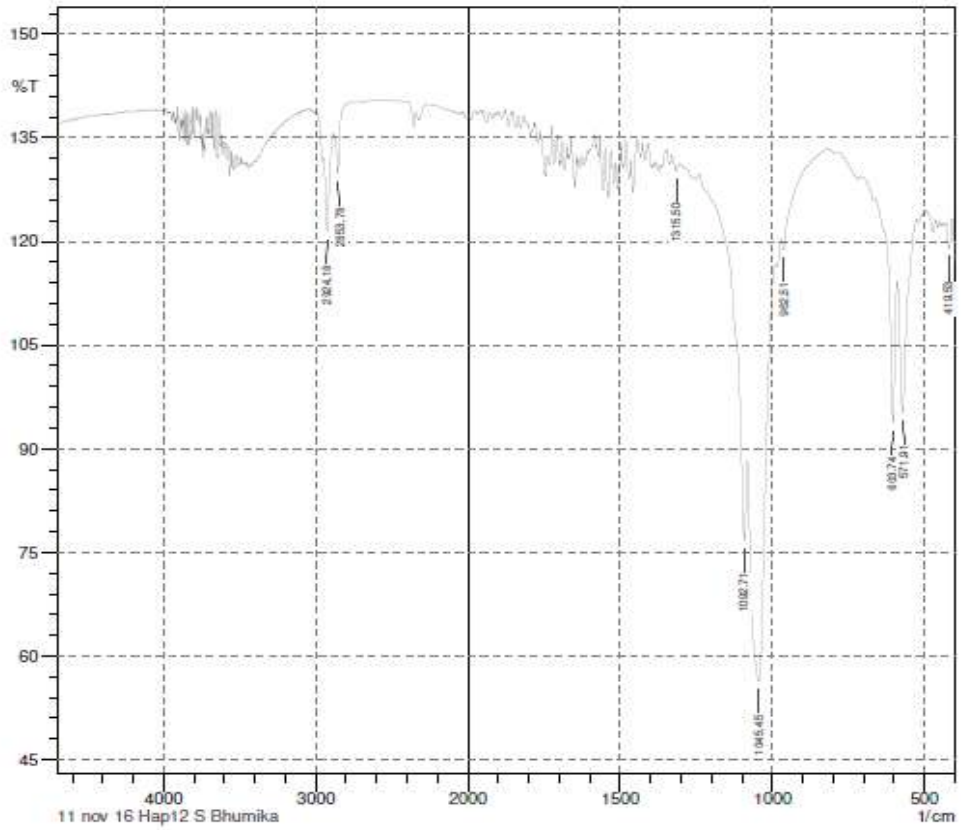

Comment;
11 nov 16 Hap12 S Bhumika

Date/Time; 11/11/2016 2:33:34 PM
No. of Scans;
Resolution;
Apodization;
User; Administrator

SHIMADZU

	Peak	Intensity	Corr. Inte	Base (H)	Base (L)	Area	Corr. Are
1	419.53	118.951	4.025	427.25	409.89	-1.408	0.153
2	571.91	95.198	21.621	590.24	525.62	-2.837	1.966
3	603.74	93.663	22.947	659.68	590.24	-4.228	1.298
4	962.51	118.808	2.494	971.19	867.03	-10.802	-0.349
5	1045.45	56.328	43.224	1082.1	989.52	9.75	10.357
6	1092.71	76.745	14.335	1241.23	1082.1	-8.958	-4.242
7	1315.5	130.207	1.607	1330.93	1303.92	-3.174	0.073
8	2853.78	129.803	6.895	2880.78	2762.16	-16.361	0.199
9	2924.18	121.436	11.886	2948.29	2880.78	-7.513	1.031

Graph 12: FTIR Result of Sample 12

Sample 12

White powder obtained by chemical synthesis was subjected to FT-IR Spectroscopy for characterization. Various peaks in the graph correspond to the following compounds: Bands at 1457.27 cm^{-1} and 872.82 cm^{-1}represent CO3- group. Bands at 571.91, 603.74, 962.51, 1045.45, 1092 .71 cm^{-1} are because of $PO4^{3-}$ groups.

Table 15: List of Bands obtained in sample 12

group	bands
CO3-	1457.27 cm^{-1} and 872.82 cm^{-1}
$PO4^{3-}$	571.91, 603.74, 962.51, 1045.45, 1092 .71 cm^{-1}
hydroxyapatite Synthesis	
OH^-	

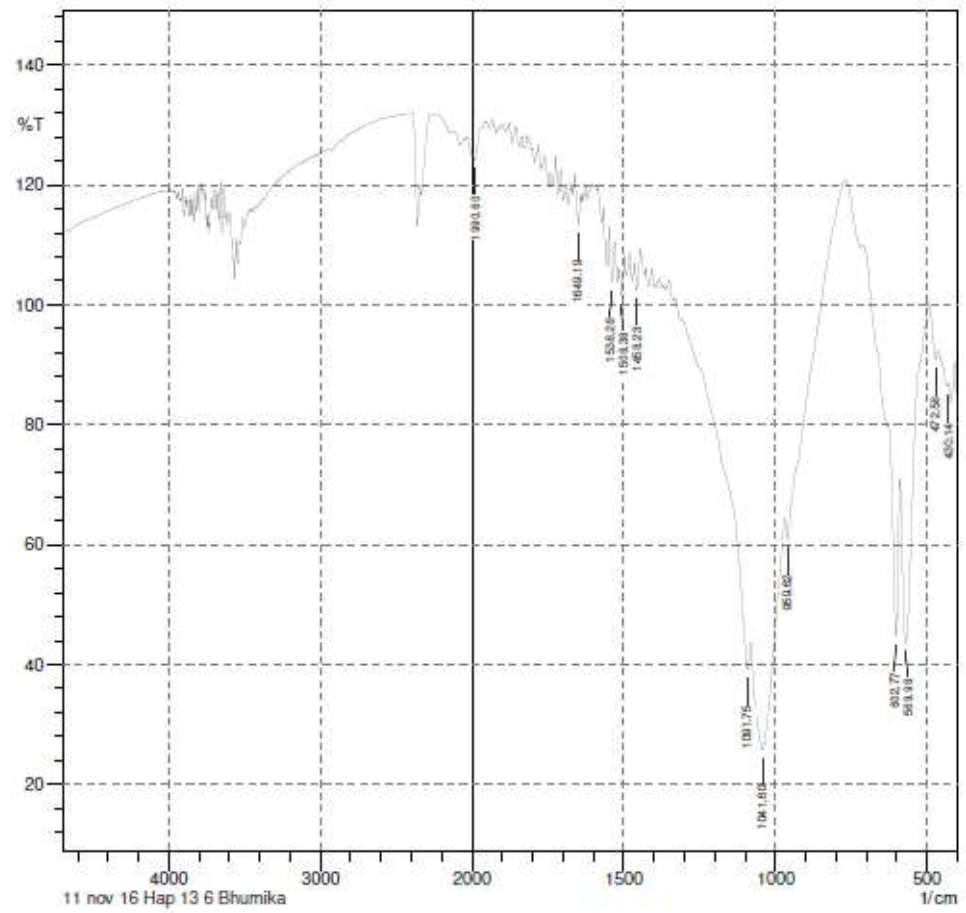

Comment;
11 nov 16 Hap 13 6 Bhumika

Date/Time; 11/11/2016 3:13:05 PM
No. of Scans;
Resolution;
Apodization;
User; Administrator

SHIMADZU

	Peak	Intensity	Corr. Inte	Base (H)	Base (L)	Area	Corr. Are
1	430.14	86.29	1.01	462.93	428.21	1.76	0.11
2	472.58	90.79	4.12	492.83	462.93	0.75	0.25
3	569.98	43.67	33.23	589.27	492.83	13.77	6.68
4	602.77	44.83	29.34	627.85	589.27	8.06	3.32
5	959.62	60.94	6.13	969.26	769.62	8.26	-2.63
6	1041.6	25.74	25.39	1082.1	969.26	47.5	16.43
7	1091.75	39.12	6.91	1308.75	1082.1	30.43	-11.42
8	1458.23	102.36	5.53	1464.98	1445.7	-0.4	0.26
9	1508.38	101.63	1.5	1515.14	1506.46	-0.12	0.03
10	1538.28	103.68	7.94	1548.89	1529.6	-0.57	0.36
11	1649.19	113.33	6.3	1661.73	1643.41	-1.24	0.23
12	1990.6	124.2	2.38	2000.25	1970.35	-3.03	0.11

Graph 13: FTIR Result of Sample 13

Sample 13

White powder obtained by chemical synthesis was subjected to FT-IR Spectroscopy for characterization. Various peaks in the graph correspond to the following compounds: Bands at 1424.48 cm-1 and 873.78 cm-1, cm^{-1}represent CO3- group. Bands at 1033.88, 962 .51and 603.74 cm^{-1} are because of $PO4^{3-}$ groups. Hydroxyapatite Synthesis is indicated by absence of peak at at 3422.8 cm^{-1} . Band at 565.16 cm^{-1} is due to OH− grouping. The bands of the $PO4^{3-}$ group are seen at at1650.16 and 711.76 cm^{-1}.

Table 16: List of Bands obtained in sample 13

group	bands
CO3-	1458.23 cm^{-1}
$PO4^{3-}$	472.58, 569.98, 602.77, 959.62 , 1041.6, 1091.75 cm^{-1}
hydroxyapatite Synthesis	
OH−	

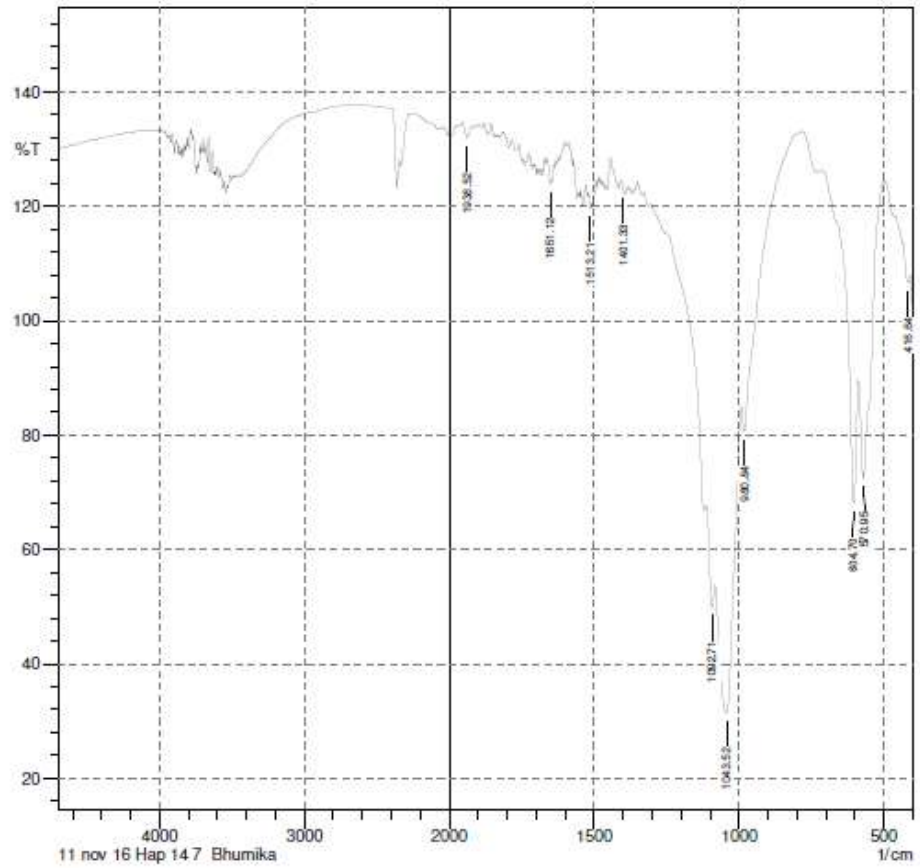

Comment;
11 nov 16 Hap 14 7 Bhumika

Date/Time; 11/11/2016 2:49:23 PM
No. of Scans;
Resolution;
Apodization;
User; Administrator

SHIMADZU

	Peak	Intensity	Corr. Inte	Base (H)	Base (L)	Area	Corr. Are
1	416.64	106.6	3.07	432.07	409.89	-0.78	0.2
2	570.95	72.36	24.35	588.31	503.44	1.83	3.83
3	604.7	68.16	26.97	681.86	588.31	0.28	1.96
4	980.84	80.59	7.34	993.37	782.16	-11.66	-5.94
5	1043.52	31.37	36	1082.1	993.37	29.68	14.6
6	1092.71	49.89	8.49	1113.93	1082.1	7.94	0.95
7	1401.33	123.02	0.26	1406.15	1400.37	-0.53	0
8	1513.21	119.56	0.86	1519.96	1511.28	-0.7	0.02
9	1651.12	123.9	1.48	1660.77	1648.23	-1.24	0.03
10	1938.52	131.98	2.21	1953.96	1927.92	-3.23	0.1

Graph 14: FTIR Result of Sample 14

Sample 14

White powder obtained by chemical synthesis was subjected to FT-IR Spectroscopy for characterization. Various peaks in the graph correspond to the following compounds: Bands at 1424.48 cm-1 and 873.78 cm-1, cm^{-1}represent CO3- group. Bands at 1033.88, 962 .51and 603.74 cm^{-1} are because of $PO4^{3-}$ groups. Hydroxyapatite. Synthesis is indicated by absence of peak at at 3422.8 cm^{-1} .. .Band at 565.16 cm^{-1} is due to OH− group. The bands of the PO4 3- groups are experiential at at1650.16 and 711.76 cm^{-1}.

Table 17: List of Bands obtained in sample 14

group	bands
CO3-	
$PO4^{3-}$	570.95, 604.7, 1043.52, 1092.71, cm^{-1}
hydroxyapatite Synthesis	
OH−	

Table 18: Comparison of Bands obtained in various samples

Standard	HAP 1	HAP 2	HAP 3	HAP 4	HAP 5	HAP 6	HAP 7	HAP 8	HAP 9	HAP 10	HAP 11	HAP 12	HAP 13	HAP 14
471				471.61	470.65		471.61				472.58		472.58	
564	567.09	566.13		565.16	565.16	565.16	564.2			570.95		571.91		570.95
602.7	604.7	603.74	603.74	603.74	603.74	603.74	602.77	604.7	604.7	604.7	603.74	603.74	602.77	604.7
631.1							631.71							
875.1	872.82	873.78	873.78	873.78	873.78	873.78	875.71	875.71	875.71	875.71				
961.5	962.51	961.55	962.51	962.51	962.51		961.55	960.58	960.58	961.55	962.51	962.51	959.62	
1032.92	1035.81	1036.77	1033.88	1034.84	1034.84	1033.88	1032.92							
1383.97				1385.9		1384.94	1383.97							
1417.73				1418.69	1417.73		1417.73	1416.76	1417.73	1415.8				
1457.27	1457.27			1457.27	1458.23		1457.27		1457.27		1457.27		1458.23	
1640.57		1637.62					1640.51		1639.55					
3443.03		3441.12			3443.05	3446.91	3443.05							
3567.46							3567.46			3566.5				

7.3 XRD ANALYSIS

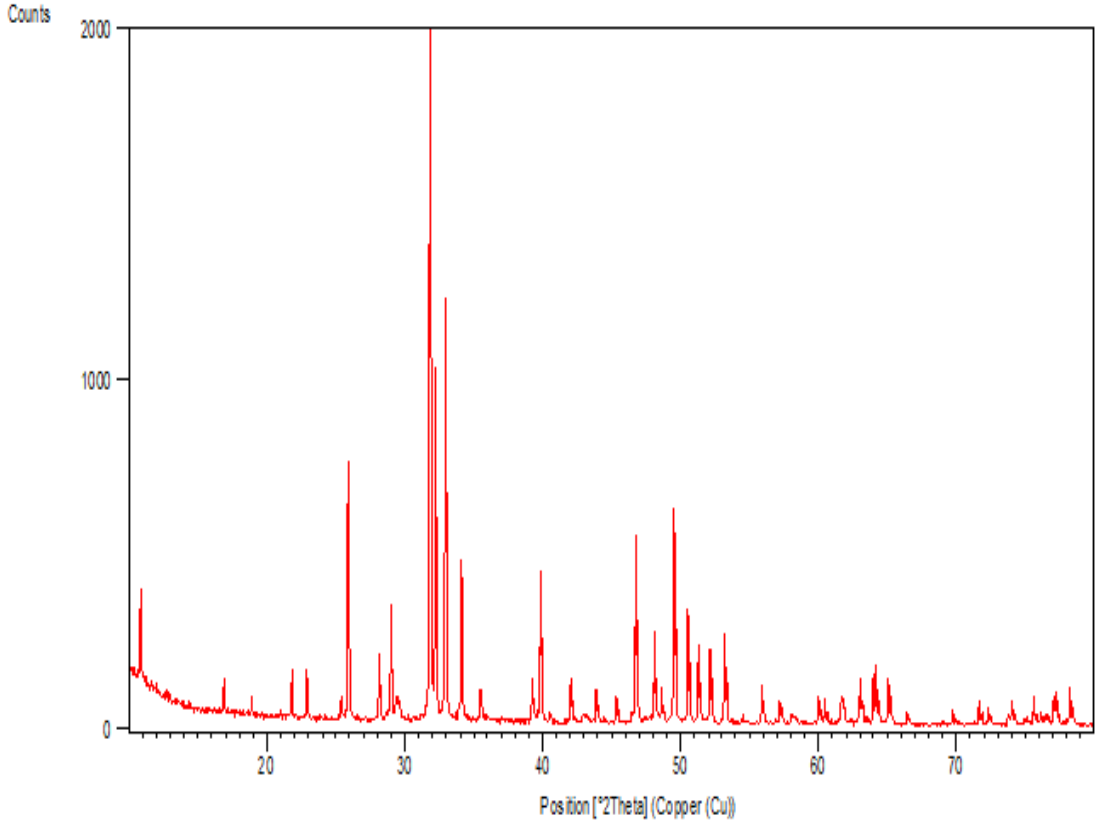

Graph 1: XRD analysis of HAP

XRD analysis of HAP prepared by Wet Chemical Method shows a peak of 200% intensity at 31.9^0 value of thata.

Various intensities obtained following XRD have been shown in table below-:

Table 19: Values of Intensity versus Theta Values

Intensity	Theta position
100	31.9

71	34.5
28.8	40

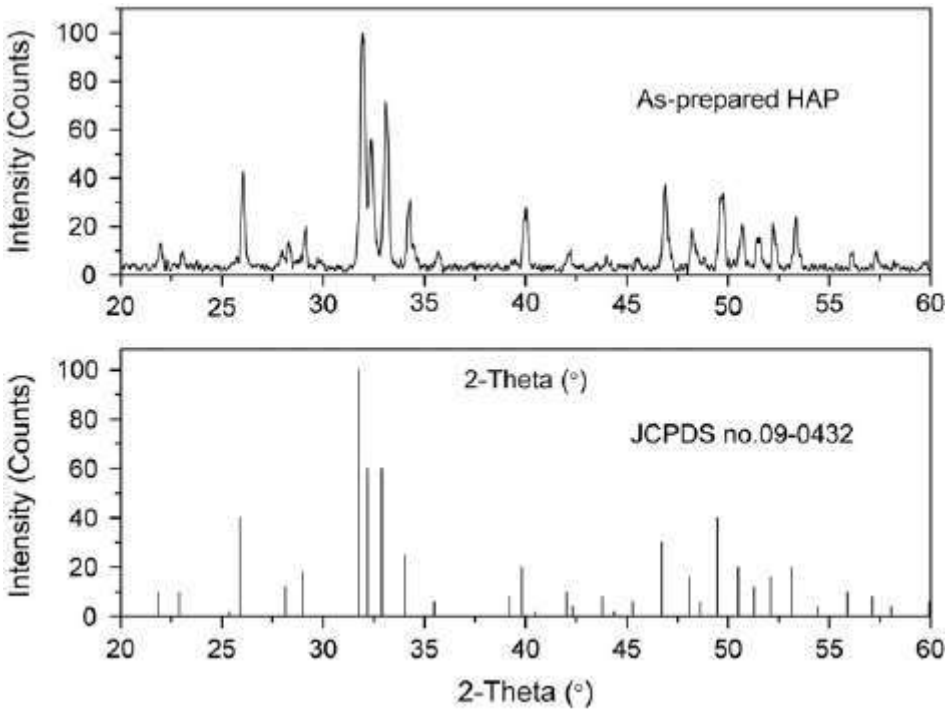

Graph 2: XRD Analysis of HAP

XRD analysis of HAP prepared by Wet Chemical Method shows a peak of 100% intensity at 31.9^0 value of thata, 71% intensity at 34.5^0 theta and 28.8% intensity at 40^0 theta.

Various intensities obtained following XRD have been shown in table below-:

Table 20: Values of Intensity versus Theta Values

Intensity	Theta position
100	31.9
71	34.5
28.8	40

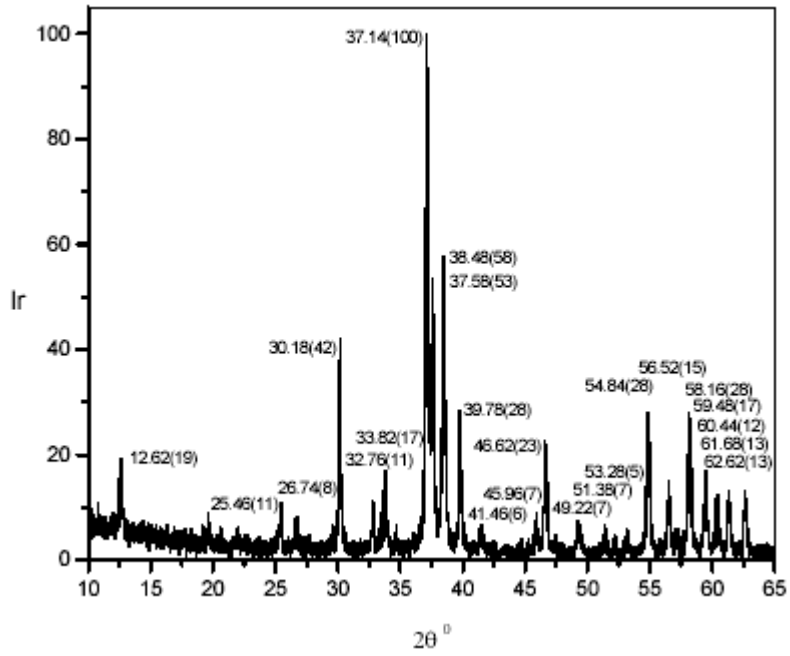

Graph 3: XRD Analysis of HAP

XRD analysis of HAP prepared by Wet Chemical Method shows a peak of 100% intensity at 37.14^0 value of thata, 58% intensity at 38.48^0 theta and 42% intensity at 30.18^0 theta.

Various intensities obtained following XRD have been shown in table below-:

Table 21: Values of Intensity versus Theta Values

Intensity	Theta position
13	62.62
17	59.48
07	51.38
06	41.46
100	37.14
58	38.48
53	37.58
42	30.18
19	12.62

The result of XRD Analysis confirms the purity sample of the HAP Sample synthesized by Wet Chemical Method and analyzed thereof. As per standards the 100% intensity is expected as a theta value lying between 30-35 degree and the sample in question satisfies the mentioned criterion .

At pH 9 peaks of X-RD Sample were obtained between 25-30 & 50-60. These disappear as pH is increased to 11 or 13. X-Ray peaks change due to: change in lattice parameter, residual stress

or impurity element, defect concentration. [Mishra, V.K. et. al. 2015] . . Silver doped HAP was synthesized at 1000^{o}C. XRD showed that the particles were fully crystalline. [Jadalannagari S. et al 2013].

7.4 SEM ANALYSIS

Morphology of Hydroxyapatite was studied by using S canning Electron Microscopy. Nanoparticles were seen. These were in an agglomerated state. These particles were spherical in shape with clump like arrangement. The powder had a significant level of agglomeration. The application and prospective use of nanodimensional and nanocrystalline calcium orthophosphates for a clinical repair of damaged bones and teeth are also known. For example, a greater viability and a better proliferation of various types of cells were detected on smaller crystals of calcium orthophosphates. [Dorozhkin, S.V. 2010]. It is notable that the aqueous temperature assumes a key part in the controlling the crystallite estimate, level of crystallinity and the stoichiometric proportion. HAP was in an exceptionally agglomerated form. [Anita L. J. 2015].

In a study conducted; needle shaped nanocrystals and capsule like nanostructures were obtained. The morphology of HAP can be varied by varying pH of the solution. The needle like structure change at microscopic level are more dense & homogeneous than at pH below 10. SEM Sample after undergoing calcination at 600^{0}C shows similar surface morphology (needle like Structure). But this is drastically changed on heating at 900^{0}C (Changes to capsule like structure). This deals with the synthesis of HAP using Calcium Nitrate & Diammonium Hydrogen ortho phosphate. [Mishra, V.K. et. al. 2015] .

Techniques used to study HAP characteristics include: X-RD, SEM, TEM, Raman Spectroscopy, [LIBS] Laser Induced Breakdown Spectroscopy. The morphology of HAP can be varied by varying pH of the solution. The needle like structure change at microscopic level are more dense & homogeneous than at pH below 10. EDTA acts as a to flower like structure on performing SEM. At pH above 10 followed by calcination the structures capping

or chelating agent. It helps to prevent agglomeration of particles. Other parameters include initial ingredients, physical & chemical conditions, Calcination temperature, Microwave Power, doping with a non-reacting metal. These lead to variation in the structure, shape, size, morphology and bonding pattern of HAP crystal. Also effects optical characteristics.

At pH 9 peaks of X-RD Sample were obtained between 25-30 & 50-60. These disappears as pH is increased to 11 or 13. X-Ray Peaks change due to: change in lattice parameter, residual stress or impurity element, defect concentration.

SEM Sample after undergoing calcination at 600^0C shows similar surface morphology (needle like Structure). But this is drastically changed on heating at 900^0C (Changes to capsule like structure). This deals with the synthesis of HAP using Calcium Nitrate & Diammonium Hydrogen ortho phosphate. Further the precipitated was made dry & washed .The chemical analysis of powders are carried out by atomic absorption spectroscopy, trimetry, gravimetry, spectrophotometry, FTIR, XRD , SEM . THE Ca : P ratio was assessed as 1.65

As per present study, the morphologies of as synthesized HAP powders are shown in figure below. Uncalcined HAP powder particles were almost regular and encircling in shape; but calcined HAP powder particles were found ouit to be agglomerated . Therefore SEM micrograph of the calcined powder established the presence of soft agglomerates that break up especially during their turnover into compact form. The microstructure as revealed from SEM is well in agreement with the particle size analysis the results.

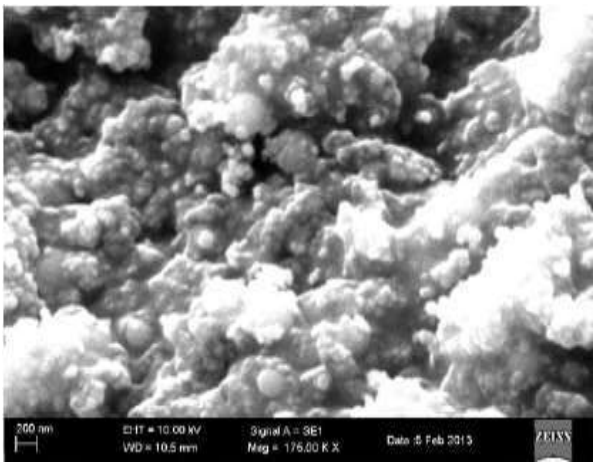

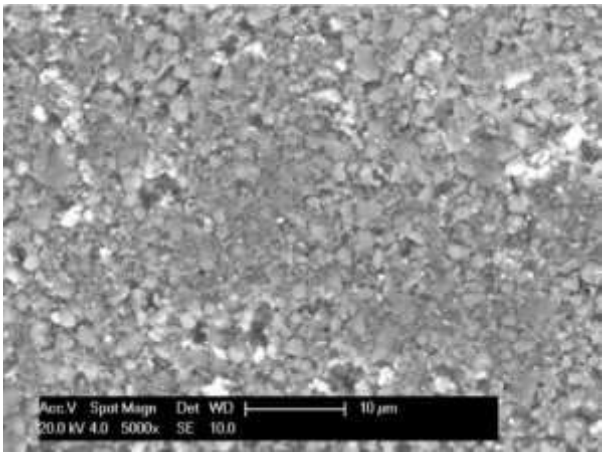

Graph 4: SEM image of hydroxyapatite

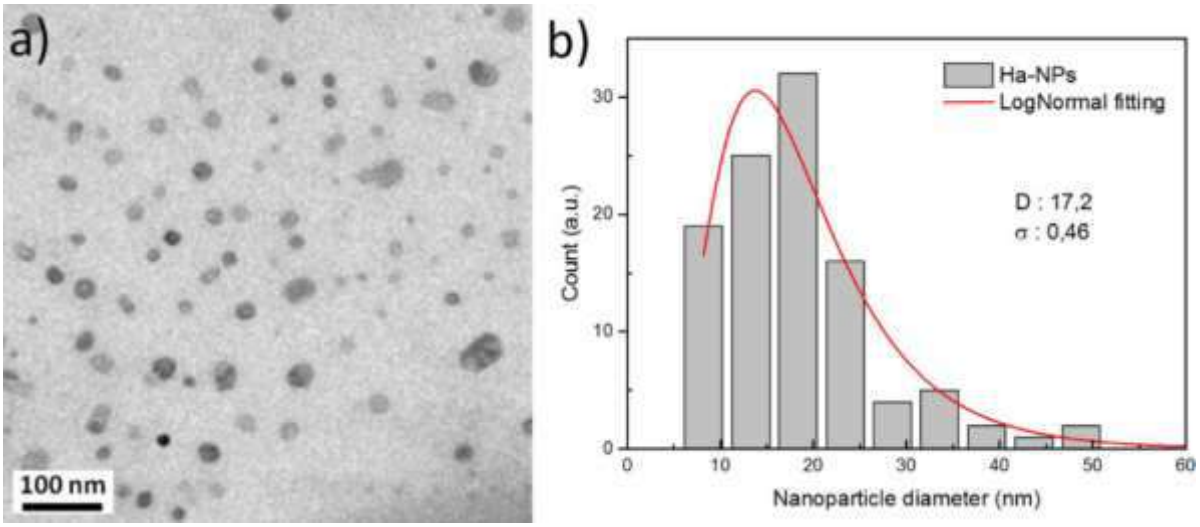

Graph5: Particle size distribution graph (for SEM)

7.5 TEM ANALYSIS

TEM is done to confirm the structure of Hydroxyapatite. Size and Morphology are confirmed by using TEM. Here particle size is about. TEM provides detailed microscopic features of a substance. The prepared Hydroxyapatite sample is found to be highly pure with minimal levels of specific impurities which can be neglected. HAP Particles look like needles. The infrastructure of crystal shows some fine holes.

Crystallinity is affected by calcination. Size of the p[articles increases with increase in calcination temperature.[Kapoor,s. et.al.,2011] . The dimension of nanorods was found to be 100nm x 10nm. [Mishra, V.K. et al 2015] . Silver doped HAP was synthesized at 1000^{o}C. These had hexagonal structure and size of 25 nm. [Jadalannagari S. et al 2013].

Hydroxyapatite particles had a size ranging between 50-70 nm.

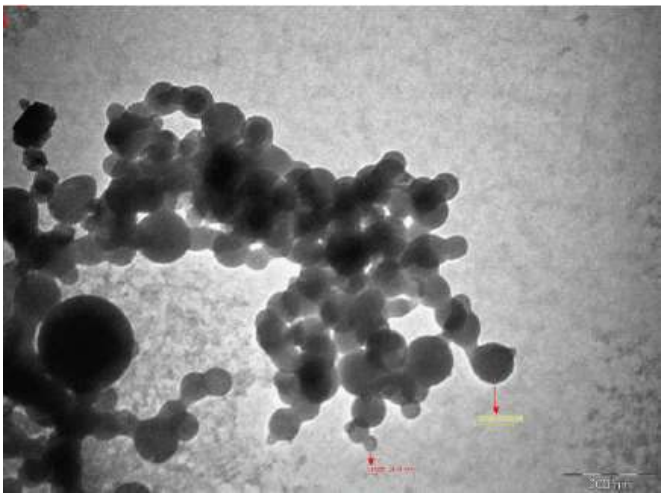

Graph6: TEM image of the HA mineral

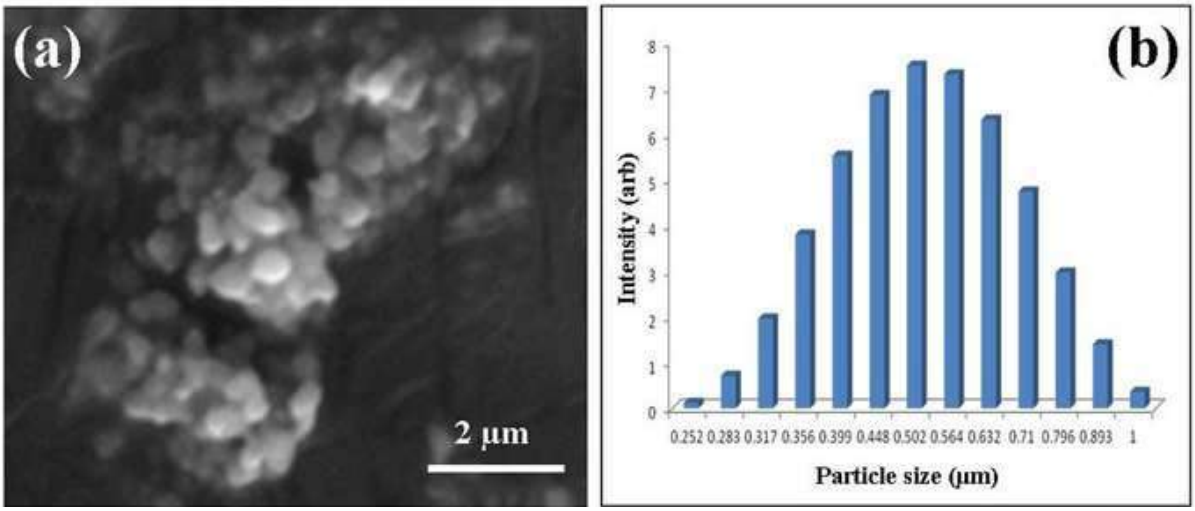

Graph7: Particle size distribution graph (for TEM image)

7.6 Preparation of Pellets

Pellets are successfully prepared using appropriate materials ie HAP, Amla, Clove, Haldi, Binders and dye and punch

7.7 STUDY OF ANTIMICROBIAL EFFCACY

7.7.1 Well Diffusion Method

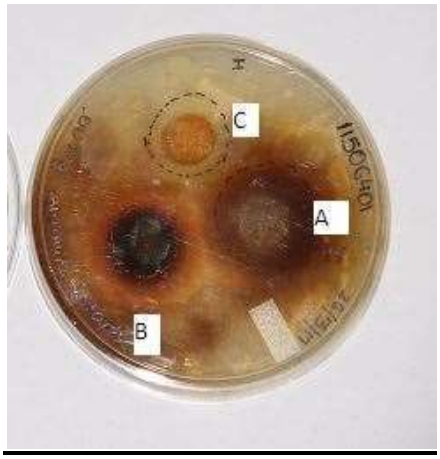

Figure 1. Nutient Agar Petri Plates with growth of E.coli having punched out wells carrying 100% Amla or Clove or Tumeric; showing Zones of Inhibition.

In this figure no.1. , A depicts amla, B depicts Clove and C depicts Turmeric.

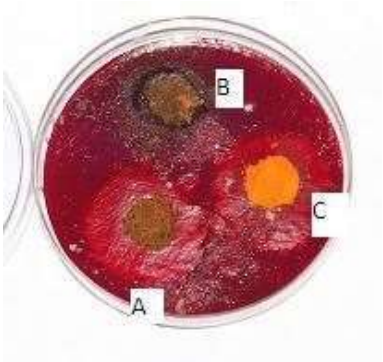

Figure 2. MacConkey's Agar Petri Plates with growth of E.coli having punched out wells carrying 100% Amla or Clove or Tumeric; showing Zones of Inhibition
In this figure no.2. , A depicts amla, B depicts Clove and C depicts Turmeric.

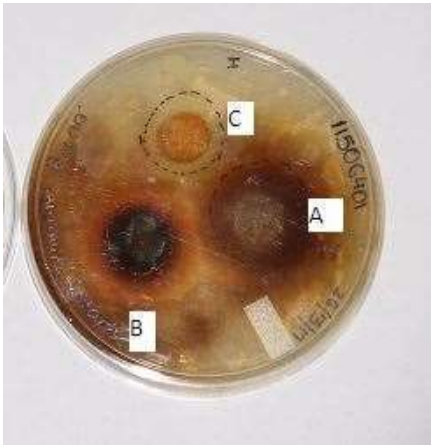

Figure 3. Nutient Agar Petri Plates with growth of S.aureus having punched out wells carrying 100% Amla or Clove or Tumeric ; showing Zones of Inhibition

In this figure no.3., A depicts amla, B depicts Clove and C depicts Turmeric.

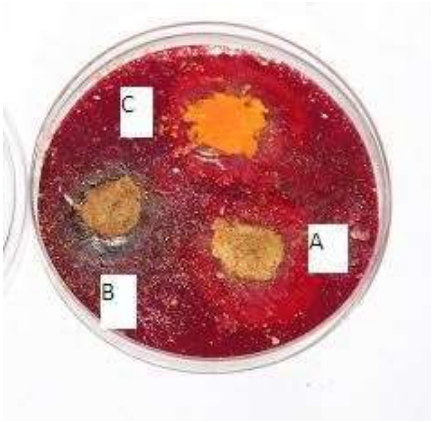

Figure 4. MacConkey's Agar Petri Plates with growth of S.aureus having punched out wells carrying 100% Amla or Clove or Tumeric; showing Zones of Inhibition
In this figure no.4., A depicts amla, B depicts Clove and C depicts Turmeric.

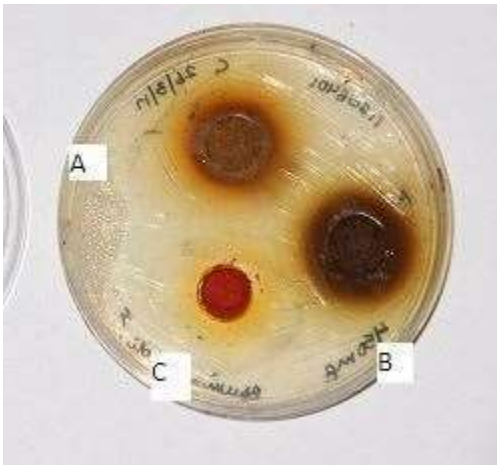

Figure 5. Nutient Agar Petri Plates with growth of E.coli having punched out wells carrying 20% HAP and 80% Amla or Clove or Tumeric ; showing Zones of Inhibition

In this figure no.5., A depicts amla, B depicts Clove and C depicts Turmeric.

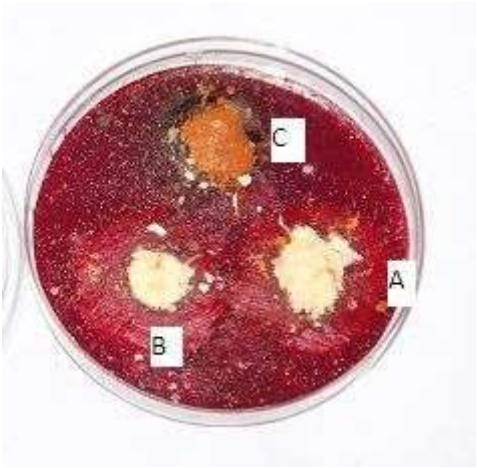

Figure 6. MacConkey's Agar Petri Plates with growth of E.coli having punched out wells carrying20% HAP and 80% Amla or Clove or Tumeric ; showing Zones of Inhibition
In this figure no.6., A depicts amla, B depicts Clove and C depicts Turmeric.

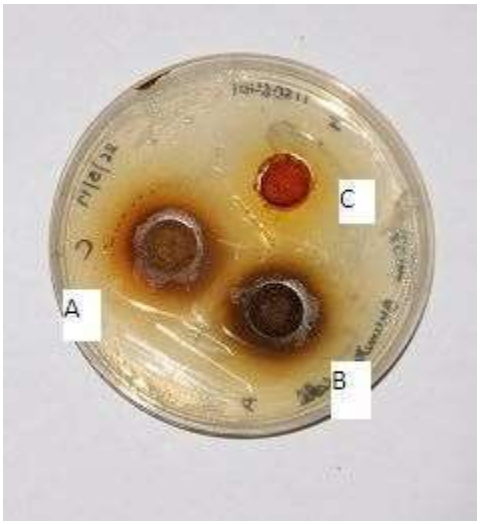

Figure 7. Nutient Agar Petri Plates with growth of S.aureus having punched out wells carrying 20% HAP and 80% Amla or Clove or Tumeric ; showing Zones of Inhibition

In this figure no.7., A depicts amla, B depicts Clove and C depicts Turmeric.

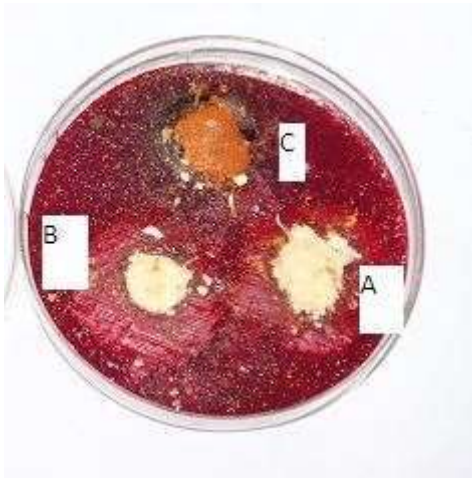

Figure 8. MacConkey's Agar Petri Plates with growth of S.aureus having punched out wells carrying 20% HAP and 80% Amla or Clove or Tumeric ; showing Zones of Inhibition
In this figure no.8., A depicts amla, B depicts Clove and C depicts Turmeric.

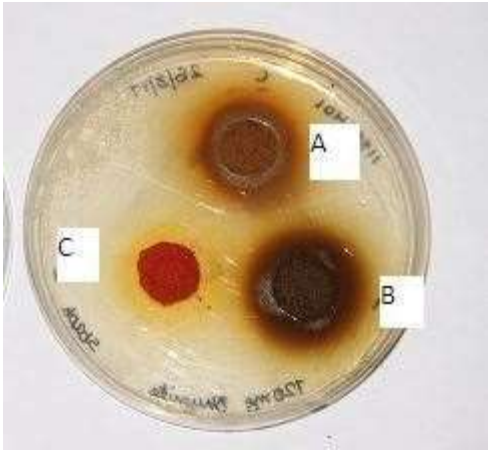

Figure 9. Nutient Agar Petri Plates with growth of E.coli having punched out wells carrying 50% HAP and 50% Amla or Clove or Tumeric ; showing Zones of Inhibition
In this figure no.9., A depicts amla, B depicts Clove and C depicts Turmeric.

Figure 10. MacConkey's Agar Petri Plates with growth of E.coli having punched out wells carrying 50% HAP and 50% Amla or Clove or Tumeric ; showing Zones of Inhibition

In this figure no.10., A depicts amla, B depicts Clove and C depicts Turmeric.

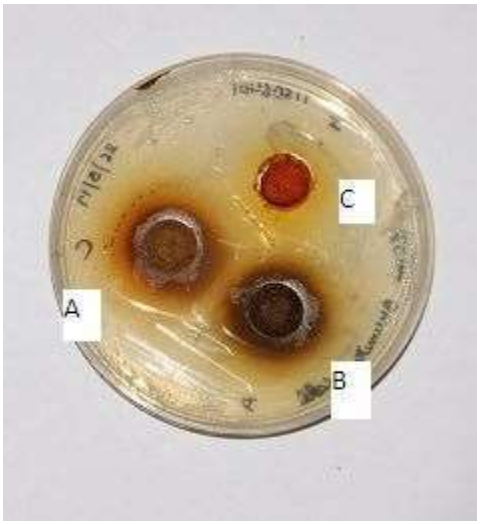

Figure 11. Nutient Agar Petri Plates with growth of S.aureus having punched out wells carrying wells containing 50% HAP and 50% Amla or Clove or Tumeric ; showing Zones of Inhibition

In this figure no.11., A depicts amla, B depicts Clove and C depicts Turmeric.

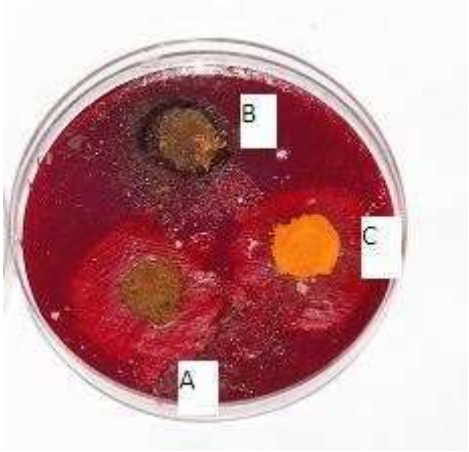

Figure 12. MacConkey's Agar Petri Plates with growth of S.aureus having punched out wells carrying 50% HAP and 50% Amla or Clove or Tumeric ; showing Zones of Inhibition

In this figure no.12., A depicts amla, B depicts Clove and C depicts Turmeric.

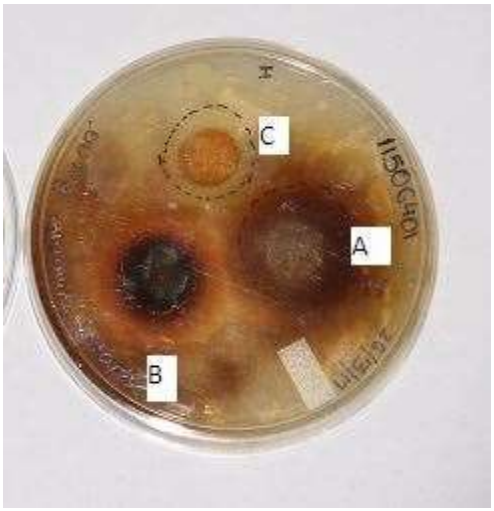

Figure 13. Nutient Agar Petri Plates with growth of E.coli having punched out wells carrying 20% HAP and 80% Amla or Clove or Tumeric ; showing Zones of Inhibition

In this figure no.13., A depicts amla, B depicts Clove and C depicts Turmeric.

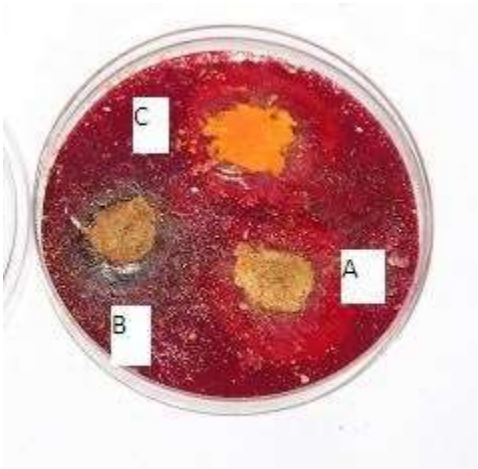

Figure 14. MacConkey's Agar Petri Plates with growth of E.coli having punched out wells carrying 20% HAP and 80% Amla or Clove or Tumeric ; showing Zones of Inhibition.

In this figure no.14., A depicts amla, B depicts Clove and C depicts Turmeric**.**

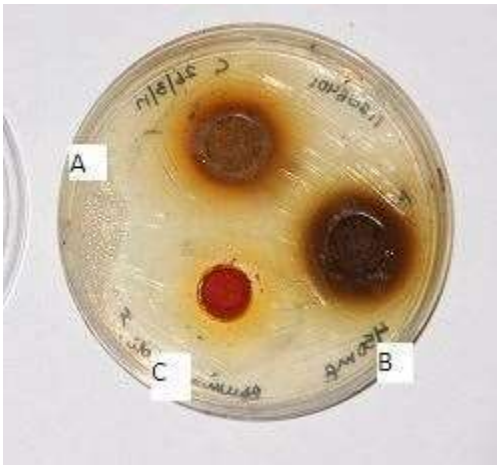

Figure 15. Nutient Agar Petri Plates with growth of S.aureus having punched out wells carrying 20% HAP and 80% Amla or Clove or Tumeric ; showing Zones of Inhibition

In this figure no.15., A depicts amla, B depicts Clove and C depicts Turmeric.

Figure 16. MacConkey's Agar Petri Plates with growth of S.aureus having punched out wells carrying 20% HAP and 80% Amla or Clove or Tumeric ; showing Zones of Inhibition

In this figure no.16., A depicts amla, B depicts Clove and C depicts Turmeric.

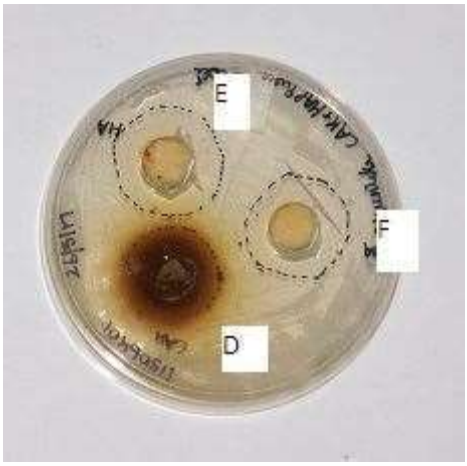

Figure 17. Nutient Agar Petri Plates with growth of E.coli having punched out wells carrying 100% HAP in two wells and a mixture of equal amounts of Amla, Clove and Tumericie 33.33% each in third well ; showing Zones of Inhibition

In this figure no. 17., A depicts a mixture of Clove, Amla and Turmeric. B and C depict pure HAP.

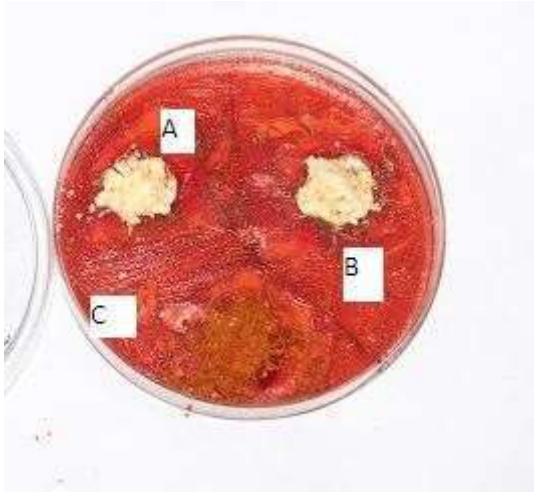

Figure 18. MacConkey's Agar Petri Plates with growth of E.coli having punched out wells carrying 100% HAP in two wells and a mixture of equal amounts of Amla, Clove and Tumericie 33.33% each in third well ; showing Zones of Inhibition
In this figure no. 18., A depicts a mixture of Clove, Amla and Turmeric. B and C depict pure HAP.

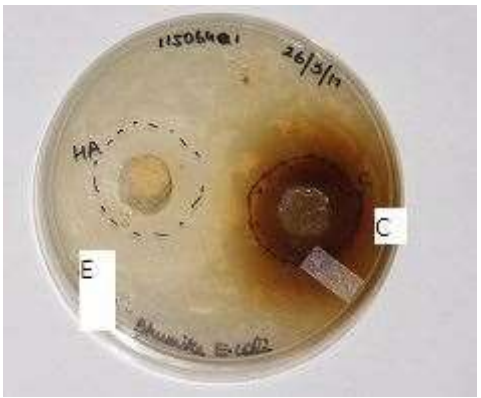

Figure 19. Nutient Agar Petri Plates with growth of S.aureus having punched out wells carrying 100% HAP in two wells and a mixture of equal amounts of Amla, Clove and Tumericie 33.33% each in third well ; showing Zones of Inhibition

In this figure no. 19., A depicts a mixture of Clove, Amla and Turmeric. B and C depict pure HAP.

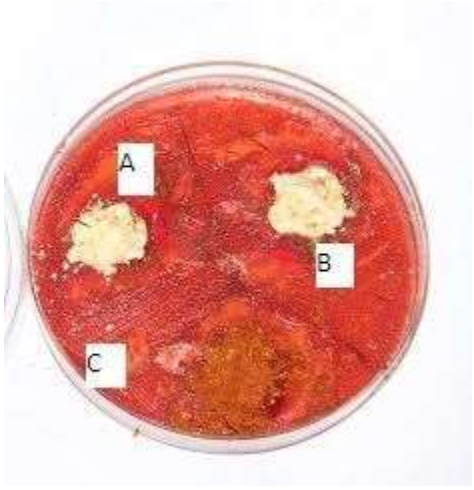

Figure 20. MacConkey's Agar Petri Plates with growth of S.aureus having punched out wells carrying 100% HAP in two wells and a mixture of equal amounts of Amla, Clove and Tumericie 33.33% each in third well ; showing Zones of Inhibition

In this figure no. 20., A depicts a mixture of Clove, Amla and Turmeric. B and C depict pure HAP.

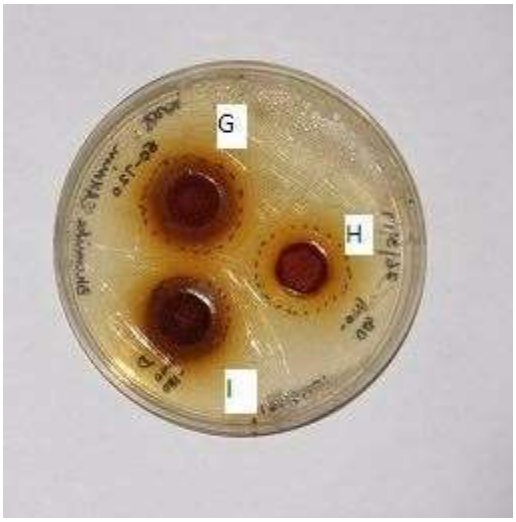

Figure 21. Nutient Agar Petri Plates with growth of E.coli having punched out wells carrying a mixture of 80% HAP and 20% Amla , Clove and Tumeric in equal amounts in first well ; a mixture of 50% HAP and 50% Amla , Clove and Tumeric in equal amounts in second well; a mixture of 20% HAP and 80% Amla , Clove and Tumeric in equal amounts in third well ; showing Zones of Inhibition

In this figure no. 21., A depicts a mixture of 80% HAP and 20% Amla , Clove and Turmeric in equal amounts. B depicts a mixture of 50% HAP and 50% Amla , Clove and Turmeric in

equal amounts. C depicts a mixture of 20% HAP and 80% Amla , Clove and Turmeric in equal amounts.

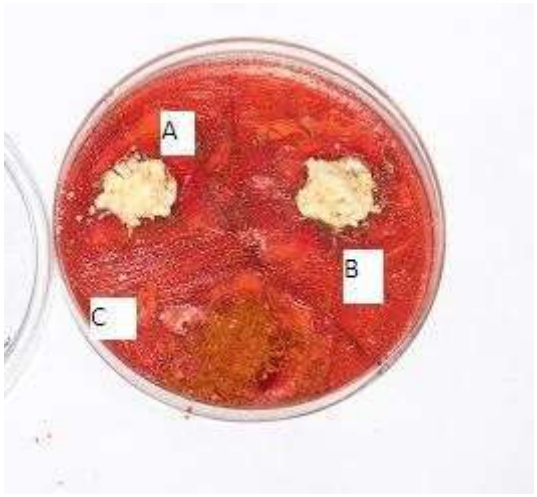

Figure 22. MacConkey's Agar Petri Plates with growth of E.coli having punched out wells carrying a mixture of 80% HAP and 20% Amla , Clove and Tumeric in equal amounts in first well ; a mixture of 50% HAP and 50% Amla , Clove and Tumeric in equal amounts in second well; a mixture of 20% HAP and 80% Amla , Clove and Tumeric in equal amounts in third well ; showing Zones of Inhibition

In this figure no. 22., A depicts a mixture of 80% HAP and 20% Amla , Clove and Turmeric in equal amounts. B depicts a mixture of 50% HAP and 50% Amla , Clove and Turmeric in equal amounts. C depicts a mixture of 20% HAP and 80% Amla , Clove and Turmeric in equal amounts.

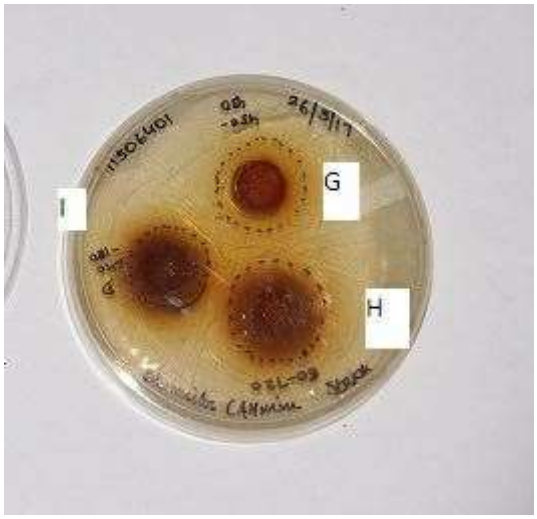

Figure 23. Nutient Agar Petri Plates with growth of S.aureus having punched out wells carrying a mixture of 80% HAP and 20% Amla , Clove and Tumeric in equal amounts in first well ; a mixture of 50% HAP and 50% Amla , Clove and Tumeric in equal amounts in second well; a mixture of 20% HAP and 80% Amla , Clove and Tumeric in equal amounts in third well ; showing Zones of Inhibition

In this figure no. 23., A depicts a mixture of 80% HAP and 20% Amla , Clove and Turmeric in equal amounts. B depicts a mixture of 50% HAP and 50% Amla , Clove and Turmeric in

equal amounts. C depicts a mixture of 20% HAP and 80% Amla , Clove and Turmeric in equal amounts.

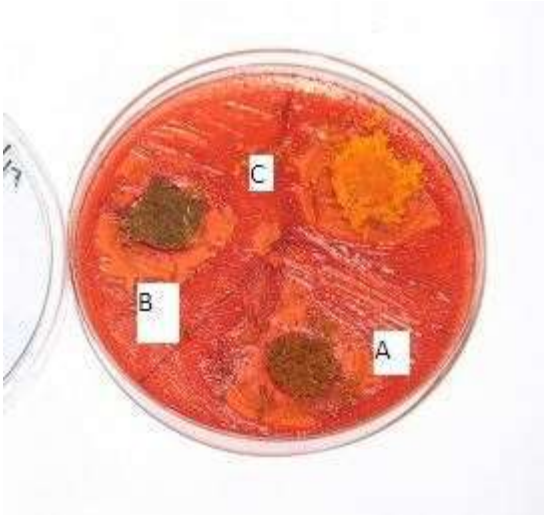

Figure 24. MacConkey's Agar Petri Plates with growth of S.aureus having punched out wells carrying a mixture of 80% HAP and 20% Amla , Clove and Tumeric in equal amounts in first well ; a mixture of 50% HAP and 50% Amla , Clove and Tumeric in equal amounts in second well; a mixture of 20% HAP and 80% Amla , Clove and Tumeric in equal amounts in third well ; showing Zones of Inhibition

In this figure no. 24., A depicts a mixture of 80% HAP and 20% Amla , Clove and Turmeric in equal amounts. B depicts a mixture of 50% HAP and 50% Amla , Clove and Turmeric in equal amounts. C depicts a mixture of 20% HAP and 80% Amla , Clove and Turmeric in equal amounts.

7.7.2 Pellet [Disk] Diffusion Method

Figure 1. Nutient Agar Petri Plates with growth of E.coli having punched out wells carrying 100% Amla or Clove or Tumeric; showing Zones of Inhibition

In this figure no.1., A depicts amla, B depicts Clove and C depicts Turmeric.

Figure 2. MacConkey's Agar Petri Plates with growth of E.coli having punched out wells carrying 100% Amla or Clove or Tumeric; showing Zones of Inhibition

In this figure no.2., A depicts amla, B depicts Clove and C depicts Turmeric.

Figure 3. Nutient Agar Petri Plates with growth of S.aureus having punched out wells carrying 100% Amla or Clove or Tumeric ; showing Zones of Inhibition

In this figure no.3., A depicts amla, B depicts Clove and C depicts Turmeric.

Figure 4. MacConkey's Agar Petri Plates with growth of S.aureus having punched out wells carrying 100% Amla or Clove or Tumeric; showing Zones of Inhibition
In this figure no.4., A depicts amla, B depicts Clove and C depicts Turmeric.

Figure 5. Nutrient Agar Petri Plates with growth of E.coli having punched out wells carrying 20% HAP and 80% Amla or Clove or Tumeric; showing Zones of Inhibition
In this figure no.5., A depicts amla, B depicts Clove and C depicts Turmeric.

Figure 6. MacConkey's Agar Petri Plates with growth of E.coli having punched out wells carrying20% HAP and 80% Amla or Clove or Tumeric showing Zones of Inhibition
In this figure no.6., A depicts amla, B depicts Clove and C depicts Turmeric.

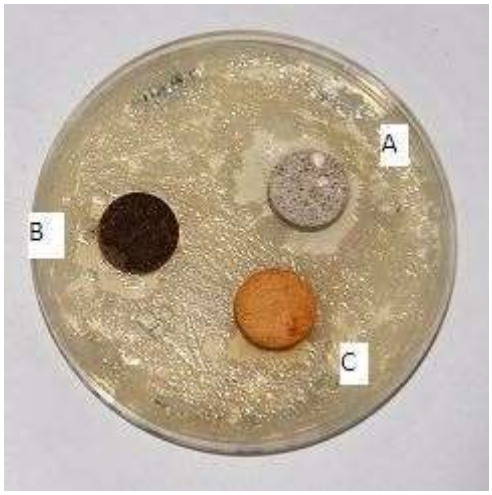

Figure 7. Nutient Agar Petri Plates with growth of S.aureus having punched out wells carrying 20% HAP and 80% Amla or Clove or Tumeric ; showing Zones of Inhibition
In this figure no.7., A depicts amla, B depicts Clove and C depicts Turmeric.

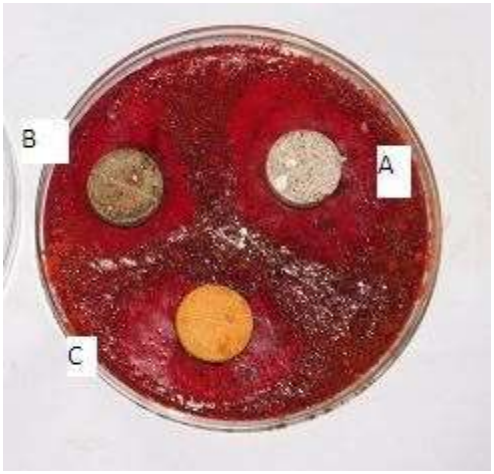

Figure 8. MacConkey's Agar Petri Plates with growth of S.aureus having punched out wells carrying 20% HAP and 80% Amla or Clove or Tumeric ; showing Zones of Inhibition
In this figure no.8., A depicts amla, B depicts Clove and C depicts Turmeric.

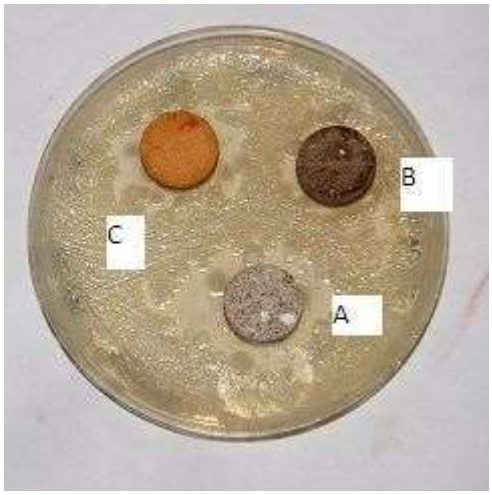

Figure 9. Nutient Agar Petri Plates with growth of E.coli having punched out wells carrying 50% HAP and 50% Amla or Clove or Tumeric ; showing Zones of Inhibition
In this figure no.9., A depicts amla, B depicts Clove and C depicts Turmeric.

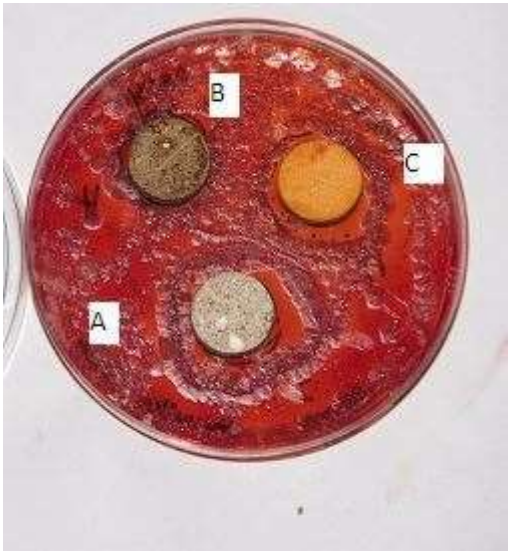

Figure 10. MacConkey's Agar Petri Plates with growth of E.coli having punched out wells carrying 50% HAP and 50% Amla or Clove or Tumeric ; showing Zones of Inhibition

In this figure no.10., A depicts amla, B depicts Clove and C depicts Turmeric.

.

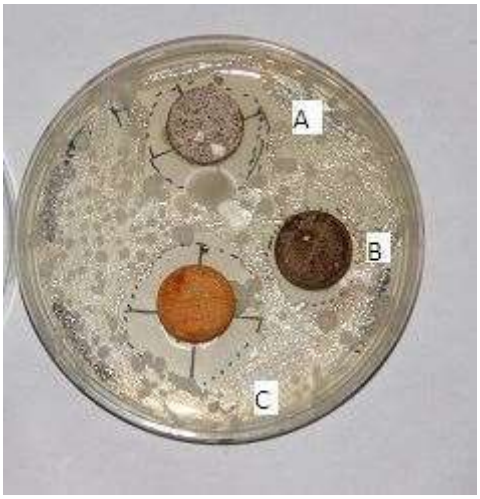

Figure 11. Nutient Agar Petri Plates with growth of S.aureus having punched out wells carrying wells containing 50% HAP and 50% Amla or Clove or Tumeric ; showing Zones of Inhibition

In this figure no.11., A depicts amla, B depicts Clove and C depicts Turmeric.

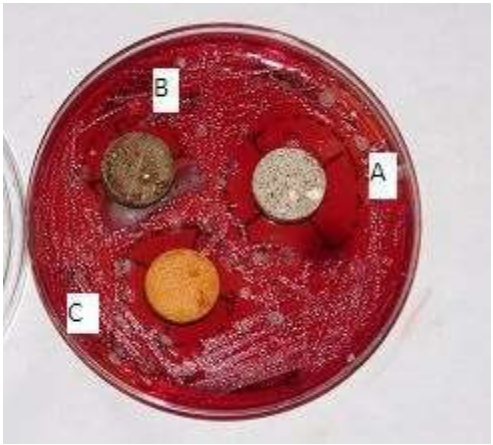

Figure 12. MacConkey's Agar Petri Plates with growth of S.aureus having punched out wells carrying 50% HAP and 50% Amla or Clove or Tumeric ; showing Zones of Inhibition

In this figure no.12., A depicts amla, B depicts Clove and C depicts Turmeric.

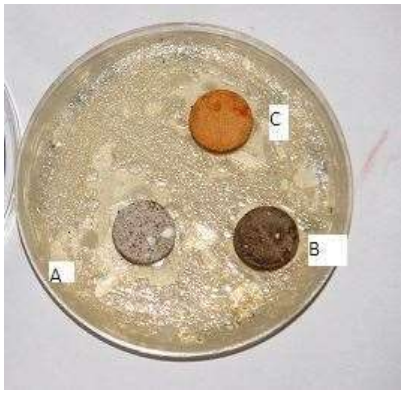

Figure 13. Nutient Agar Petri Plates with growth of E.coli having punched out wells carrying 20% HAP and 80% Amla or Clove or Tumeric ; showing Zones of Inhibition

In this figure no.13., A depicts amla, B depicts Clove and C depicts Turmeric

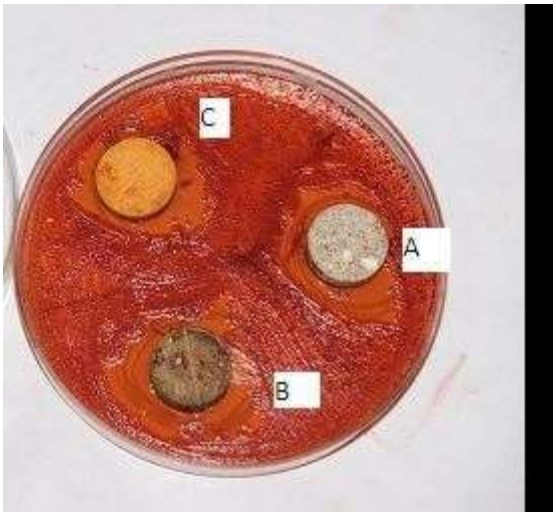

Figure 14. MacConkey's Agar Petri Plates with growth of E.coli having punched out wells carrying 20% HAP and 80% Amla or Clove or Tumeric ; showing Zones of Inhibition

In this figure no.14., A depicts amla, B depicts Clove and C depicts Turmeric**.**

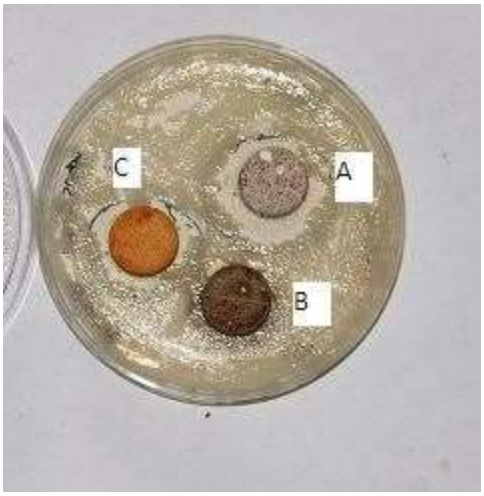

Figure 15. Nutient Agar Petri Plates with growth of S.aureus having punched out wells carrying 20% HAP and 80% Amla or Clove or Tumeric ; showing Zones of Inhibition

In this figure no.15., A depicts amla, B depicts Clove and C depicts Turmeric.

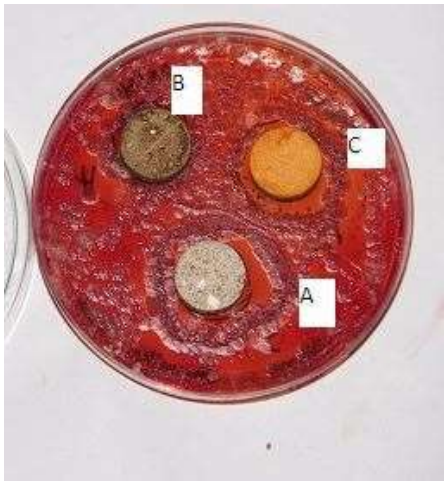

Figure 16. MacConkey's Agar Petri Plates with growth of S.aureus having punched out wells carrying 20% HAP and 80% Amla or Clove or Tumeric ; showing Zones of Inhibition

In this figure no.16., A depicts amla, B depicts Clove and C depicts Turmeric.

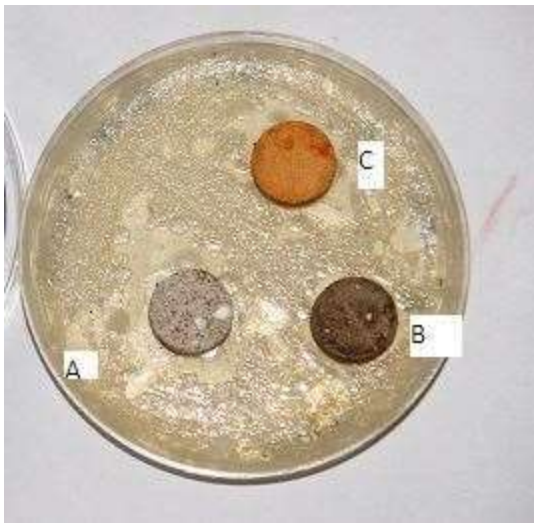

Figure 17. Nutient Agar Petri Plates with growth of E.coli having punched out wells carrying 100% HAP in two wells and a mixture of equal amounts of Amla, Clove and Tumericie 33.33% each in third well ; showing Zones of Inhibition

In this figure no. 17., A depicts a mixture of Clove, Amla and Turmeric. B and C depict pure HAP.

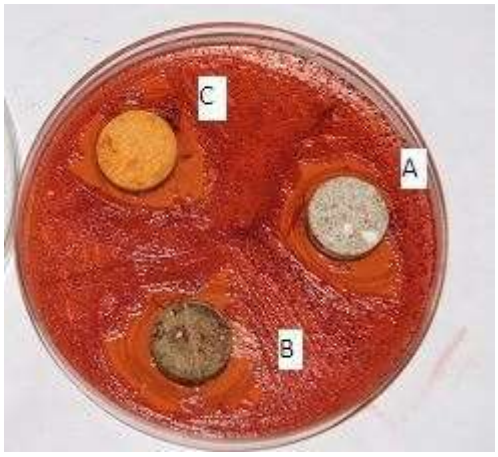

Figure 18. MacConkey's Agar Petri Plates with growth of E.coli having punched out wells carrying 100% HAP in two wells and a mixture of equal amounts of Amla, Clove and Tumericie 33.33% each in third well ; showing Zones of Inhibition

In this figure no. 18., A depicts a mixture of Clove, Amla and Turmeric. B and C depict pure HAP.

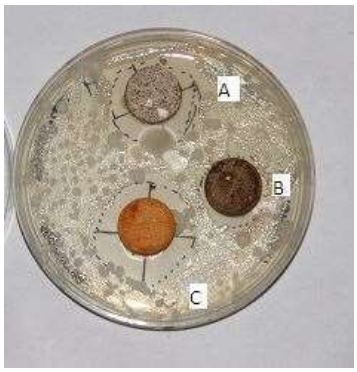

Figure 19. Nutient Agar Petri Plates with growth of S.aureus having punched out wells carrying 100% HAP in two wells and a mixture of equal amounts of Amla, Clove and Tumericie 33.33% each in third well ; showing Zones of Inhibition

In this figure no. 19., A depicts a mixture of Clove, Amla and Turmeric. B and C depict pure HAP.

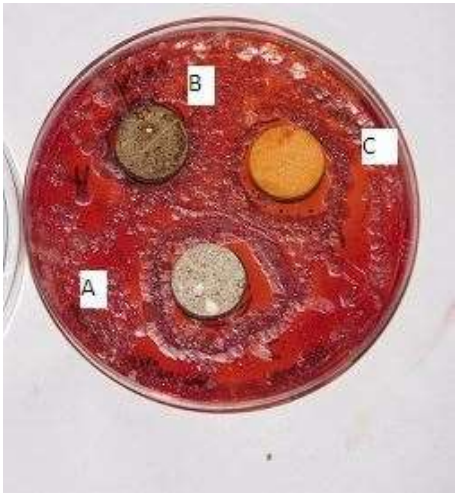

Figure 20. MacConkey's Agar Petri Plates with growth of S.aureus having punched out wells carrying 100% HAP in two wells and a mixture of equal amounts of Amla, Clove and Tumericie 33.33% each in third well ; showing Zones of Inhibition

In this figure no. 20., A depicts a mixture of Clove, Amla and Turmeric. B and C depict pure HAP.

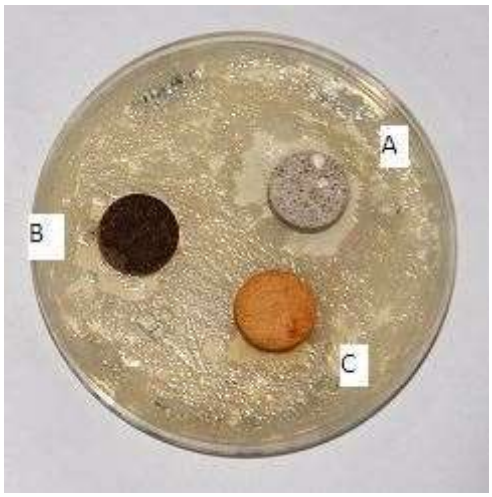

Figure 21. Nutient Agar Petri Plates with growth of E.coli having punched out wells carrying a mixture of 80% HAP and 20% Amla , Clove and Tumeric in equal amounts in first well ; a mixture of 50% HAP and 50% Amla , Clove and Tumeric in equal amounts in second well; a mixture of 20% HAP and 80% Amla , Clove and Tumeric in equal amounts in third well ; showing Zones of Inhibition

In this figure no. 21., A depicts a mixture of 80% HAP and 20% Amla , Clove and Turmeric in equal amounts. B depicts a mixture of 50% HAP and 50% Amla , Clove and Turmeric in equal amounts. C depicts a mixture of 20% HAP and 80% Amla , Clove and Turmeric in equal amounts.

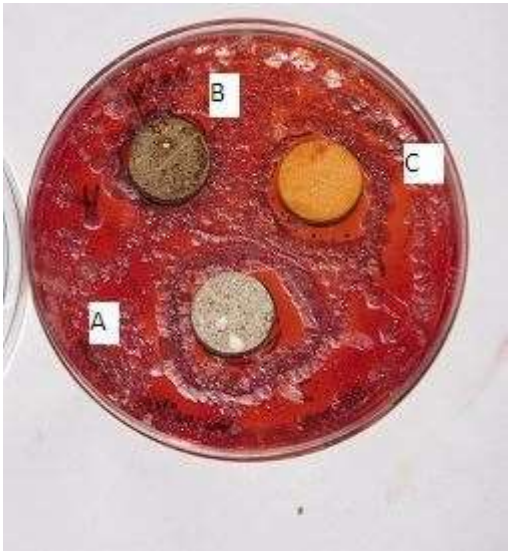

Figure 22. MacConkey's Agar Petri Plates with growth of E.coli having punched out wells carrying a mixture of 80% HAP and 20% Amla , Clove and Tumeric in equal amounts in first well ; a mixture of 50% HAP and 50% Amla , Clove and Tumeric in

equal amounts in second well; a mixture of 20% HAP and 80% Amla , Clove and Tumeric in equal amounts in third well ; showing Zones of Inhibition

In this figure no. 22., A depicts a mixture of 80% HAP and 20% Amla , Clove and Turmeric in equal amounts. B depicts a mixture of 50% HAP and 50% Amla , Clove and Turmeric in equal amounts. C depicts a mixture of 20% HAP and 80% Amla , Clove and Turmeric in equal amounts.

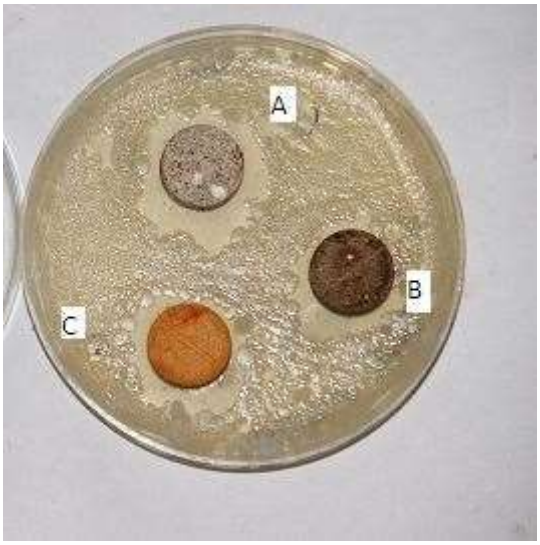

Figure 23. Nutient Agar Petri Plates with growth of S.aureus having punched out wells carrying a mixture of 80% HAP and 20% Amla , Clove and Tumeric in equal amounts in first well ; a mixture of 50% HAP and 50% Amla , Clove and Tumeric in equal amounts in second well; a mixture of 20% HAP and 80% Amla , Clove and Tumeric in equal amounts in third well ; showing Zones of Inhibition

In this figure no. 23., A depicts a mixture of 80% HAP and 20% Amla , Clove and Turmeric in equal amounts. B depicts a mixture of 50% HAP and 50% Amla , Clove and Turmeric in equal amounts. C depicts a mixture of 20% HAP and 80% Amla , Clove and Turmeric in equal amounts.

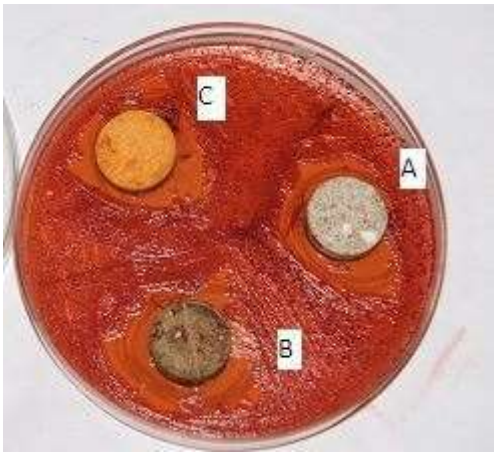

Figure 24. MacConkey's Agar Petri Plates with growth of S.aureus having punched out wells carrying a mixture of 80% HAP and 20% Amla, Clove and Tumeric in equal amounts in first well ; a mixture of 50% HAP and 50% Amla , Clove and Tumeric in equal amounts in second well; a mixture of 20% HAP and 80% Amla , Clove and Tumeric in equal amounts in third well ; showing Zones of Inhibition

In this figure no. 24., A depicts a mixture of 80% HAP and 20% Amla , Clove and Turmeric in equal amounts. B depicts a mixture of 50% HAP and 50% Amla , Clove and Turmeric in equal amounts. C depicts a mixture of 20% HAP and 80% Amla , Clove and Turmeric in equal amounts.

7.7.3 ANTIMICROBIAL ACTIVITY TABLES

Table 1. Zone of Inhibition values against E.coli by Well Diffusion Method on Nutrient Agar

Table 1.1 Conc. of Amla in comparison to Zone of Inhibition

Conc of Amla (mg) (Percentage)	Conc of HAP (mg) (Percentage)		Zone of Inhibition (mm)			
			Sample 1	Sample 2	Sample 3	Mean
900 (100%)	0(0%)	Control	2.3	2.1	1.9	2.1
720 (80%)	180(20%)		4.8	5.3	4.9	5
450(50%)	450(50%)		9.3	8.8	8.9	9
180(20%)	720(80%)		12.9	13.1	13	13
0(0%)	900(100%)	Control	17.6	18.5	17.9	18

Table 1.2 Conc. of Clove in comparison to Zone of Inhibition

Conc of Clove (mg)	Conc of HAP (mg)		Zone of Inhibition (mm)			
			Sample 1	Sample 2	Sample 3	Mean
900	0	Control	11.6	12.1	12.3	12
720	180		13.4	13.1	12.5	13
450	450		14.4	13.8	13.8	14
180	720		15	14.9	15.1	15
0	900	Control	17.6	18.5	17.9	18

Table 1.3 Conc. Of Turmeric in comparison to Zone of Inhibition

Conc of Tumeric (mg)	Conc of HAP (mg)		Zone of Inhibition (mm)			
			Sample 1	Sample 2	Sample 3	Mean
900	0	Control	8.3	7.8	7.9	8
720	180		9.5	10.3	10.2	10
450	450		11.8	12.1	12.1	12
180	720		14.4	13.9	13.7	14
0	900	Control	17.6	18.5	17.9	18

Table 1.4 Conc. Of Amla, Clove & Turmeric in comparison to Zone of Inhibition

Conc of Amla (mg)	Conc of Clove (mg)	Conc of Tumeric (mg)	Conc of HAP(mg)		Zone of Inhibition (mm)			
					Sample 1	Sample 2	Sample 3	Mean

0	0	0	900	Control	17.6	18.5	17.9	18
60	60	60	720		14	13	12	13
150	150	150	450		11	12	13	12
240	240	240	180		9.05	9.06	9.07	9.06
300	300	300	0	Control	7.2	7.3	7.4	7.3

Table 2. Zone of Inhibition values against E.coli by Well Diffusion Method on MacConkey's Agar

Table 2.1 Conc. Of Amla in comparison to Zone of Inhibition

Conc of Amla (mg)	Conc of HAP (mg)		Zone of Inhibition (mm)			
			Sample 1	Sample 2	Sample 3	Mean
900	0	Control	2.0	1.8	1.6	1.8
720	180		4.6	5.1	4.7	4.8
450	450		9.3	8.8	8.9	9
180	720		12.7	12.9	12.8	12.8
0	900	Control	17.3	18.2	17.6	17.7

Table 2.2 Conc. Of Clove in comparison to Zone of Inhibition

Conc of Clove (mg)	Conc of HAP (mg)		Zone of Inhibition (mm)			
			Sample 1	Sample 2	Sample 3	Mean
900	0	Control	11.7	11.9	12.1	11.9
720	180		13.3	13.0	12.4	12.9
450	450		14.4	13.8	13.8	14
180	720		14.9	14.8	15.0	14.9
0	900	Control	17.4	18.3	17.7	17.8

Table 2.3 Conc. Of Turmeric in comparison to Zone of Inhibition

			Sample 1	Sample 2	Sample 3	Mean
Conc of Tumeric (mg)	Conc of HAP (mg)		Zone of Inhibition (mm)			
900	0	Control	8.3	7.8	7.9	8
720	180		9.4	9.2	9.6	9.4

450	450		11.8	12.1	12.1	12
180	720		14.3	13.8	13.4	13.9
0	900	Control	17.4	18.3	17.7	17.8

Table 2.4 Conc. Of Amla, Clove & Turmeric in comparison to Zone of Inhibition

Conc of Amla (mg)	Conc of Clove (mg)	Conc of Tumeric (mg)	Conc of HAP(mg)		Zone of Inhibition (mm)			
					Sample 1	Sample 2	Sample 3	Mean
0	0	0	900	Control	17.5	18.4	17.8	17.9
60	60	60	720		12.6	12.7	12.8	12.7
150	150	150	450		11	12	13	12
240	240	240	180		9.05	9.06	9.07	9.06
300	300	300	0	Control	7.2	7.3	7.4	7.3

Table 3. Zone of Inhibition values against S.aureus by Well Diffusion Method on Nutrient Agar

Table 3.1 Conc. Of Amla in comparison to Zone of Inhibition

Conc of Amla (mg)	Conc of HAP (mg)		Zone of Inhibition (mm)			
			Sample 1	Sample 2	Sample 3	Mean
900	0	Control	2.3	2.1	1.9	2.1
720	180		4.8	5.3	4.9	5
450	450		9.3	8.8	8.9	9
180	720		12.9	13.1	13	13
0	900	Control	17.6	18.5	17.9	18

Table 3.2 Conc. Of Clove in comparison to Zone of Inhibition

Conc of Clove (mg)	Conc of HAP (mg)		Zone of Inhibition (mm)			
			Sample 1	Sample 2	Sample 3	Mean
900	0	Control	11.6	12.1	12.3	12
720	180		13.4	13.1	12.5	13
450	450		14.4	13.8	13.8	14
180	720		15	14.9	15.1	15

0	900	Control	17.6	18.5	17.9	18

Table 3.3 Conc. Of Turmeric in comparison to Zone of Inhibition

Conc of Tumeric (mg)	Conc of HAP (mg)		Zone of Inhibition (mm)			
			Sample 1	Sample 2	Sample 3	Mean
900	0	Control	8.3	7.8	7.9	8
720	180		9.5	10.3	10.2	10
450	450		11.8	12.1	12.1	12
180	720		14.4	13.9	13.7	14
0	900	Control	17.6	18.5	17.9	18

Table 3.4 Conc. Of Amla, Clove & Turmeric in comparison to Zone of Inhibition

Conc of Amla (mg)	Conc of Clove (mg)	Conc of Tumeric (mg)	Conc of HAP(mg)		Zone of Inhibition (mm)			
					Sample 1	Sample 2	Sample 3	Mean
0	0	0	900	Control	17.6	18.5	17.9	18
150	150	150	450		11.6	12.0	11.8	11.8
240	240	240	180		9.0	9.05	9.01	9.02
300	300	300	0	Control	7.3	7.2	6.8	7.1

Table 4. Zone of Inhibition values against S.aureus by Well Diffusion Method on MacConkey's Agar

Table 4.1 Conc. Of Amla in comparison to Zone of Inhibition

Conc of Amla (mg)	Conc of HAP (mg)		Zone of Inhibition (mm)			
			Sample 1	Sample 2	Sample 3	Mean
900	0	Control	2.0	1.8	1.6	1.8
720	180		4.4	4.9	4.5	4.6
450	450		8.5	8.6	8.7	8.6

180	720		12.4	12.8	12.6	12.6
0	900	Control	17.2	18.0	17.6	17.6

Table 4.2 Conc. Of Clove in comparison to Zone of Inhibition

Conc of Clove (mg)	Conc of HAP (mg)		Zone of Inhibition (mm)			
			Sample 1	Sample 2	Sample 3	Mean
900	0	Control	11.6	12.1	12.3	12
720	180		13.2	12.9	12.3	12.8
450	450		14.3	13.7	13.7	13.9
180	720		14.9	14.8	15.0	14.9
0	900	Control	17.6	18.5	17.9	18

Table 4.3 Conc. Of Turmeric in comparison to Zone of Inhibition

Conc of Tumeric (mg)	Conc of HAP (mg)		Zone of Inhibition (mm)			
			Sample 1	Sample 2	Sample 3	Mean
900	0	Control	8.2	7.7	7.8	7.9
720	180		9.3	10.1	10.0	9.8
450	450		11.7	12.0	12.0	11.9
180	720		14.2	13.7	13.5	13.8
0	900	Control	17.6	18.5	17.9	18

Table 4.4 Conc. Of Amla, Clove & Turmeric in comparison to Zone of Inhibition

Conc of Amla (mg)	Conc of Clove (mg)	Conc of Tumeric (mg)	Conc of HAP(mg)		Zone of Inhibition (mm)			
					Sample 1	Sample 2	Sample 3	Mean
0	0	0	900	Control	17.6	18.5	17.9	17.9
60	60	60	720		11.6	12.0	11.8	13

150	150	150	450		9.0	9.05	9.01	12
240	240	240	180		7.3	7.2	6.8	9.06
300	300	300	0	Control	17.8	18.1	18.3	18

Table 5. Zone of Inhibition values against E.coli by Pellet (Disk) Diffusion Method on Nutrient Agar

Table 5.1 Conc. Of Amla in comparison to Zone of Inhibition

Conc of Amla (mg)	Conc of HAP (mg)		Zone of Inhibition (mm)			
			Sample 1	Sample 2	Sample 3	Mean
900	0	Control	2.5	2.5	1.9	2.3
720	180		4.9	5.5	4.9	5.3
450	450		9.2	9.4	9.6	9.4
180	720		12.9	13.1	13	13
0	900	Control	19.6	18.9	19.4	19.3

Table 5.2 Conc. Of Clove in comparison to Zone of Inhibition

Conc of Clove (mg)	Conc of HAP (mg)		Zone of Inhibition (mm)			
			Sample 1	Sample 2	Sample 3	Mean
900	0	Control	11.6	12.1	12.3	12
720	180		13.4	13.1	12.5	13
450	450		14.4	13.8	13.8	14
180	720		15	14.9	15.1	15
0	900	Control	17.6	18.5	17.9	18

Table 5.3 Conc. Of Turmeric in comparison to Zone of Inhibition

Table 5.4 Conc. Of Amla, Clove & Turmeric in comparison to Zone of Inhibition

Conc of Tumeric (mg)	Conc of HAP (mg)		Zone of Inhibition (mm)			
			Sample 1	Sample 2	Sample 3	Mean
900	0	Control	8.3	7.8	7.9	8
720	180		9.5	10.3	10.2	10
450	450		11.8	12.1	12.1	12
180	720		14.4	13.9	13.7	14
0	900	Control	17.6	18.5	17.9	18

Conc of Amla (mg)	Conc of Clove (mg)	Conc of Tumeric (mg)	Conc of HAP(mg)		Zone of Inhibition (mm)			
					Sample 1	Sample 2	Sample 3	Mean
0	0	0	900	Control	17.6	18.5	17.9	18
60	60	60	720		13.3	13.5	13.4	13.4
150	150	150	450		11.7	12.1	11.9	11.9
240	240	240	180		9.6	9.4	9.5	9.5
300	300	300	0	Control	7.9	7.6	7.9	7.8

Table 6. Zone of Inhibition values against E.coli by Pellet (Disk) Diffusion Method on MacConkey's Agar

Table 6.1 Conc. Of Amla in comparison to Zone of Inhibition

Conc of Amla (mg)	Conc of HAP (mg)		Zone of Inhibition (mm)			
			Sample 1	Sample 2	Sample 3	Mean
900	0	Control	2.5	2.3	2.1	2.3
720	180		4.9	5.5	4.9	5.1
450	450		9.5	8.9	9.2	9.2
180	720		13.1	13.3	13.2	13.2
0	900	Control	17.8	18.7	18.1	18.2

Table 6.2 Conc. Of Clove in comparison to Zone of Inhibition

Conc of Clove (mg)	Conc of HAP (mg)		Zone of Inhibition (mm)			
			Sample 1	Sample 2	Sample 3	Mean
900	0	Control	11.7	12.2	12.4	12.1
720	180		13.6	13.3	12.7	13.2
450	450		14.5	13.9	13.9	14.1
180	720		15.1	14.9	15.3	15.1
0	900	Control	17.8	18.6	17.9	18.1

Table 6.3 Conc. Of Turmeric in comparison to Zone of Inhibition

Conc of Tumeric (mg)	Conc of HAP (mg)		Zone of Inhibition (mm)			
			Sample 1	Sample 2	Sample 3	Mean
900	0	Control	8.3	7.8	7.9	8
720	180		9.7	10.5	10.4	10.2
450	450		11.9	12.2	12.2	12.1
180	720		14.8	13.9	13.9	14.2
0	900	Control	17.9	18.5	17.9	18.1

Table 6.4 Conc. Of Amla, Clove & Turmeric in comparison to Zone of Inhibition

Conc of Amla (mg)	Conc of Clove (mg)	Conc of Tumeric (mg)	Conc of HAP(mg)		Zone of Inhibition (mm)			
					Sample 1	Sample 2	Sample 3	Mean
0	0	0	900	Control	17.9	18.5	17.9	18.1
60	60	60	720		18.8	13.5	13.5	13.6
150	150	150	450		11.9	12.2	11.9	12
240	240	240	180		9.2	9.8	9.5	9.5
300	300	300	0	Control	7.9	7.7	7.8	7.8

Table 7. Zone of Inhibition values against S.aureus by Pellet (Disk) Diffusion Method on Nutrient Agar

Table 7.1 Conc. Of Amla in comparison to Zone of Inhibition

Conc of Amla (mg)	Conc of HAP (mg)		Zone of Inhibition (mm)			
			Sample 1	Sample 2	Sample 3	Mean
900	0	Control	2.3	2.1	1.9	2.1
720	180		4.8	5.3	4.9	5
450	450		9.3	8.8	8.9	9
180	720		12.9	13.1	13	13
0	900	Control	17.6	18.5	17.9	18

Table 7.2 Conc. Of Clove in comparison to Zone of Inhibition

Conc of Clove (mg)	Conc of HAP (mg)		Zone of Inhibition (mm)			
			Sample 1	Sample 2	Sample 3	Mean
900	0	Control	11.6	12.1	12.3	12
720	180		13.4	13.1	12.5	13
450	450		14.4	13.8	13.8	14
180	720		15	14.9	15.1	15
0	900	Control	17.6	18.5	17.9	18

Table 7.3 Conc. Of Turmeric in comparison to Zone of Inhibition

Conc of Tumeric (mg)	Conc of HAP (mg)		Zone of Inhibition (mm)			
			Sample 1	Sample 2	Sample 3	Mean
900	0	Control	8.3	7.8	7.9	8
720	180		9.5	10.3	10.2	10
450	450		11.8	12.1	12.1	12
180	720		14.4	13.9	13.7	14
0	900	Control	17.6	18.5	17.9	18

Table 7.4 Conc. Of Amla, Clove & Turmeric in comparison to Zone of Inhibition

Conc of Amla (mg)	Conc of Clove (mg)	Conc of Tumeric (mg)	Conc of HAP(mg)		Zone of Inhibition (mm)			
					Sample 1	Sample 2	Sample 3	Mean
0	0	0	900	Control	17.9	18.8	17.9	18.2
60	60	60	720		13.5	13.2	13.2	13.3
150	150	150	450		13.1	13.3	13.2	13.2
240	240	240	180		9.3	9.7	8.9	9.3
300	300	300	0	Control	7.8	7.5	7.8	7.7

Table 8. Zone of Inhibition values against S.aureus by Pellet (Disk) Diffusion Method on MacConkey's Agar

Table 8.1 Conc. Of Amla in comparison to Zone of Inhibition

Conc of Amla (mg)	Conc of HAP (mg)		Zone of Inhibition (mm)			
			Sample 1	Sample 2	Sample 3	Mean
900	0	Control	2.3	2.4	1.9	2.3
720	180		4.9	5.5	4.9	5.1
450	450		9.3	9.7	8.9	9.3
180	720		13.1	13.3	13.2	13,2
0	900	Control	17.8	18.6	17.9	18.1

Table 8.2 Conc. Of Clove in comparison to Zone of Inhibition

Conc of Clove (mg)	Conc of HAP (mg)		Zone of Inhibition (mm)			
			Sample 1	Sample 2	Sample 3	Mean
900	0	Control	12.1	12.6	12.8	12.5
720	180		13.4	13.4	12.8	13.2
450	450		14.5	13.9	13.9	14.1
180	720		15.2	14.9	15.2	15.1
0	900	Control	17.8	18.9	17.9	18.2

Table 8.3 Conc. Of Turmeric in comparison to Zone of Inhibition

Conc of Tumeric (mg)	Conc of HAP (mg)		Zone of Inhibition (mm)			
			Sample 1	Sample 2	Sample 3	Mean
900	0	Control	8.3	7.8	7.9	8
720	180		9.5	10.4	10.3	10.4
450	450		11.9	12.3	12.1	12.1
180	720		14.5	13.9	13.9	14.3
0	900	Control	17.5	18.3	17.9	17.9

Table 8.4 Conc. Of Amla, Clove & Turmeric in comparison to Zone of Inhibition

Conc of Amla (mg)	Conc of Clove (mg)	Conc of Tumeric (mg)	Conc of HAP(mg)		Zone of Inhibition (mm)			
					Sample 1	Sample 2	Sample 3	Mean
0	0	0	900	Control	17.5	18.3	17.9	17.9
60	60	60	720		13.4	13.3	13.8	13.5
150	150	150	450		12.2	12.5	12.5	12.4
240	240	240	180		9.5	9.1	9.0	9.2
300	300	300	0	Control	7.2	7.6	7.7	7.5

7.7.4 Description of work

. The antimicrobial activity of clove is because of eugenol (a terpenoid), vanillin,eugeniin and casuarji-citin components. Turmeric contains terpenoids i.e., curcumin and turmeric oil as

antimicrobials. And Indian gooseberry has phosphatides, tannins, vitamin C and chebulinic acid as antimicrobial substances.(Ahmad, I. et al., 2001).

Turmeric is a yellow-orange substance that is obtained from the root of the plant Curcuma longa. (Cheng, Y.et. al.2014).

Concentrates of Amla (Emblica officinalis) natural product, Neem (Azadirachta indica) leaves, (Aloe vera) leaves, Assam Tea (Camellia sinensis assamica) leaves and Clove (Syzygium aromaticum) buds were found to hinder the development of Staphylococcus aureus, Vibrio cholerae and Pseudomonas aeruginosa. Bioactive segments were steady over a scope of pH qualities and temperatures. (Shubhi, M.et. al.,2010)

It is observed that HAP produced zone of inhibition of 16-18mm diameter in pure form and thus it was found to have maximum antimicrobial efficacy. It was followed by the antimicrobial activity possessed by of clove, haldi and amla in that sequence in a decreasing manner. In a concentration of 900 mg each ; Clove showed 12 mm whereas Turmeric showed 08 mm zone of inhibition in pure form.Indian Gooseberry (Amla) had 2 -4 mm zone of inhibition in pure form and hence it was least effective antimicrobial in the present study. Against Staphylococcus aureus, Turmeric exhibited a zone of 5.67 mm in comcentration of 10% W/W and that of 7 mm in concentration of 5% W/W.(Cheng, Y.et. al.2014).Wherteas in my study , the zone of inhibition obtained in case of turmeric is about 8mm on an average . It is a little bit higher than that reported in the mentioned study. Alteration may be because of variation in the degree of purity of turmeric utilized in the study.

From fig 1, 5, 9 and 13 it is observed that with addition of HAP in other pure compound [amla, clove, turmeric] the anti microbial activity tends to increase. This is because we get a greater zone of inhibition. Similar case is observed on comparing fig 2,6,10,14 ; 3,7,11,15 and 4,8,12,16

The antimicrobial activity is more against S.aureus when compared with E.coli. Therefore the zones of inhibition in case of S. aureus are found to be little bit greater than those obtained in case of E. coli.

Activity of Turmeric [Curcuma longa] is due to the presence of Curcumin which belongs to class of Terpenoids. It is effective against Bacteria. In case of Clove [Syzygium aromaticum] the chemical compound present is Eugenol again belonging to Terpenoid class.

Also well diffusion was better than pellet diffusion since zones of inhibition in former methodology were comparatibly bigger than those formed by later technique.

Various values of zones of inhibition have been depicted in the tables framed below.

Antimicrobial action of Clove (Syzygium aromaticum) and Garlic (Allium sativum) was tried against Staphylococcus aureus, Salmonella typhi and Escherichia coli. E.coli and Bacillus cereus at various conc. (1000 ppm, 1500 ppm, 2000 ppm) of their concentrates among which garlic was observed to be more viable when contrasted with clove. Bacillus cereus was observed to be most delicate while E.coli was generally safe.

Activity of Turmeric [Curcuma longa] is due to the presence of Curcumin which belongs to class of Terpenoids. It is effective against Bacteria. In case of Clove (Syzygium aromaticum), the chemical compound present is Eugenol again belonging to Terpenoid class. Also well diffusion was better than pellet diffusion since zones of inhibition in former methodology were comparatibly bigger than those formed by later technique.

Chapter 8
Experimental Work

127

Chapter 9
Conclusion And Future Scope

7.1 Conclusion

Hydroxyapatite was synthesized by precipitation method as a wet chemical technique. Hydroxyapatite was synthesized using Wet Chemical Technique in two disparate sub manners. In the former technique, the pair of chemicals used in producing HAP included Calcium Hydroxide and Ortho-Phosphoric Acid; whereas the second tactic utilized the chemicals named Calcium Nitrate and be a better resource Diamino Hydrogen-Orthophosphate. The earlier method was established out to a better means to create HAP in uncontaminated or pure form ; and that has been concluded following FTIR studies dones and graphs obtained being analysed thereof. Purity is important here since it is to be implanted in human bodies. The need to produce HAP lies in the fact that it is a suitable biocompatible substance that can be used; but rather it is being used widely in medical implants for human bones. Its applicability in other fields can be established by conducting vast research especially in the fields of dental caries filling up and also for denture replacements on the whole.

Following production of HAP by using Calcium Hydroxide And Orthophosphoric Acid, calcination was done at 800^0C. The synthesized HAP powder was characterized on a macroscopic level by FTIR,SEM,TEM and XRD . This technique has shown that the HAP sample prepared in solution was nearly pure. HAP is assessed to be the best antimicrobial when compared with Clove, Turmeric and Indian Goosebberry. In a mixture, as percent content of HAP increases and that of Clove / Turmeric / Indian Gooseberry decreases, the Zone of Inhibition increases. The present study has revealed the supremacy of HAP as an antimicrobial over Clove, Turmeric and Indian Gooseberry which have assessed for their antimicrobial activity. It is observed that HAP had 16-18 mm zone of inhibition and was assessed to have maximum antimicrobial efficacy in the present study. In the coparative ranking in antimicrobial efficacy it was followed by clove, turmeric and Indian Gooseberry in that sequence. Clove showed 12mm zone of inhibition and Tumeric showed 8 mm zone of inhibition. But Indian Gooseberry had 2 mm zone of inhibition and hence it was found out to be least effective antimicrobial agent in the present study.

.E. coli is more pathogenic than Staphylococcus aureus. Hence the antimicrobial activity is more in case of E.coli and therefore zone of inhibition is found to be greater in case of S. aureus. Also well diffusion methodology was found to be more effective than pellet dispersion tactic. As such zones of inhibition in former methodology were comparatibly larger than those formed by later technique.

7.2 Future Scope

Also, because of having excellent biocompatibility; HAP is successful in biomedical applications , especially in the fields of Dentistry and Orthopaedics as implanting material.

Chapter 10
List of
References or Bibliography

Anita, L. J. (2015) "Influence of surfactant on synthesis of HAp by hydrothermal route", Journal of Chemical and Pharmaceutical Research,vol. 7, 3, pp. 187-190.

Azzouz, M. A. and Bullerman, L. R. 1982. Comparative antimycotic effects of selected herbs and spices, plant components and commercial antifungal agents. J. Food Protect. 45:1248-1301.

Baur, A.W. Kirby, W.M.M. Scherris, J.C. Turck, M (1966) "Antibiotic susceptibility testing by a standardized single disk method", Amer. J. Cl. Pathol, vol.45, pp. 493–496.

Beuchat, L. R. Sensitivity of *Vibrio Parahaemolyticus* to spices and organic acids. J. Food Sci. 41:899-902.

Bianco, A. Cacciotti, M. Lombardi, L. Montanaro, G. (2007) "Thermal stability and sintering behaviour of hydroxyapatite nanopowders", J. Therm. Anal. Calorim. VOL.88, pp.237–43.

Binnaz, H.Y. Yeliz,K, (2009) "Double Step Stirring: A Novel Method For Precipitation Of Nano-Sized Hydroxyapatite Powder"Digest J. Nanomaterials and biostructures, vol.4,1 pp. 73-81.

Bullerman, L. B. 1974. Inhibition of aflatoxin production by cinnamon. J. Food Sci. 39:1163-1165.

Bullerman, L. B., Lieu, F. Y., and Seier, S. A. 1977. Inhibition of growth and aflatoxin production by cinnamon and clove oils, cinnamic aldehyde and eugenol. J. Food Science. 42:1107-1109, 1116.

Cai, Y.R. Liu, Y.K. Yan, W.Q. Hu, Q.H. Tao, J.H. Zhang, M. Shi, Z.L. and Tang, R.K.(2007) "Role of hydroxyapatite nanoparticle size in bone cell proliferation", J. Mater Chem., vol. 17, pp. 3780–3787.

Craig, D. Friedman,C.D. Costantino, P.D.,Takagi,S. Chow,L.C.J. (1998) "BoneSourceTM Hydroxyapatite Cement: A Novel Biomaterial for Craniofacial Skeletal Tissue Engineering and Reconstruction" , J. Biomed Mater Res (Appl Biomater) vol. 43, pp. 428–432.

Cristina,G Sousa,F. and Julian R. G. E (2003)) "Sintered Hydroxyapatite Latticework for Bone Substitute". J. Am. Ceram. Soc.,vol. 86,3 pp, 517–519.

Dankert, J., Tromp, Th. F. J., Devries, H. and Klasen, H. J. 1979. Antimicrobial activity of crude juices of *Allium ascalonicum, Allium cepa* and *Allium sativum*. Zb. Bkr. Hyg., I. Abt. Orig. A245:229-239.

Dorozhkin, S. V. (2010). Nanosized and nanocrystalline calcium orthophosphates. Acta biomaterialia, 6(3), 715-734.

Eslami, H., Tahriri, M., & Bakhshi, F. (2010). "Synthesis and characterization of nanocrystalline hydroxyapatite obtained by the wet chemical technique". Mater. Sci. Pol, vol. 28(1), pp. 5-13.

Fabbri M., Celott G.C.i and A. Ravaglioli(1995) "Hydroxyapatite-based porous aggregates: physico-chemical nature,structure, texture and architecture". Biomaferials vol.16,3, pp. 225-228.

Giese, J. 1994. Spices and seasoning blends: A taste for all seasons. Food Technol. 48(4):87-98.

Handrasekar, A. Sagadevan, S. and Dakshnamoorthy, A*.(2013) "Synthesis and characterization of nano-hydroxyapatite (n-HAP) using the wet chemical technique" International Journal of Physical Sciences . vol. 8,32, pp. 1639-1645.

Hitokoko, H., Morozumi, S., Wauke, T., Sakai, S., and Kurata, H. 1980. Inhibitory effects of spices on growth and toxin production of toxigenic fungi. Appl. Env. Microbiol. 39:818-822.

Huhtanen, C. N. 1980. Inhibition of *Clostridium botulinum* by spice extracts and aliphatic alcohols. J. Food Protect.vol. 43:195-196.

Ito, A. Otsuka, M. and Kawamura, H. (2005) "Zinc-containing tricalcium phosphate and related materials for promoting bone formation". Curr Appl Phys vol. 5, pp 402-406.

Johnson, M. G., and Vaught, R. H. 1969. Death of *Salmonella typhimurium* and *Escherichia coli* in the presence of freshly reconstituted dehydrated garlic and onion. Appl. Microbiol. 17:903-905.

José, R.G, Esmeralda, L.M. , Galois, R. Á , Gaby, E. Tiznado, O.Ramiro, G. and Etienne, F. B. (2013) " XRD and FTIR crystallinity indices in sound human tooth enamel and synthetic hydroxyapatite". Materials Science and Engineering vol.33, pp. 4568–4574

Julseth. R. M. and Deibel, R. H. 1974. Microbial profile of selected spices and herbs at import. J. Milk Food Technol. 37:414-419.

Kapoor, S., Batra, U., Kohli, S. (2011) "Transformations in Sol Gel Synthesized nanoscale Hydroxyapatite Calcined under different temperatures and time conditions" Journal of Material Engineering and performance vol.21, pp.1737-1743

Kneifel, W. and Berger, E. 1994. Microbial criteria of random samples of spices and herbs retailed on the Austrian market. J. Food Protect. 57:893-901

Kobayashi, S. and Kawai, W. (2007) "Development of carbon nanofiber reinforced hydroxyapatite with enhanced mechanical properties",Composites: Part A: Applied Science and Manufacturing, vol.38 pp 114-123.

Kehoe, S., Ardhaoui, M., & Stokes, J. (2011). "Design of experiments study of hydroxyapatite synthesis for orthopaedic application using fractional factorial design." Journal of materials engineering and performance, vol.20(8), pp.1423-1437.

Kristine,S. Liga,B.C. Natalija,B.. (2010) "Calcium phosphate bioceramics prepared from wet chemically precipitated powders", Processing and Application of Ceramics, vol. 4, 1, pp. 45–51.

Kui, C.A. Shen, A.G. Weng, A.W. Han,A.G. Jose, M.F. Ferreira,B. and Yang,J. (2001) "Synthesis of hydroxyapatiterfluoroapatite solid solution by a sol–gel method" Materials Letters. vol.51 pp. 37–41.

Kumar, G. S., Sathish, L., Govindan, R., & Girija, E. K. (2015) " Utilization of snail shells to synthesise hydroxyapatite nanorods for orthopedic applications". RSC Advances, 5(49), pp. 39544-39548.

Li, B. Guo, B. Fan, H.S. Zhang, X.D. (2008) "Preparation of nano-hydroxyapatite particles with different morphology and their response to highly malignant melanoma cells in vitro",Appl. Surf. Sci., 255, 357–360.

Llewellyn, G.C., Burkitt, M. L., and Eadie, T. 1981. Potential mold growth, aflatoxin production and antimycotic activity of selected natural spices and herbs. J. Assoc. Off. Anal. Chem. 64(4):955-960

Lim, G.K., Wang, J. S.C. Gan N.L.M. (1996)."Processing of fine hydroxyapatite powders via an inverse microemulsion route", Materials Letters, vol. 28 pp. 431-436.

Lopez, M.A, Rodriguez,C.R. Hidalgo,L. Garcia,G.M.V. Zivera, E. Castano,V.M. (1998) "Wet Chemical Synthesis of Hydroxyapatite Particles from Nonstoichiometric Solutions." Journal of pp.Materials Synthesis and Processing, vol. 6, I, pp. 21-26.

López, P., Sánchez, C., Batlle, R., & Nerín, C. (2007). Development of flexible antimicrobial films using essential oils as active agents. Journal of Agricultural and Food Chemistry, 55(21), pp.8814-8824.

Maisara,S. Arsad,M. Pat,M.L. (2011) "Synthesis and Characterization of Hydroxyapatite Nanoparticles and β-TCP Particles",2nd International Conference on Biotechnology and Food Science IPCBEE vol.7 pp. 1-11.

Mansour, S. F., El-dek, S. I., Ahmed, M. A., Abd-Elwahab, S. M., & Ahmed, M. K. (2016). "Effect of preparation conditions on the nanostructure of hydroxyapatite and brushite phases." Applied
Nanoscience, vol. 6(7), pp. 991-1000.

Merheb, J., Temmerman, A., Rasmusson, L., Kübler, A., Thor, A., & Quirynen, M. (2016). "Influence of skeletal and local bone density on dental implant stability in patients with osteoporosis". Clinical implant dentistry and related research.vol.18(02) pp.253-260.

Mishra, V.K. Bhattacharya,B.N. Kumar, D. Rai,S.B. and Prakash, O. (2015) "Effect of Chelating Agent at Different pH on Spectroscopic and Structural Properties of Microwave Derived Hydroxyapatite Nanoparticles: A Bone Mimetic Material" New Journal of Chemistry (The Royal Society of Chemistry),vol.1 pp1-11.

Mohammad, N.F. Othman, R. and Yee-Yeoh,F. (2014) "Nanoporous hydroxyapatite preparation methods for drug delivery applications", Rev.Adv. Mater. Sci., vol. 38 pp138-147.

Mohandes, F. 1, M. Salavati, N,(2013) "Influence of morphology on the in vitro bioactivity of hydroxyapatite nanostructures prepared by precipitation method", New Journal of Chemistry RSC Publishing Article 00, 1-3

Monda, S.l. Dey,A. and Pal,U. (2o16) "Low temperature wet-chemical synthesis of spherical hydroxyapatite nanoparticles and their in situ cytotoxicity study", **Advances in Nano Research**, vol. 4, 4 , pp. 295.

Mukherjeea,S. Biswanath,K. Swarnendu,S. Chanda,A. (2014) "Improved properties of hydroxyapatite–carbon nanotube biocomposite: Mechanical, invitro bioactivity and biological studies", Ceramics International vol.40, pp. 5635–5643.

Nonam, T. H. Taoda, N.T. Hue, E. Watanabe, K. Iseda, M.T. and Fukaya, M. "Apatite Formation on TiO2 Photocatalyst Film in a Pseudo BodySolution", Mater Res Bull, vol. 33,1, pp 125-131.

Novesar Jamarun1*, Sri Elfina1, Syukri Arief1, Akmal Djamaan2 and Mufitra(2016) "Hydroxyapatite Material: Synthesis by Using Precipitation Method from Limestone" Der Pharma Chemica,vol.8 no.13. pp. 302-306.

Pafumi, J. 1986. Assessment of microbiological quality of spices and herbs. J. Food Protect. 49:958-963

Pandya, H. M. "Modelling Scenario in Nanotechnology Today", (2012) .J. Environmental Nano Technology, vol.1 pp. 1 01-104.

Paster, N., Menasherov, M., Ravid, U., and Juven, B. 1995. Antifungal activity of oregano and thyme essential oils applied as fumigants against fungi attacking stored grain. J. Food Protect. 58:81-85.

Peltola, T. M. Patsi, H. Rahiala, I. K. and Yli-Urpo,A. (1998) "Calcium phosphate induction by solgel-derived titania coatings on titanium substrates in vitro", J Biomed Mater Res, vol. 41, 3, pp. 504-510.

Powers, E. M., Layer, R., and Masuoka, Y. 1975. Microbiology of processed spices. J. Milk Food Technol. 38:683-687.

Raizda,*P. Gautam,S. Priya,B. and Singh,P. (2016) "Preparation and photocatalytic activity of hydroxyapatite supported BiOCl nanocomposite for oxytetracyline removal", Adv. Mater. Lett. **7**,4, pp. 312-318

Ramay, H.R.R. and Zhang,M. "Biphasic calcium phosphate nanocomposite porous scaffolds for loadbearing bone tissue engineering", Biomaterials vol.25, pp. 5171-5180.

Sadat,S. 1. Khorasani, M.T. Dinpanah,K. E. and Jamshidi, A. (2013) "Synthesis methods for nanosized hydroxyapatite with diverse structures", Acta Biomater, vol.9, pp. 7591–7621.

Sadjadi, M.S. Meskinfam, M. Sadeghi, B. Jazdarreh,H. and Zare, K. (2010) "In situ biomimetic synthesis, characterization and in vitro investigation of bone-like nanohydroxyapatite in starch matrix" Materials Chemistry and Physics, vol,124 pp. 217–222.

Safrono, T. V. Shekhirev, M. A. and Putlyaev,V.I. (2007), "Ceramics Based on Calcium Hydroxyapatite Synthesized in the Presence of PVA", Glass and Ceramics, vol. 64, Nos. 11 – 12, pp. 408-412.

Sakthivel,* P. Senthilarasan, K. and Ragu, A. (2014) "Synthesis and Characterization of Nano Hydroxyapatite with Agar-Agar Bio-Polymer" Int. Journal of Engineering Research and Applications, vol. 4, 7, pp. 55-59.

Sasikumar, S. and Vijayaraghavan, R.(2006)" Low Temperature Synthesis of Nanocrystalline Hydroxyapatite from Egg Shells by Combustion Method",Trends Biomater. Artif. Organs, vol. 19,2, pp. 70-73.

Sharma, A., Tewari, G. M., Shrikhande, A. J., Padwal-Desai, S. R., and Bandyopadhyay, C. (1979). Inhibition aflatoxin producing fungi by onion extracts. J. Food Sci. 44:1545-1547.

Shelef, L. A. (1983). Antimicrobial effects of spices. J. Food Safety.vol. 6, 29-44.

Shelef, L. A., Jyothi, E. K., and Bulgarelli, M. 1984. Effect of sage on growth of enteropathogenic and spoilage bacteria in sage containing broths and foods. J. Food Sci. 737-740, 809.

Shelef, L. A., Naglik, O. A., and Bogen, D. W. (1980). Sensitivity of some common food-borne bacteria to the spices sage, rosemary, and allspice. J. Food Sci. 45(4):1045-1044.

Singh, A. Mehta, D. and George, S. (2016) "Assessment of Different Synthesis Route of Hydroxyapatite and Study of its Biocompatibility in Synthetic Body Fluids", International J. Chem Tech Research vol. 9,3, pp. 267-276.

So, W.W. Park, S.B. Kim, K.J. and Moon, S.J. (1997). "Phase Transformation Behavior at Low Temperature in Hydrothermal Treatment of Stable and Unstable Titania Sol". J Colloid Interf Sci, Vol. 191, No. 2, pp 398-406.

Sooksaen, P. Jumpanoi1, N. Suttiphan, P. Kimchaiyong, E. (2010) "Crystallization of Nano-Sized Hydroxyapatite via Wet Chemical Process under Strong Alkaline Conditions**"** Sci. J. UBU, Vol. 1, No. 1 pp. 20-27.

Sridhara, R. D. V. Muraleedharan, K. and Humphreys, C. J. (2010) "TEM specimen preparation techniques", Microscopy: Science, Technology, Applications and Education A. Méndez-Vilas and J. Díaz (Eds.)

Sunada, K. Watanabe, T. and Hashimoto, K. (2003)"Bactericidal activity of copper-deposited TiO2 thin film under weak UV light illumination". Environ.Sci. Technol , vol. 37, pp. 4785-4789.

Tolba, E., Müller, W. E., El-Hady, B. M. A., Neufurth, M., Wurm, F., Wang, S., Wang, X. (2016). "High biocompatibility and improved osteogenic potential of amorphous calciumCarbonate /
vaterite." Journal of Materials Chemistry B,vol. 4(3), pp.376-386.

Tiwari, B. K., Valdramidis, V. P., O'Donnell, C. P., Muthukumarappan, K., Bourke, P., & Cullen, P. J. (2009). Application of natura antimicrobials for food preservation. Journal of Agricultural and Food Chemistry, *57*(14), pp.5987-6000.

Tripathi, A. Saravanan, S. and Pattnaik, S.(2012) "Bio composite scaffolds containing chitosan/nano-hydroxyapatite/nanocopper-zinc for bone tissue engineering", International J. Biological Macromolecules,2012, vol. 50, pp. 294–299.

Werner , E.G.M. Meik, N. Emad, T. Shunfeng ,W. Werner, G. Qingling, F. Heinz C. Schrödera, X. W. (2 0 1 6) "A biomimetic approach to ameliorate dentalhypersensitivity by amorphous polyphosphate microparticles" Dental- Science Direct 2752; no. of pp 9.

Wu, W.J.and George, H.N. (1998)"Kinetics of Heterogeneous Nucleation of Calcium Phosphates on Anatase and Rutile Surfaces". J Colloid Interf Sci, vol.199, pp. 206-211.

Yukai, S. Yuyue, Q. Yongming, C.1., Hongl,i L.1. and Minglong, Y,* (2013) “The Synthesis and Characterization of Hydroxyapatite-β-Alanine Modified by Grafting Polymerization of γ-Benzyl-L-glutamate-N-carboxyanhydride”. Molecules,vol.18,pp 13979-13991.

Zaika, L. L. 1988. Spices and herbs: Their antimicrobial activity and its determination. J. Food Safety. 9:97-118.

Zakaria, S. M., Sharif Zein, S. H., Othman, M. R., Yang, F., & Jansen, J. A. (2013). Nanophase hydroxyapatite as a biomaterial in advanced hard tissue engineering: a review. Tissue Engineering Part B: Reviews, 19(5), 431-441.

Zhou,W.Y. Wang,M. Cheung,W. L. Guo,B.C. and Jia,D.M. (2008). “Synthesis of carbonated hydroxyapatite nanospheres through Nanoemulsion”, J Mater Sci: Mater Med. vol. 19,pp.103–110.

Chapter 11
Appendix

111